

For Reference

NOT TO BE TAKEN FROM THIS ROOM

Ex LIBRIS
UNIVERSITATIS
ALBERTAENSIS





Digitized by the Internet Archive
in 2021 with funding from
University of Alberta Libraries

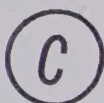
<https://archive.org/details/West1972>

THE UNIVERSITY OF ALBERTA

$\text{H}_2\text{O}^{18}/\text{H}_2\text{O}^{16}$ VARIATIONS IN ICE AND SNOW

OF MOUNTAINOUS REGIONS OF CANADA

BY



KENNETH ERNEST WEST

A THESIS SUBMITTED TO THE FACULTY OF GRADUATE STUDIES AND
RESEARCH IN PARTIAL FULFILMENT OF THE REQUIREMENTS FOR THE DEGREE
OF DOCTOR OF PHILOSOPHY

DEPARTMENT OF PHYSICS

EDMONTON, ALBERTA

SPRING 1972

UNIVERSITY OF ALBERTA

FACULTY OF GRADUATE STUDIES AND RESEARCH

The undersigned certify that they have read, and recommend to the Faculty of Graduate Studies and Research for acceptance, a thesis entitled $\text{H}_2\text{O}^{18}/\text{H}_2\text{O}^{16}$ VARIATIONS IN ICE AND SNOW OF MOUNTAINOUS REGIONS OF CANADA, submitted by Kenneth Ernest West in partial fulfilment of the requirements for the degree of Doctor of Philosophy.

Thesis
1972
74D

ABSTRACT

Ice and snow samples for $\text{H}_2\text{O}^{18}/\text{H}_2\text{O}^{16}$ analysis were collected in four mountainous regions of Canada (St. Elias Mountain Ranges, Yukon; Peyto Glacier, Alberta; United States Mountain Range, Northern Ellesmere Island, N.W.T.; Mt. Seymour, B.C.) with the objective of correlating the isotopic variations with meteorological trends and investigating glacier flow.

In the summer of 1968, the snow and ice collected in the St. Elias Mountains varied isotopically from -45.1 ‰ (S.M.O.W.) on Mt. Logan, elevation 5680 m, to -14.8 ‰ (S.M.O.W.), rainfall at Fox Glacier. The $\text{H}_2\text{O}^{18}/\text{H}_2\text{O}^{16}$ results helped to elucidate complex weather patterns caused by the St. Elias Mountains acting as an obstacle against easterly flow, as well as giving an insight into the flow pattern of the Fox Glacier, which is a supposed surging glacier.

The ablation area of the Peyto Glacier was sampled in the summer of 1969. A computed contour map of the $\text{H}_2\text{O}^{18}/\text{H}_2\text{O}^{16}$ results, δ values ranging from -19.1 ‰ (S.M.O.W.) to -25.4 ‰ (S.M.O.W.), revealed a general flow pattern. Also, a correlation between the topographical shape and the δ -values of the glacier was noted.

In May 1970, annual accumulation in a 7 m snow pit, and 22 m core from the bottom of the pit, in Northern Ellesmere Island were studied. The δ -values ranged from

-22 ‰ (S.M.O.W.) to -37 ‰ (S.M.O.W.) with a mean of -28.7 ‰ (S.M.O.W.). Discrepancies between the stratigraphic and isotopic identifications of annual layers preserved in the firn were found. Stratigraphic evidence indicated a mean annual accumulation of about 140 mm of H₂O while the isotopic results gave a mean annual accumulation of 197 mm of H₂O.

Due to the small amount of sampling and the dynamic meteorological effects encountered in snow storms on Mt. Seymour, B.C., in the winters of 1969 and 1970, the isotopic results were inconclusive. The isotopic values ranged from -8.9 ‰ (S.M.O.W.) to -21.4 ‰ (S.M.O.W.).

ACKNOWLEDGEMENTS

I wish to express my thanks to my supervisor Dr. H.R. Krouse for his guidance during the course of this work. I would also like to thank Dr. G. Hattersley-Smith, J. LaBelle, J. Underwood, Dr. R. Goodman, R. Pajowski, C. Keeler and B. Fitzharris for their cooperation in obtaining samples. The extensive help and suggestions made by the field parties of the A.I.N.A. under Dr. M. Marcus and Dr. S. Collins, and the D.R.B. field party under Dr. G. Hattersley-Smith were very much appreciated. Assistance in computing was given by Dr. G. Cumming and R. Hunt. The laboratory assistance of R. Shaw is gratefully acknowledged.

Financial support for this project came from D.R.B., N.R.C. and Boreal Institute (University of Alberta) grants.

CONTENTS

	<u>Page</u>
CHAPTER I : $\text{H}_2\text{O}^{18}/\text{H}_2\text{O}^{16}$ ABUNDANCE VARIATIONS	1
Introduction	1
I.1 Designation of Isotopic Variation	3
I.2 Fractionation of Isotopic Species of Water	4
I.3 Applications in Mountainous Regions	10
a) Latitude Effects	11
b) Altitude Effects	11
c) Preservation of Seasonal Isotopic Variations in Ice and Snow	12
d) Paleoclimatology	14
e) Glacier Flow	15
f) Projects of this Thesis	16
CHAPTER II : EXPERIMENTAL PROCEDURES	18
II.1 Field Sampling	18
a) Snow-Pits	18
b) Snow and Ice Cores	19
c) Surface Sampling	20
II.2 Sample Preparation for Isotopic Analysis	20
a) Theory	20
b) Equilibration of H_2O with CO_2	22
II.3 Mass Spectrometry	25

	<u>Page</u>
CHAPTER III : ICEFIELD RANGES: ST. ELIAS MOUNTAINS, YUKON	27
III.1 Introduction	27
III.2 Divide	28
a) Introduction	28
b) Climatology	29
c) Data	30
III.3 Mt. Logan	38
a) Introduction	38
b) Results	39
c) Discussion	45
III.4 The "Fox" Glacier	48
a) Introduction	48
b) Glaciers	50
c) Results	56
d) Discussion	70
CHAPTER IV : PEYTO GLACIER	73
IV.1 Introduction	73
a) Description	73
b) Other Investigations	74
IV.2 Isotopic Data	75
CHAPTER V : NORTHERN ELLESMERE ISLAND	81
V.1 Introduction	81

Page

CHAPTER V (cont'd)

V.2	Isotopic Data	83
a)	Snow-Pit	83
b)	Isotopic and Stratigraphic Discrepancies	89
c)	Climatic Trends	94
d)	Ice Lens Systems	95
e)	Temperatures	96
f)	Relationship with Other Studies	97
CHAPTER VI :	CONCLUSIONS	100
APPENDIX A :	CONTOUR PLOTTING OF RAW DATA, TREND SURFACES AND RESIDUALS	103
APPENDIX B :	$\text{H}_2\text{O}^{18}/\text{H}_2\text{O}^{16}$ VARIATIONS ON MT. SEYMOUR, B.C.	109
BIBLIOGRAPHY		113

LIST OF FIGURES

<u>Figure</u>		<u>Page</u>
1a)	Evaporation Fractionation	4A
1b)	Reaction Rates	4A
2	Rayleigh Condensation Process	6A
3	An Ideal Snow-Pit	18A
4	Standard Equilibration Flask (glass joints)	24A
5	New Equilibration Flask	24B
6	P.D.P.-8 Output	26A
7	St. Elias Mountains (Mt. Logan, Divide, Fox Glacier, after MARCUS, 1965)	27A
8	Rain Shadow of Mt. Logan (after TAYLOR-BARGE, 1969)	30A
9	Temperature Profile of Divide Pit	30B
10	Density Profile of Divide Pit	33A
11	Isotopic Profile of Divide Pit	33A
12	Pit 1 of MACPHERSON and KROUSE, 1967 (June 30, 1963, alt. 8396 ft.)	35A
13	Deuterium Traverse of the Sierra Nevadas (after FRIEDMAN and SMITH, 1970)	36A
14	Map of Mt. Logan Plateau (after LABELLE, in Press)	39A
15	Density of Pit I (Mt. Logan, Northwest Col, elev. 5400 m.)	40A
16	Temperature of Pit I (Mt. Logan, Northwest Col, elev. 5400 m.)	40A
17	Isotope Profile of Pit I (Mt. Logan, Northwest Col, elev. 5400 m.)	40B
18	Density of Pit II (Mt. Logan, A.I.N.A. Peak, elev. 5680 m.)	41A

<u>Figure</u>		<u>Page</u>
19	Isotope Profile of Pit II (Mt. Logan, A.I.N.A. Peak, elev. 5680 m.)	41A
20	Temperature of Pit II (Mt. Logan, A.I.N.A. Peak, elev. 5680 m.)	42A
21	The Snow-Core from the Logan Plateau (elev. 5400 m.)	42B
22	$\text{H}_2\text{O}^{18}/\text{H}_2\text{O}^{16}$ Composition of Fox Glacier in relation to Locations at other Latitudes (after SHARP, 1960)	45A
23	δO^{18} vs δD for Mt. Logan, Divide and Fox Glacier Samples	46A
24	Glacial Zones (after MÜLLER, 1962)	50A
25a)	Longitudinal Profile of Glacier Flow (after REID, 1896)	52A
25b)	Top View of Glacier Flow (after REID, 1896)	52A
25c)	Isotopic Variation of a Longitudinal Profile	52A
26	The Fox Glacier	56A
27	Snow Pit 36E8, Fox Glacier	57A
28a)	Snow Pit 32E8, Fox Glacier	59A
28b)	Snow Pit 28E4, Fox Glacier	59A
29	Snow Pit 36, Fox Glacier	60A
30a)	Snow Pit 24W2, Fox Glacier	61A
30b)	Snow Pit 28W4, Fox Glacier	61A
31a)	Firn Core at Stake 24 (29/7/68)	63A
31b)	Firn Core at Stake 24 (15/8/68)	63A
32	Isotopic Traverses of the Fox Glacier	64A
33	Uncorrected Longitudinal Profile	65A

<u>Figure</u>		<u>Page</u>
34	Corrected Longitudinal Profile	66A
35	Ice Core at Stake 7, Fox Glacier	66B
36	Ice Core at Stake 2, Fox Glacier	67A
37	Icefalls Traverses on Fox Glacier	67B
38	The Fox Glacier Icefall's Longitudinal Profile	67C
39	Longitudinal Profile, Peyto Glacier	75A
40	Raw Data Plot, Peyto Glacier	76A
41	5 th Degree Trend Surface, Peyto Glacier	77A
42	5 th Degree Residual Plot	77B
43	6 th Degree Trend Surface, Peyto Glacier	77C
44	6 th Degree Residual Plot	77D
45	7 th Degree Trend Surface, Peyto Glacier	77E
46	7 th Degree Residual Plot	77F
47	8 th Degree Trend Surface, Peyto Glacier	77G
48	8 th Degree Residual Plot	77H
49	Peyto Glacier: Concavity/Convexity (after YOUNG, 1970)	79A
50	Location of the Northern Ellesmere Island Snow-Pit	81A
51	Snow-Pit, 0-2.8 m., Northern Ellesmere Island	84A
52	Snow-Pit, 2.7-4.4 m., Northern Ellesmere Island	86A
53	Snow-Pit, 4.4-7.3 m., Northern Ellesmere Island	88A
54	Water Equivalent Profile of Northern Ellesmere Island Snow-Pit and Core	91A

<u>Figure</u>		<u>Page</u>
55	Autocorrelation Function of $\text{H}_2\text{O}^{18}/\text{H}_2\text{O}^{16}$ Profile of Snow-Pit and Core (W.E.)	91B
56	Power Spectra of the Isotope Profile of the Northern Ellesmere Island Snow-Pit (0-128 cm)	93A
57	Power Spectra of the Isotope Profile of the Northern Ellesmere Island Snow-Pit (0-256 cm)	93B
58	Power Spectra of the Isotope Profile of the Northern Ellesmere Island Snow-Pit (0-512 cm)	93C
59	Power Spectra of the Isotope Profile of the Northern Ellesmere Island Snow-Pit (441-956 cm)	93D
60	Power Spectra of the Isotope Profile of the Northern Ellesmere Island Snow-Pit (0-1024 cm)	93E
61	Temperatures at Upernivik, Greenland and Alert, N.W.T. (after HATTERSLEY-SMITH, 1963)	94A

ERRATUM

The official names of the Fox, Jackal and Hyena Glaciers have been chosen after the completion of this text. The glaciers' proper names are listed below (see page 48);

<u>Old</u>	<u>New</u>
Fox	Rusty
Jackal	Backe
Hyena	Trapridge

CROSSLEY D.J. and G.K.C. CLARKE (1970), Gravity Measurements on the "Fox Glacier", Yukon Territory, Canada, J. of Glac. 9, No. 57, pp. 363-374.

KRUMBEIN W.C. and F.A. GRAYBILL (1965), An Introduction to Statistical Models in Geology, McGraw-Hill, New York.

CHAPTER I

 $\text{H}_2\text{O}^{18}/\text{H}_2\text{O}^{16}$ ABUNDANCE VARIATIONSIntroduction

Isotopes of an element differ in their masses. Hence, many properties of substances are altered by isotopic composition and the abundances of isotopic species vary in nature.

The fact that specific gravity variations of waters were principally due to differences in the isotopic composition of these waters was pointed out by DOLE (1936). Development of mass spectrometry in the early 1950's made precise measurements and meaningful interpretations of these variations possible.

The most important isotopic components of water are H_2O^{16} , HDO and H_2O^{18} . Their average relative occurrences are approximately 997680 : 320 : 2000 ppm (parts per million) respectively (DANSGAARD, 1964). For the most part, the deuterium and O^{18} concentrations vary linearly, with the fractional separation for deuterium in meteoric waters being about 8 times that for O^{18} (CRAIG, 1961b; DANSGAARD, 1964).

Isotopic fractionation of water in nature may be attributed to a number of physical, chemical and biological processes. The most significant processes in the hydrological cycle are evaporation and condensation.

Fractionation in these cases is due to the different vapour pressures of H_2O^{16} , HDO and H_2O^{18} .

A number of laboratories have been engaged in measuring natural $\text{H}_2\text{O}^{18}/\text{H}_2\text{O}^{16}$ and HDO/ H_2O abundance variations for the purpose of elucidating processes in the hydrological cycle. Our laboratory has extended these investigations in mountainous regions of Canada. This thesis summarizes data from four such locations and evaluates the potential of isotopic abundance techniques in interpreting the associated climatological and glaciological phenomena.

Some of the observations of the fractionation of isotopic species of water in nature can be summarized as follows:

- a) Fresh waters are depleted in heavy isotopes in comparison to sea water (GILFILLAN, 1934).
- b) The isotopic composition of the oceans is fairly uniform except near regions of fresh water contributories (EPSTEIN and MAYEDA, 1953).
- c) The isotopic composition of precipitation varies with temperature, latitude and altitude.
- d) The deuterium and oxygen-18 concentrations in sea water, and the vapour above it, vary parallelly, except when kinetic effects, i.e. fast evaporation, upset this parallelism (DANSGAARD, 1964).

I.1 Designation of Isotopic Variation

Whereas absolute abundances of isotopic species are difficult to determine, the relative abundances of isotopes in two samples can be compared with very high precision. Hence a δ scale was defined as follows:

$$\delta O^{18} (\text{in } \text{‰}) = \left[\frac{(O^{18}/O^{16})_x}{(O^{18}/O^{16})_s} - 1 \right] \times 1000 \quad (1)$$

x = unknown sample

s = standard sample

The δD (deuterium) scale is defined as equation (1) with D instead of O^{18} and H (hydrogen) instead of O^{16} .

The reference standard for studies of water is S.M.O.W. (Standard Mean Ocean Water) i.e. by definition, δO^{18} and δD for S.M.O.W. equal zero. Other water standards were introduced by the National Bureau of Standards, U.S.A. and subsequently by the International Atomic Energy Agency, Vienna, Austria. These are;

	δD (S.M.O.W.)	δO^{18} (S.M.O.W.)
NBS - 1	- 47.6 ‰	- 7.94 ‰
NBS - 1A	-183.3 ‰	-24.33 ‰

These are working standards. When a sample has been measured in terms of a working standard, it can be expressed on the S.M.O.W. scale by using the following formula:

$$\delta_{\text{S.M.O.W.}} = \delta_{\text{SAMPLE}} + \delta_{\text{STANDARD}} + \delta_{\text{SAMPLE}} \times \delta_{\text{STANDARD}} \quad (2)$$

$\delta_{\text{S.M.O.W.}}$ — value of sample relative to S.M.O.W.

δ_{SAMPLE} — value of sample relative to secondary standard

δ_{STANDARD} — value of secondary standard relative to S.M.O.W.

I.2 Fractionation of Isotopic Species of Water

In order to understand these trends, it is necessary to consider the isotopic fractionation which accompanies evaporation and condensation. Evaporation can proceed so slowly that near equilibrium conditions occur at the boundary between the liquid and vapour phases. Then the isotopic fractionation factor between the liquid and vapour phases (α) becomes the ratio of the vapour pressures, p , of the light and heavy isotopic components:

$$\alpha = \frac{[\text{H}_2\text{O}^{18}/\text{H}_2\text{O}^{16}]_{\text{water}}}{[\text{H}_2\text{O}^{18}/\text{H}_2\text{O}^{16}]_{\text{vapour}}} = \frac{p_1}{p_2} \quad (3)$$

where subscripts 1 and 2 refer to the light and heavy isotopes respectively. At 20°C, $\alpha_{18} \approx 1.009$ and $\alpha_D \approx 1.08$ (MERLIVAT ET AL, 1963; REISENFELD and CHANG, 1963; ZHAVORONKOV ET AL, 1955; fig. 1a).

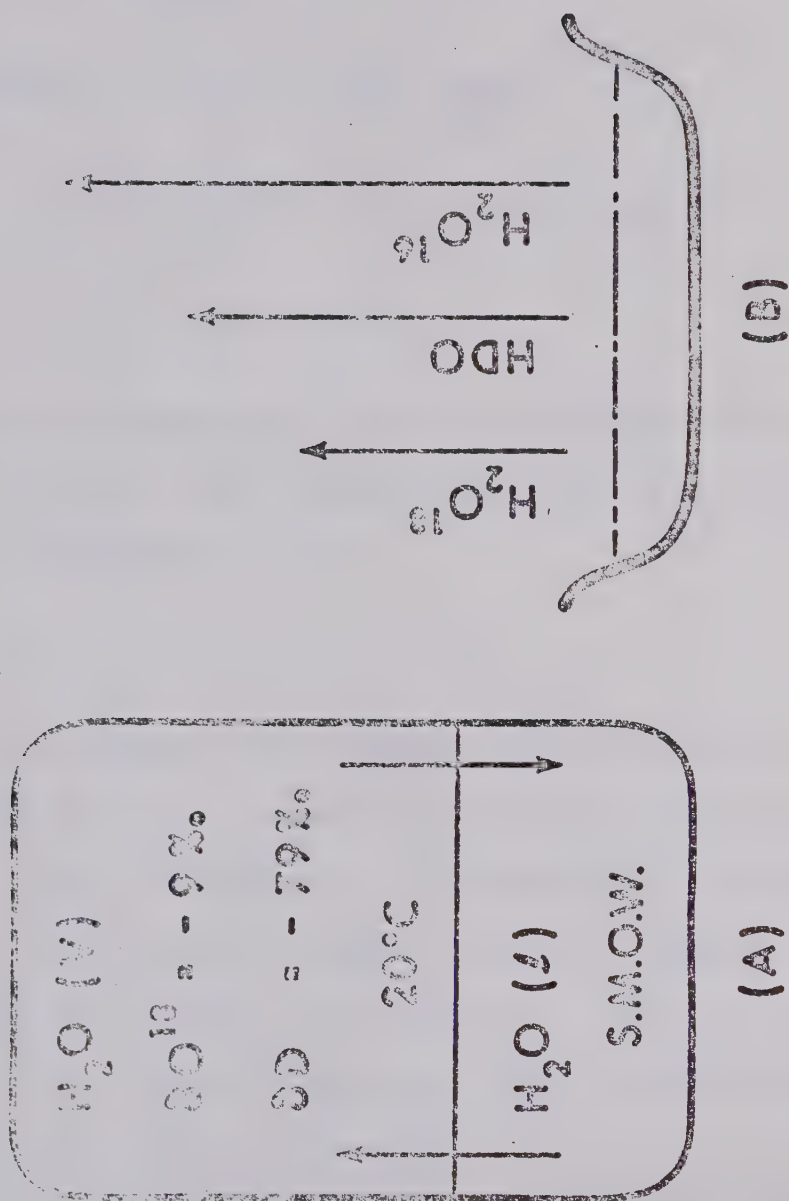


Fig. 1a) Evaporation Fractionation Fig. 1b) Reaction Rates

If the water is S.M.O.W. ($\delta_w = 0$) and letting,

$$Y = \left(\frac{H_2O^{18}}{H_2O^{16}} \right) \quad (4)$$

then the δO^{18} value for the vapour

$$\delta_v = \left(\frac{Y_v - Y_w}{Y_w} \right) \times 1000 \quad (\text{from equation 1}) \quad (5)$$

$$= \left(\frac{1}{\alpha} - 1 \right) \times 1000 . \quad (6)$$

Under equilibrium conditions, the water condensing at any moment has the same isotopic composition as the liquid already present i.e.

$$\delta_c = \delta_w = 0 \quad \text{or} \quad Y_c = Y_w . \quad (7)$$

In nature, such a system may not be effectively "closed" and thus become displaced from isotopic equilibrium. Then evaporation and condensation processes may be best described in terms of kinetic effects. Obvious examples are removal of condensate from the vapour phase in the form of snow and rapid evaporation of limited reservoirs under low humidity conditions.

Condensation as snow may be described as a Rayleigh process (DANSGAARD, 1964) whereby

$$\frac{Y_o}{Y_1} = F_v^{(\alpha-1)} \quad (8)$$

where

F_v = remaining fraction of vapour phase;

Y_1 = initial phase (water or vapour);

Y_o = final phase (vapour or condensation).

δ_c and δ_v will change as follows:

$$\delta_v = \left(\frac{1}{\alpha_o} F_v^{(\alpha_m - 1)} - 1 \right) \times 1000 \quad (9)$$

$$\delta_c = \left(\frac{\alpha}{\alpha_o} F_v^{(\alpha_m - 1)} - 1 \right) \times 1000 \quad (10)$$

from equations (1), (3) and (8).

α = instantaneous α

α_o = initial α

α_m = mean α for overall system

F_v = remaining fraction of vapour.

Therefore δ_c becomes more negative as F_v becomes smaller or the condensate becomes poorer in the heavier isotopes as the vapour reservoir loses its moisture (fig. 2).

In considering the net vaporization on the world's surface, the oceans can be approximated as an infinite source and the Rayleigh process does not apply. Also the equilibrium process described earlier does not strictly apply. This is due to the superposition of kinetic effects (wind, etc.) on the system. Such kinetic effects can be described qualitatively by the difference in evaporation rates R of the isotopic species;

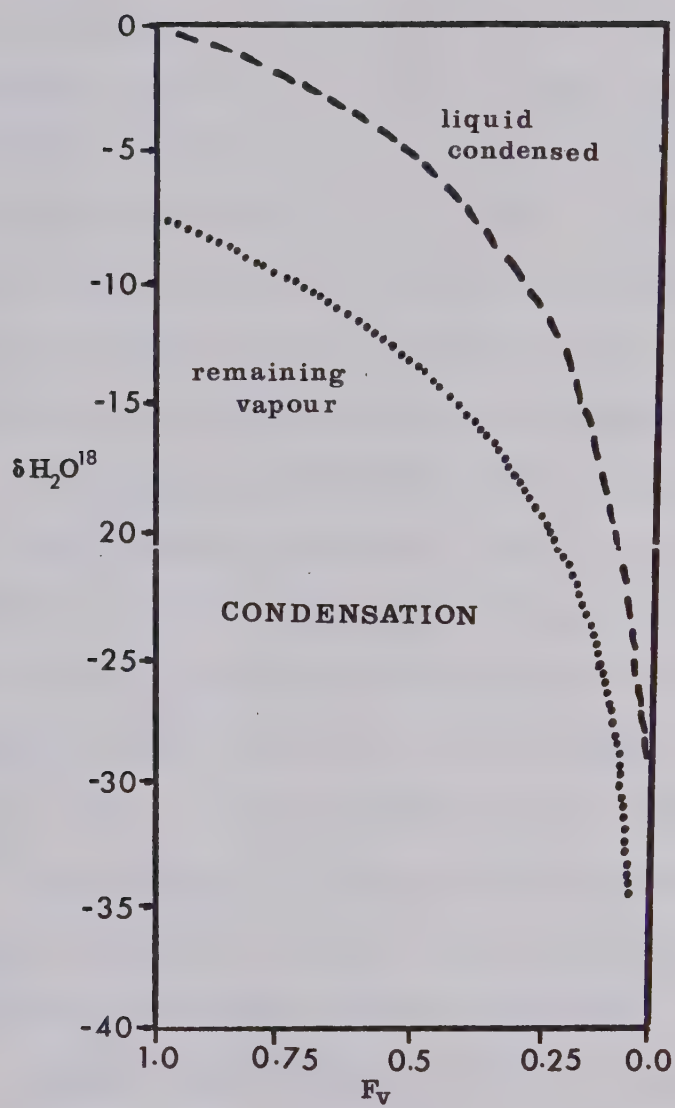


Fig. 2. Rayleigh Condensation Process

$R_{H_2O^{16}} > R_{HDO} > R_{H_2O^{18}}$ (fig. 1b). Under these conditions much higher isotope fractionations are realized.

DANSGAARD (1961) found α values up to 1.019, while under reduced pressure conditions, in a fume hood, BAKR (1971) obtained values of $\alpha = 1.03$. Since R_{HDO} and $R_{H_2O^{18}}$ are different, it has been suggested by DANSGAARD (1964) that by comparing δD and δO_{18} , it may be possible to measure the relative surplus of δD and therefore assess the kinetic history of the precipitation. He called this relative deuterium surplus the d-index.

Analysis by DANSGAARD (1964) shows that if evaporation from water of isotopic composition S.M.O.W. (the oceans) occurred under near equilibrium conditions and subsequent condensation at different temperatures also occurred under equilibrium conditions, then a plot of δD vs δO^{18} for the condensation would yield a slope of 8 and a d value of zero. Non-equilibrium evaporation from a limited amount of water reduces the d-index of the water as long as exchange does not dominate. Fast evaporation of a limited reservoir of S.M.O.W. yields a δD vs δO^{18} plot for the remaining water with a slope < 8 , i.e. the d-index becomes more and more negative as the water reservoir decreases in size. Similarly, if the arrows of figure 1(b) were reversed during condensation, then the d-index of a limited vapour supply should decrease during condensation. However, this process does not seem to be common in nature.

Non-equilibrium evaporation from an infinitely large and well mixed reservoir, an ocean, leaves the d of the water unchanged, and disregarding exchange, the d -index of the vapour is positive and increases with the rate of reaction. In this case, therefore, d is not only a non-equilibrium indicator, but also an index of rate of evaporation. So, assuming condensation to be an equilibrium process in nature, the averaged d of precipitation at a given locality may reflect the rate of evaporation in the source area.

Two attempts have been made to correlate the isotopic composition of terrestrial precipitation with the temperature of formation. DANSGAARD (1953) measured rain from a warmfront, in which the air was moist-adiabatically cooled from 12°C to -8°C . The observed change in δO^{18} over this temperature range was $8\text{ }^{\circ}/\text{oo}$. This was corrected to $11\text{ }^{\circ}/\text{oo}$ because of evaporation and exchange effects. In the low temperature range (-18°C to -30°C) PICCIOTTO ET AL (1960) found $8\text{ }^{\circ}/\text{oo}/^{\circ}\text{C}$ and $0.9\text{ }^{\circ}/\text{oo}/^{\circ}\text{C}$ for $\delta\text{D}/dt$ and $\delta\text{O}^{18}/dt$ in Antarctic snow. These values compare favourably with theoretical calculations of DANSGAARD (1964) at -20°C after an isobaric cooling from 20°C (vapour-ice equilibrium from 0°C). The mathematical derivation of $d\delta/dt$ is performed by taking the log of equation (9) and then differentiating

with respect to temperature. The results obtained were:

$$\frac{d\delta D}{dt} = 7.7 \text{ } ^\circ/\text{oo}/^\circ\text{C} \quad \frac{d\delta O^{18}}{dt} = 0.95 \text{ } ^\circ/\text{oo}/^\circ\text{C} \quad (11)$$

DANSGAARD (1964) also plotted the annual means of the O^{18} content in precipitation and the surface air temperature of North Atlantic coast stations and Greenland Ice Cap stations. Assuming the mean surface temperatures vary parallel to the mean condensation temperatures, $d\delta O^{18}/dt$ was $0.7 \text{ } ^\circ/\text{oo}/^\circ\text{C}$. This compared extremely well with DANSGAARD's (1964) calculation of $0.66 \text{ } ^\circ/\text{oo}/^\circ\text{C}$ in the temperature range, $0 < t < 10^\circ\text{C}$.

When δD is plotted against δO^{18} for precipitation at a large number of locations in the Northern Hemisphere, a line results which can be described by the following equation:

$$\delta D = (8.1 \pm 0.1) \delta O^{18} + (11.0 \pm 1.0) \text{ } ^\circ/\text{oo} \quad (12)$$

The slope of 8.1 is consistent with the theoretical ratio:

$$\frac{d\delta D/dt}{d\delta O^{18}/dt} = \frac{7.7 \text{ } ^\circ/\text{oo}/^\circ\text{C}}{0.95 \text{ } ^\circ/\text{oo}/^\circ\text{C}} \quad (\text{from equation 11})$$

Thus, the assumption that the condensation part of the water cycle, at high latitudes in nature, is a simple Rayleigh process starting at 20°C seems justified. The fact that the d-index in equation (12) is positive means

that there are minor kinetic isotope contributions during evaporation. It is not surprising that some locations throughout the world deviate from equation (12). One such location of interest to this report is Whitehorse, Yukon where $d\delta D/d\delta O^{18} = 5.5$. This is probably due to the fact that the precipitation is sparse and although the summer rain samples have higher δ -values, the d-index is lower than that of the winter δ -values. This suggests that non-equilibrium evaporation from the liquid precipitation probably accounts for the low slope (DANSGAARD, 1964).

During the preceding discussion, exchange between the falling precipitation and the vapour phase has been ignored. Exchange between snow and vapour should only affect the surface molecules and is therefore considered negligible. This is not true in the case of raindrops. Therefore interpretations of the isotopic composition of rain should consider the vapour content of the area.

I.3 Applications in Mountainous Regions

The logistical problem of supporting a research team in remote mountain regions usually restricts investigation of these regions to the summer. Remote stations are seldom used because of the cost and difficulty of operation and maintenance. This situation lends itself

to isotopic investigations since spring samples may provide a record of the previous winter provided that the isotopic trends are preserved. Indeed, sometimes in areas of no melting, meteorological data of centuries are preserved as an isotopic record. Therefore isotopic investigation seems a feasible and fairly inexpensive method to study certain aspects of mountainous regions.

a) Latitude Effects

Continental temperatures generally decrease with increasing latitude. As a greater temperature gradient between the source and the location of precipitation is realized, greater isotopic selectivity also occurs, showing up as a depletion of H_2O^{18} and HDO with increasing latitude. This trend has been used to identify the origin of icebergs (DANSGAARD, 1961) and also delineate fresh and seawater stratifications in an Arctic Lake (KROUSE, 1970).

b) Altitude Effects

These effects are due to the preferential loss of the heavier isotopic species at lower altitudes, and the fact that higher elevations usually have lower temperatures, i.e. air masses cool as they rise, causing Rayleigh condensation, which means lower δ -values, as the vapour reservoir becomes depleted, at higher

elevations. SHARP, ET AL (1960) found δO^{18} of snow on the Blue Glacier, Washington, to decrease with increasing altitude at the rate of 0.5‰ per 100 metres, while FRIEDMAN and SMITH (1970) found δD values for snow cores in the Sierra Nevadas to decrease 4‰ per 100 metres increase in altitude on the west side of the mountains. The altitude effect was obliterated on the east side of the range. Possible explanations are turbulence created as the air mass moved across the highly irregular Sierra Nevada crest and non-uniformities in the temperature profiles.

c) Preservation of Seasonal Isotopic Variations in Ice and Snow

Seasonal variations in the isotopic composition of precipitation arise mainly from the temperature dependence of α . The temperature gradients between the source and the precipitation area vary with season. Minimum δ -values are encountered in the winter and maxima in the summer or early fall.

Mixing of snow layers by high winds, especially in areas of sparse precipitation often obscures this seasonal dependence. This has been found especially true in Antarctica (EPSTEIN and SHARP, 1962). It is also possible that molecular diffusion may erase this

trend over a long period of time. In areas of moderate summer temperatures, the seasonal variations in snow may be partially or totally erased by homogenization processes such as downward percolation of meltwater.

However, records of seasonal variations have been recorded in the snow fields of a number of glaciers and ice caps (EPSTEIN and SHARP, 1959a; GONFIANTINI, ET AL, 1963; MACPHERSON and KROUSE, 1967).

DANSGAARD (1964) plotted the mean annual air temperature of 6 Greenland stations against the δ -values for the same periods and obtained the following relationships:

$$\begin{aligned}\delta O^{18} &= 0.69 t - 13.6 \text{ }^{\circ}/\text{oo} & (t \text{ in } ^{\circ}\text{C}) & (13) \\ \delta D &= 5.6 t - 100.0 \text{ }^{\circ}/\text{oo}\end{aligned}$$

It may be possible in simple circumstances to match monthly temperatures and δ -values to obtain equations for monthly temperatures. However, in areas such as Antarctica serious complications arise. Antarctica is surrounded by a relatively warm ocean, and a location on the ice cap may receive precipitation from various directions and from air masses with essentially different histories. Topographical as well as ablation factors also may upset the temperature- δ -value correlations (EPSTEIN and SHARP, 1962).

d) Paleoclimatology

Isotopic studies of deep cores from ice caps have recently been utilized to evaluate long term climatic changes over the past 100,000 years. DANSGAARD, ET AL (1969b) reported data from 1,600 samples of a 1,390 metre ice core from Camp Century, Greenland. He was able to identify, in the upper parts such well-known events as the warming trend in the 1920's and 1930's, the "Little Ice Ages" of the 17th and 18th centuries and the warm period between 550 and 1150 A.D. when the Vikings came to North America. At 10,000 years B.P., the H_2O^{18} content fell rapidly corresponding to the final stages of the Wisconsin ice age.

The Allerød and Boelling interstadials are also suggested in the lower core. EPSTEIN, ET AL (1970) have reported a similar, if less detailed, analysis from a core from the Antarctic Ice Sheet at Byrd Station. Synchronism between major climatic changes in Antarctica and the Northern Hemisphere was strongly indicated. Again the Wisconsin cold interval extended from approximately 75,000 to 10,000 years ago. However, as DANSGAARD (1969a) pointed out, due to the large amount of water removed from the hydrological cycle, you have to be careful in the interpretation of δO^{18} variations as paleoclimatic indicators. These considerations apply not only to glacier ice, but also oxygen isotope

determinations in carbonates of sea shells. The extents to which the isotopic composition of the oceans and the temperature fluctuated during the Wisconsin Ice Age have been subjects of much debate.

e) Glacier Flow

The snow that falls in the accumulation area of a glacier is affected by all of the fore-mentioned effects. Latitude normally affects only the average δ -value of the glacier. Altitude effects have a much more important role.

Since the majority of snow basins of glaciers have a fairly steep gradient, the δ -values of the snows decrease from the firn line (line between areas of total ablation and accumulation) to the top. Upon disappearing below the surface the snow transforms into glacier ice to reappear later below the firn line. Since the altitude effect places an isotopic label on the original snow, in principle, it should be possible to elucidate the origin of the ice and the mechanics of glacier flow. However, other parameters can hinder the application of this principle. Paleoclimatic variations may be greater than the altitude effect. Exchange may take place between meltwater and the exposed ice. One might sample superimposed ice rather than real glacier ice. Minor ablation might allow preferential evaporation of the lighter isotopic species, and

uneven ablation may expose deep layers of ice in some areas and not in others. Several workers have used O^{18}/O^{16} abundances to study glacier dynamics with some degree of success (EPSTEIN and SHARP, 1959a; SHARP, ET AL, 1960; MACPHERSON and KROUSE, 1967).

f) Projects of this Thesis

i) Icefield Ranges; St. Elias Mountains, Yukon.

Three areas in the St. Elias Mountains were sampled in the summer of 1968;

1) A snow pit at Divide camp, on the snow field of the Kaskawulsh and Hubbard glaciers was sampled to compare with the data of MACPHERSON (1965) and also to correlate with data collected on Mt. Logan.

2) Mt. Logan, the tallest mountain in Canada (6,100 m.), is a formation of six peaks and a central plateau. Joe Labelle and Jim Underwood brought back samples from two pits, at 5,250 m. and 5,520 m. These were analysed with the idea of determining whether it actually snowed at these altitudes (as opposed to mechanical lifting by the winds) and to see if seasonal variations were recognizable. Later, in cooperation with James Keeler (C.R.R.E.L., U.S. Army), a 16 metre firn core was also analysed.

3) The Fox Glacier was studied for two reasons. It had already been intensively studied by other geophysical means and isotopes would possibly help make a more

complete picture. Also the Fox was thought to be a surging glacier (one that advances in periodic surges, but otherwise remains quiescent) and no known isotopic work had been done on this particular type of glacier.

ii) Peyto Glacier, Alberta;

The Peyto Glacier is another Canadian glacier that has undergone geophysical investigations. This study was therefore done to add further information to that already available. Further, since the Peyto is a normal temperate glacier, it provides an interesting contrast to the Fox, which is a polar, and suspected surging glacier. The sampling of Peyto Glacier was done by a summer student, Robert Pajowski in 1969 under the supervision of Dr. R. Goodman, D.E.M.R.

iii) Northern Ellesmere Island;

In the summer of 1970, with G. Hattersley-Smith of D.R.B., a snow pit of 7 metres and a core which extended another 22 m. (total depth 29 m.) were sampled in an unexplored ice cap, of elevation 1800 m., northwest of Tanquary Fiord in Northern Ellesmere Island. The motives for this project were to:

- 1) assess the annual accumulation in an area where deep coring may be undertaken in the future;
- 2) compare classical stratigraphic and isotopic methods of identification in a zone of percolation facies.

CHAPTER II

EXPERIMENTAL PROCEDURES

II.1 Field Sampling

a) Snow Pits

This type of sampling is the most accurate of all the sampling techniques as the researcher is able to observe the snow, or firn in situ before making any measurements on it, whereas in core sampling, the fine stratigraphic detail is usually lost. When digging a snow pit, one wall is called the working wall. This wall should be shaded from the sun as much as possible and no snow piled on top of it. It is from this wall that all the data are taken. If sampling of the wall is not possible soon after it has been exposed, then the wall should be recut before sampling and data are taken. The pits are usually dug in a step fashion (see fig. 3) with the snow being thrown on the steps above, until this becomes impractical because of the depth. Then snow can be removed by bucket and tripod. A small board should be placed at the edge of the working wall to supply a base for the depth measurements. Density and temperatures were taken, using a snow kit designed by C.R.R.E.L. (U.S. Army) and now produced by Testlab of Chicago. The density was determined by carefully inserting 500 cc capacity stainless steel tubes into

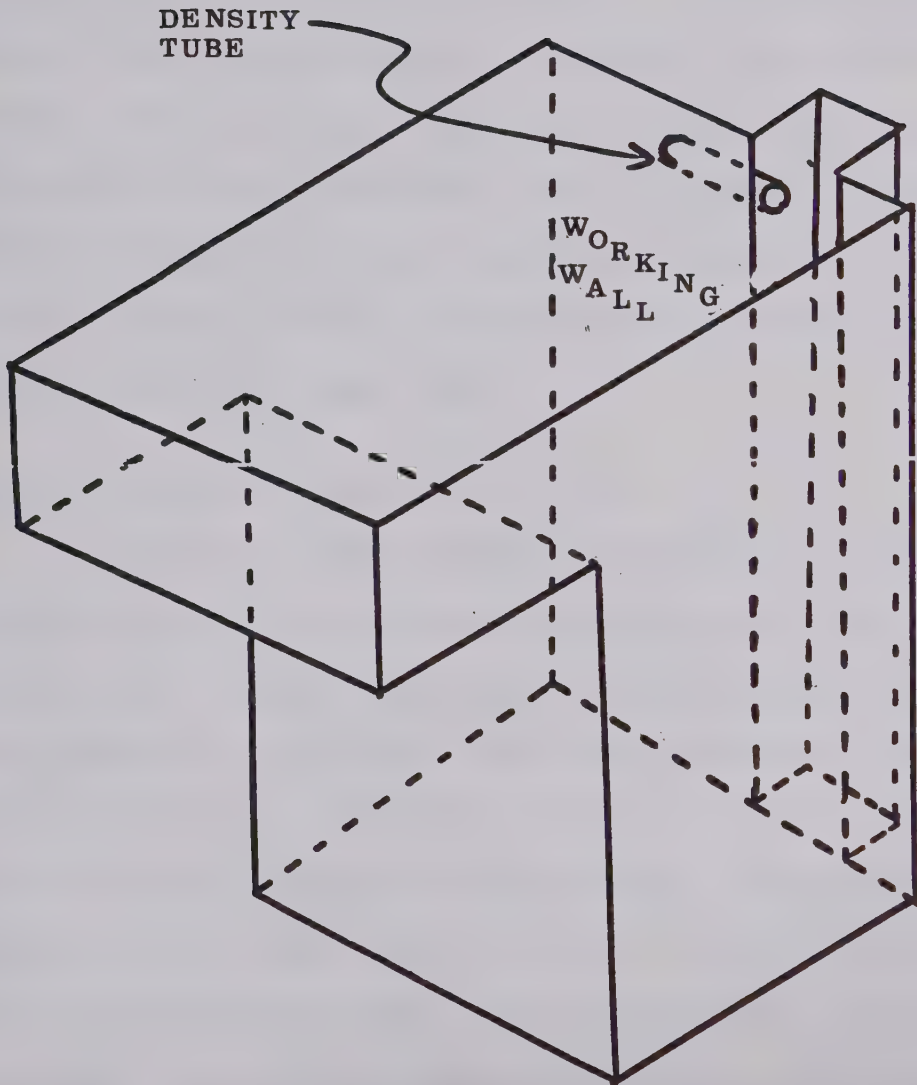


Fig. 3. An Ideal Snow-Pit

the snow, cutting them out with a snow knife, capping them and weighing the filled tubes on the tare spring scale. A notch in the working wall often facilitates removal of the density tubes. The snow was then transferred into plastic bottles which were tightly capped using parafilm as a sealer. Wide necked bottles were found to be the most convenient. The density measurements were usually taken horizontally (see fig. 3). Temperatures were measured with a bimetallic stainless steel thermometer, which was first zeroed in a slush bath. Grain size was judged with the aid of a graduated grid plate and a hand lens.

b) Snow and Ice Cores

A 3" ice coring auger developed by S.I.P.R.E. (later called C.R.R.E.L.) was used to retrieve all the cores in this work. A chain saw motor with a standard $\frac{1}{2}$ " chuck was adapted to the auger and used extensively while on the Fox Glacier. It proved invaluable while drilling ice cores and holes for survey poles, but its rotation speed was too high for firn cores. After the cores were retrieved they were cut into segments with a saw and bottled. Careful measurement had to be taken of depth since the core often became slightly compacted during the drilling, and retrieval was sometimes incomplete. Densities were measured by weighing certain lengths of

segments, 2" or 4", when the cores would hold together. Temperatures were taken by means of a thermocouple.

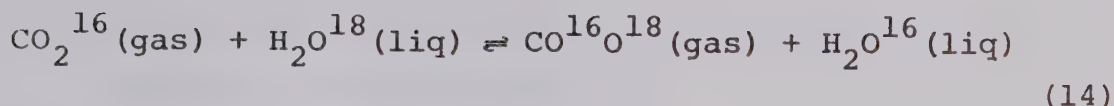
c) Surface Sampling

Sampling of hard ice below the firn line presented other problems. When working just below the firn line, it is very easy to sample superimposed ice rather than real glacier ice. This is also true of the ice under or near dirt layers, such as moraines. Exchange of molecules between meltwater and glacier ice also must be avoided. Therefore sampling should be done on local high points and the first 10 cm or so of ice scraped away. This should also take care of the problem of ice saturated with meltwater. SHARP, ET AL (1960) found systematic variations in the O^{18} content of clear and bubbly ice, therefore only one type of ice, in this case bubbly ice, was sampled to avoid introducing more variables.

II.2 Sample Preparation for Isotopic Analysis

a) Theory

Water poses problems when introduced into the mass spectrometer for analysis. However, oxygen isotopic abundances can be determined by analyzing carbon dioxide equilibrated with the water. The overall exchange reaction can be written as:



For less precise requirements, it is not necessary to know the fractionation factor, α_1 , for the exchange where:

$$\alpha_1 = \frac{[\text{O}^{18}/\text{O}^{16}]_{\text{CO}_2}}{[\text{O}^{18}/\text{O}^{16}]_{\text{H}_2\text{O}}} \quad (15)$$

If water is by far the dominant component of the system then

$$\delta\text{O}^{18}_{\text{system}} \approx \delta\text{O}^{18}_{\text{water}} \quad (16)$$

Since we are interested in relative isotopic abundances of water samples, the $\Delta\delta\text{O}^{18}$ of any two water sample is close to the $\Delta\delta\text{O}^{18}$ value of two CO_2 samples that have been equilibrated with these waters at the same temperature (i.e. α_1 is the same for both equilibrations).

However, for more precise determinations, the amount of CO_2 used for equilibration must be considered particularly if its isotopic composition differs significantly from the water. Corrections require a reasonable evaluation of α_1 . CRAIG (1957) derived the following correction formula:

$$\delta_{\text{corrected}} = \delta_{\text{measured}} \frac{(\rho + \alpha_1)}{\rho} - \frac{\alpha_1}{\rho} (\delta\text{O}^{18}) (\text{tank CO}_2) \quad (17)$$

$$\alpha_1 = 1.039 \text{ at } 25^\circ\text{C}$$

ρ = gram atoms of oxygen in water sample/gram atoms of oxygen in introduced CO_2 .

In our case, the correction would be as follows:

$$\delta^{18}\text{O}_{\text{Tank CO}_2} \approx +20.0 \pm 1.0 \text{ } ^\circ/\text{oo SMOW} .$$

Equilibration conditions were 25 mls. of water and 250 mls. of CO_2 at 37 mm pressure and 25°C . This gave

$$\rho = 2.04 \times 10^2 .$$

Substituting into equation (17)

$$\delta_{\text{final}} = 1.005 \delta_{\text{measured}} - .09 \text{ } ^\circ/\text{oo} \quad (18)$$

This correction is smaller than our reproducibility ($\pm 0.2 \text{ } ^\circ/\text{oo}$). Other corrections, such as cross-talk in the magnetic valve system on the mass spectrometer, leak differences and fractionations within the standard's reservoir with time were applied when necessary.

b) Equilibration of H_2O with CO_2

The method of equilibrating water with CO_2 , used in this study, is outlined below:

- i) The water samples were pipetted (25 mls.) into the equilibration flasks, twelve at a time. A drop of nitric acid was added as a catalyst for rapid equilibration.

- ii) The flasks were attached to the vacuum line and the water samples frozen with liquid air. They were then pumped out with a fore pump.
- iii) The flasks were then closed off and the samples melted to release trapped gas and then refrozen with a dry-ice-ethanol bath.
- iv) The samples were then pumped out with a mercury diffusion pump for about 5 minutes.
- v) Dry, commercial CO₂ was then introduced into the flasks. 36 mm was found to be sufficient pressure.
- vi) Equilibration was carried out in a temperature controlled bath, set at 25.6°C. The entire flask containing the CO₂ was below the bath surface. The flasks were left in the bath for between 24-36 hours. Shaking was found to reduce the equilibration time.
- vii) After equilibration, the flasks were again attached to the equilibration line and the water samples frozen in a dry-ice-ethanol bath.
- viii) The CO₂ gas was then transferred from each flask through two dry-ice-ethanol traps (to remove any water vapour) into a breakseal cooled by liquid air.
- iv) The breakseal was then sealed and labelled, ready for the mass spectrometer.

In every set of twelve, one sub-standard was equilibrated to check equilibration reproducibility (± 0.2 ‰), and also to provide a check for the standard used on the mass spectrometer. These standards were usually tank CO₂ or large amounts of CO₂ which had been equilibrated with water standards. They were stored in large bulbs on the introduction line of the mass spectrometer. The standards used in this study were:

	δO^{18} (‰)
FX1-SST (Fox Glacier Meltwater)	-24.5
SC-1 (Lecture Bottle of CO ₂)	-21.9
SC-2 (Large cylinder of CO ₂)	-19.3
SC-3 (Large cylinder of CO ₂)	-19.3
HS-8 (Yelverton Glacier Meltwater)	-33.2

These standards were corrected to SMOW by comparisons with, SMOW, NBS-1 NBS-1A and standards of other laboratories. Use of the standard closer to the expected value of the sample reduced instrument errors.

Two types of equilibration flasks were used. The one in figure 4 was used for most of this study while the one in figure 5 was designed here and built by Ace Glass. The advantages of the latter design are the lack of vacuum grease and a reduction in the number of joints. One disadvantage was that over zealous tightening of the teflon stop-cock caused the glass thread to crumble. With care, however, this system is easier to handle.

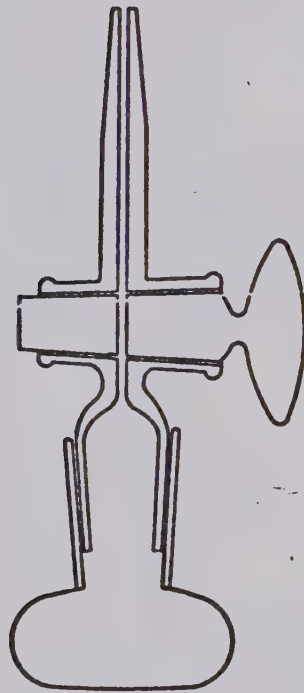


Fig. 4. Standard Equilibration Flask

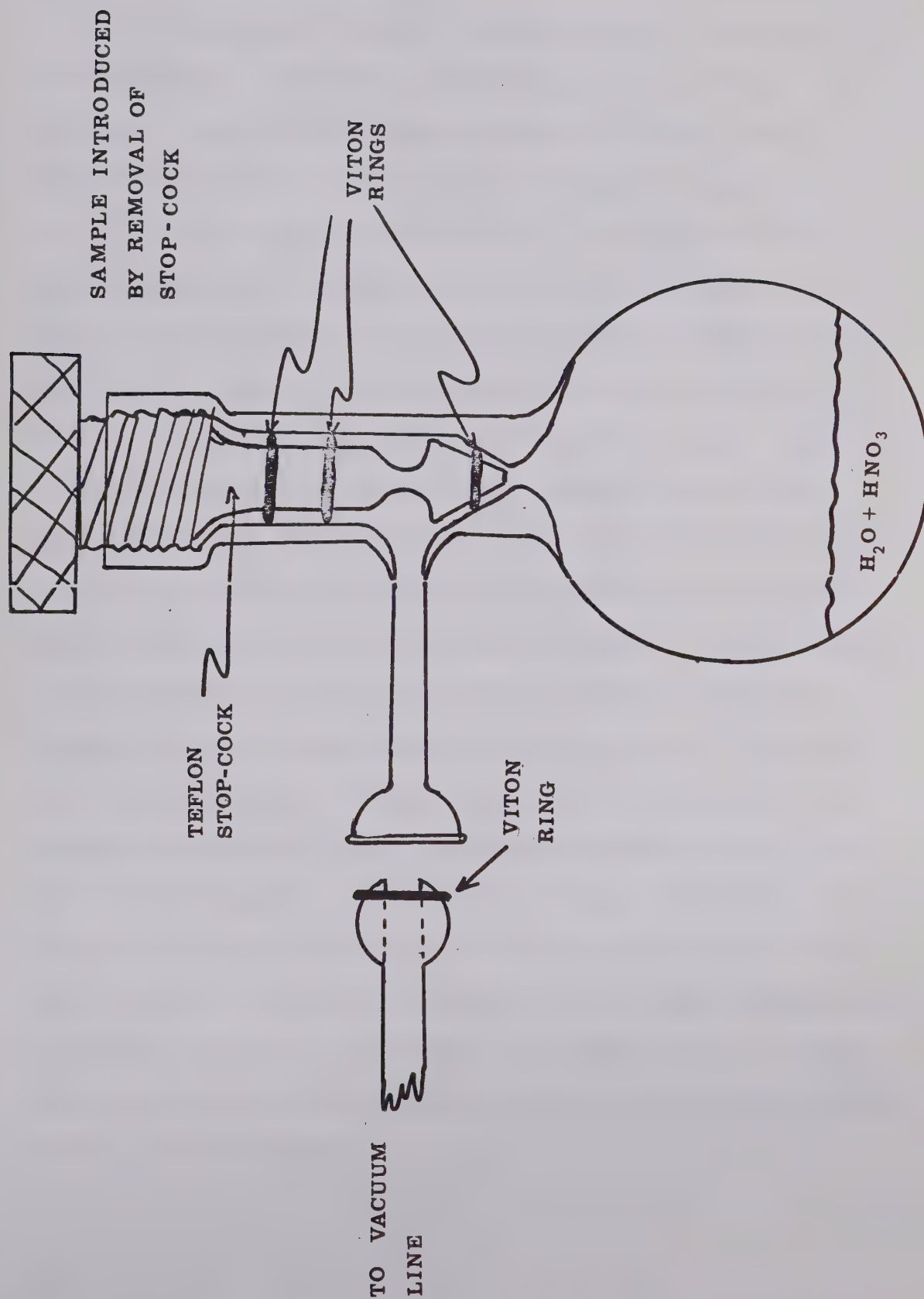


Fig. 5. New Equilibration Flask

II.3 Mass Spectrometry

A 90 degree, 12 inch radius magnetic analyzer Nier-McKinney type mass spectrometer was used for the analysis (NIER, 1947; MCKINNEY, ET AL, 1950). The $\text{H}_2\text{O}^{18}/\text{H}_2\text{O}^{16}$ ratio is measured by comparing mass 46 ($\text{C}^{12}\text{O}^{16}\text{O}^{18}$) to mass 44 ($\text{C}^{12}\text{O}^{16}\text{O}^{16}$). The gases were introduced into the machine through small leaks to reduce the pressure. The back pressure on these leaks was kept constant by adjustment of the mercury level in the gas reservoirs in the introduction line. By a set of 4 magnetic values the standard and unknown gas samples could be let into the machine alternately. The CO_2 was then ionized and accelerated by a potential difference of 4kV into the magnetic field. Ion currents corresponding to masses 44 and 46 were collected in Faraday cups and amplified by a pair of Cary vibrating reed electrometers. The pressures of the standard and unknown samples and peak shape were monitored by a two pen chart recorder. The output voltages from the V.R.E.'s were converted to frequencies and their ratios printed using Hewlett-Packard equipment as described by McCULLOUGH and KROUSE (1965). Later this was replaced by a Fluke Digital Voltmeter with ratio option, which was interfaced with a PDP-8 computer.

The digitizing interval for the Fluke equipment was 18 m sec compared to 1 sec with the Hewlett-Packard integrating voltmeter. The faster response time coupled with the ability of the computer to handle larger amounts of data increased the precision significantly. A sample of the computer output is shown in figure 6. $INTIME = 2^{**}7$ means that each value in a sub-set is the average of 2^7 readings of the Fluke (this number was 10 readings when Hewlett-Packard equipment was used). $GMTIME = 2^{**}2$ means there were 2^2 sub-sets of 2^7 intervals averaged to give the final ratio of ion currents, 46/44, in both the s (standard) or x (unknown) case. The final ratio of x/s was then calculated by taking the average value of the first two s ratios and dividing this into the first x value. Then the average value of the first two x ratios was divided by the second value of the s ratio and so on for the eight s and x ratios. This gave six values of x/s which were then averaged and the standard deviation calculated. A delete clause enabled deletion of any of the x/s ratios if it was desirable. Also 3 more sets could be taken. In each of these cases the final x/s ratio and the standard deviation were recalculated. A standard deviation of under .00020 was considered acceptable but generally one of under .00010 was achieved. This programme was written by R. Hunt, University of Alberta.

TEST

INTIME=2**7

GMTIME=2**2

FIRST SET MUST BE S !

THIS SET IS S

00.43017 00.43022 00.43026 00.43034

00.43025 S

THIS SET IS X

00.43043 00.43049 00.43034 00.43045

00.43043 X

THIS SET IS S

00.43057 00.43045 00.43052 00.43054

00.43052 S

THIS SET IS X

00.43067 00.43056 00.43067 00.43076

00.43067 X

THIS SET IS S

00.43075 00.43081 00.43087 00.43082

00.43081 S

THIS SET IS X

00.43085 00.43099 00.43103 00.43103

00.43098 X

THIS SET IS S

00.43107 00.43117 00.43113 00.43114

00.43113 S

THIS SET IS X

00.43123 00.43134 00.43127 00.43132

00.43129 X

01.00010 01.00007 01.00001 01.00003 01.00002 01.00001

MEAN RATIO 01.00004

STD DEV IS 00.00004

TYPE Y IF DEV SATISFACTORY? Y

Fig. 6. P.D.P.-8 Output

CHAPTER III

ICEFIELD RANGES: ST. ELIAS MOUNTAINS, YUKON

III.1 Introduction

The St. Elias Mountains form a major element of the Pacific mountain systems of the North American cordillera between latitudes 59°N and 62°N and longitudes 137°W and 142°W . Rising as a high barrier between the Pacific Ocean and the continental interior, they comprise a number of roughly parallel ranges that form a shallow arc through nearly 300 miles. In width, they span a distance of more than 100 miles between the Gulf of Alaska and the Yukon plateau. The topography is that of a high alpine region and its major valleys are largely submerged beneath the most extensive mantle of snow and ice in continental North America (see fig. 7).

This mountain belt is characterized by a wet-cold climate on the slopes that fringe the Gulf of Alaska, and by a dry-cold, even semi-arid climate in the continental interior. Records at Yakutat, Alaska, on the Pacific coast show that an annual precipitation of 125 inches is common there whereas, at Kluane, 110 miles away at the foot of the eastern scarp of the mountains, precipitation does not average much more than 15 inches per year.

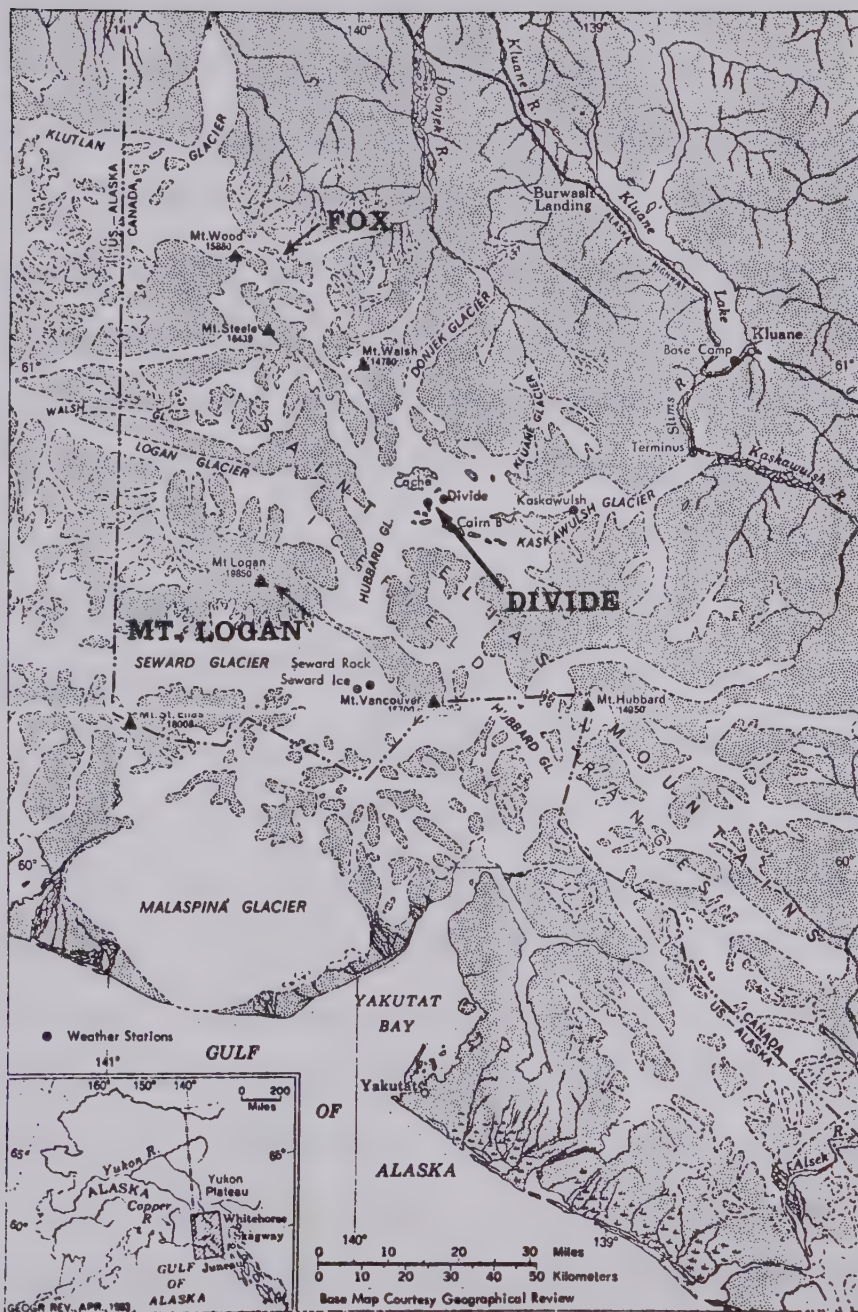


Fig. 7. St. Elias Mountains (Mt. Logans, Divide, Fox Glacier, after MARCUS, 1965).

Logistical support for the research camps was provided from the base camp at the south end of Kluane Lake, mile 1054 on the Alaska Highway. Food and personnel were flown in by either a Helio Courier or helicopter from the base camp. In the case of Fox Camp it was necessary to air-drop the rations because of its location. Daily radio contact was maintained with the base camp. The three locations of this study, Divide, Fox and Mt. Logan are indicated in figure 7

III.2 Divide

a) Introduction

In mid-July of 1968, a 5.4 m deep snow-pit was dug at the Divide (elev. 2640 m) camp. Divide is the snow accumulation area for the Hubbard and Kaskawulsh Glaciers (see fig. 7). This area was the first to be sampled, as a helicopter could not be reserved to reach the Fox Glacier until late July. Transportation to the camp was achieved in the A.I.N.A. Helio Courier, piloted by Phil Upton.

Divide is surrounded on all sides by mountain peaks with the major glacial valleys, the Kaskawulsh and Hubbard, leading off to the south and east. The major topographic feature is Mt. Logan, elevation 6100 m, which lies to the southwest of Divide.

b) Climatology

Divide, at 2640 m, is well above the climatological freezing level. Summer temperatures average in the high 20's ($^{\circ}\text{C}$) and vary about 15° diurnally. Relative humidities are in the mid 80's. No winter meteorological data has been taken in this area.

Winds are low, averaging about 5.0 kn with westerlies being predominant. Southwest winds are generally the strongest except when cyclonic passages bring strong easterlies. Strong winds tend to be cold, while light winds are often accompanied by warm temperatures and clear skies. Southerlies tend to be warm and moist. Precipitation accompanies easterly, cyclonically induced winds, while westerlies drop the least snow.

At Divide there seems to be a close relationship between low pressure, cloud cover and wind maxima, and precipitation. Similarly, high pressure is followed by low winds and small cloud amounts. Thus, summer weather at Divide, despite the topographic relief, seems to follow normal synoptic behaviour.

TAYLOR-BARGE (1969) suggested that there is a climatological divide zone usually located just east of Divide camp, but this could oscillate east or west, depending on circulation patterns. The divide would not take the form of a blockage of air mass and frontal systems, but instead, would make a complex modification

of these systems and their surface effects. The effectiveness of this divide should disappear about 3,000 m. This is only 400 m above Divide.

This divide was not always found to give marine weather on the west slopes and continental on the east. To the east of the mountain barrier, relatively uncommon easterly flows produced considerable cloud precipitation and general cooling (effects normally associated with the marine slopes during a cyclonic passage). There was evidence of a föhn or chinook effect on the marine slopes. Therefore, while Divide weather would usually be that of the synoptic situation, it might experience a change from a marine to a continental weather pattern.

TAYLOR-BARGE (1969) also showed that Divide lay in the precipitation shadow of Mt. Logan (fig. 8). Seward Glacier is south of Mt. Logan and therefore would not be affected by it (fig. 7). Divide and Kaskawulsh Glaciers on the other hand lie directly west of Mt. Logan. The ideal profiles were calculated using the same method as WALKER (1961).

c) Data

i) Temperatures:

Temperature readings were taken, from a freshly cut wall, every 10 cm. The average temperature was -0.3°C down to a depth of 370 cm (fig. 9). From 370 cm to 490 cm

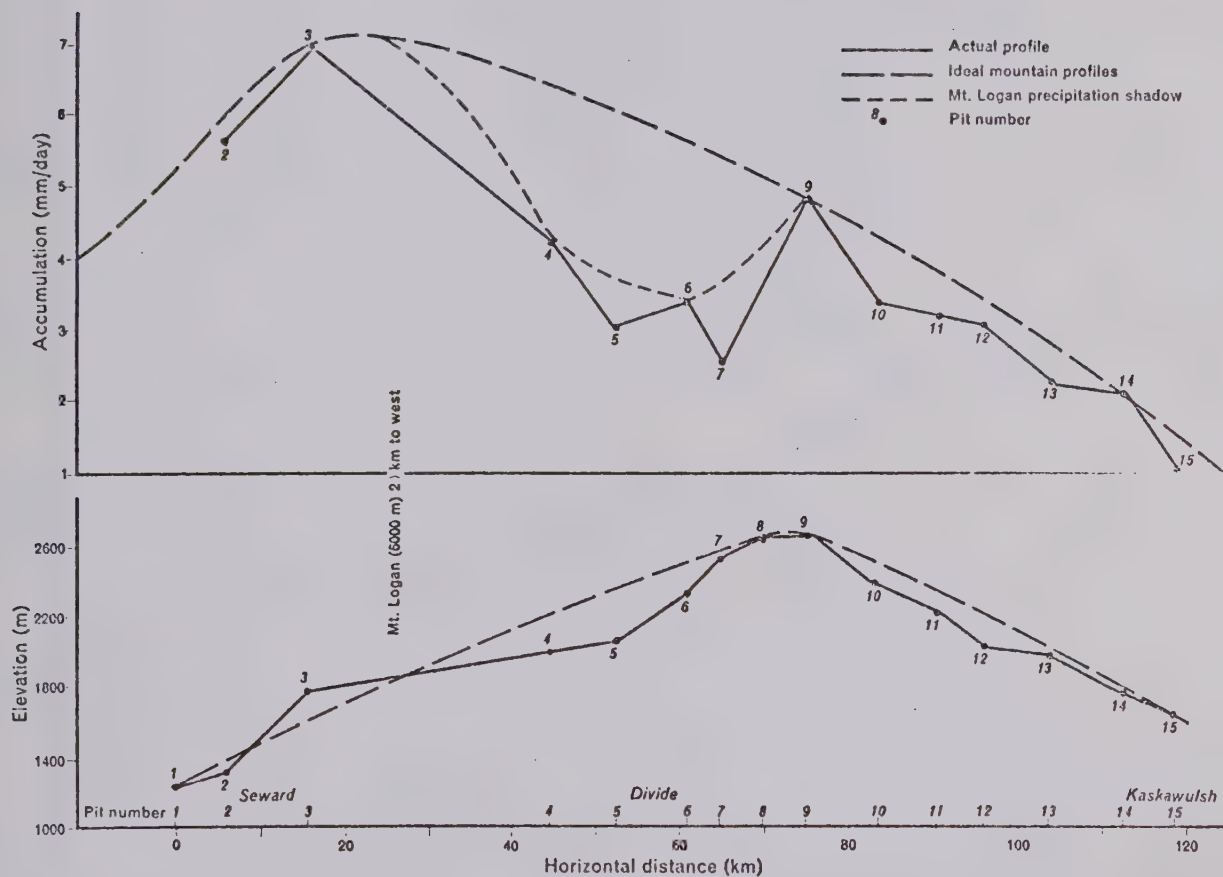


Fig. 8. Rain Shadow of Mt. Logan
(after TAYLOR-BARGE, 1969).

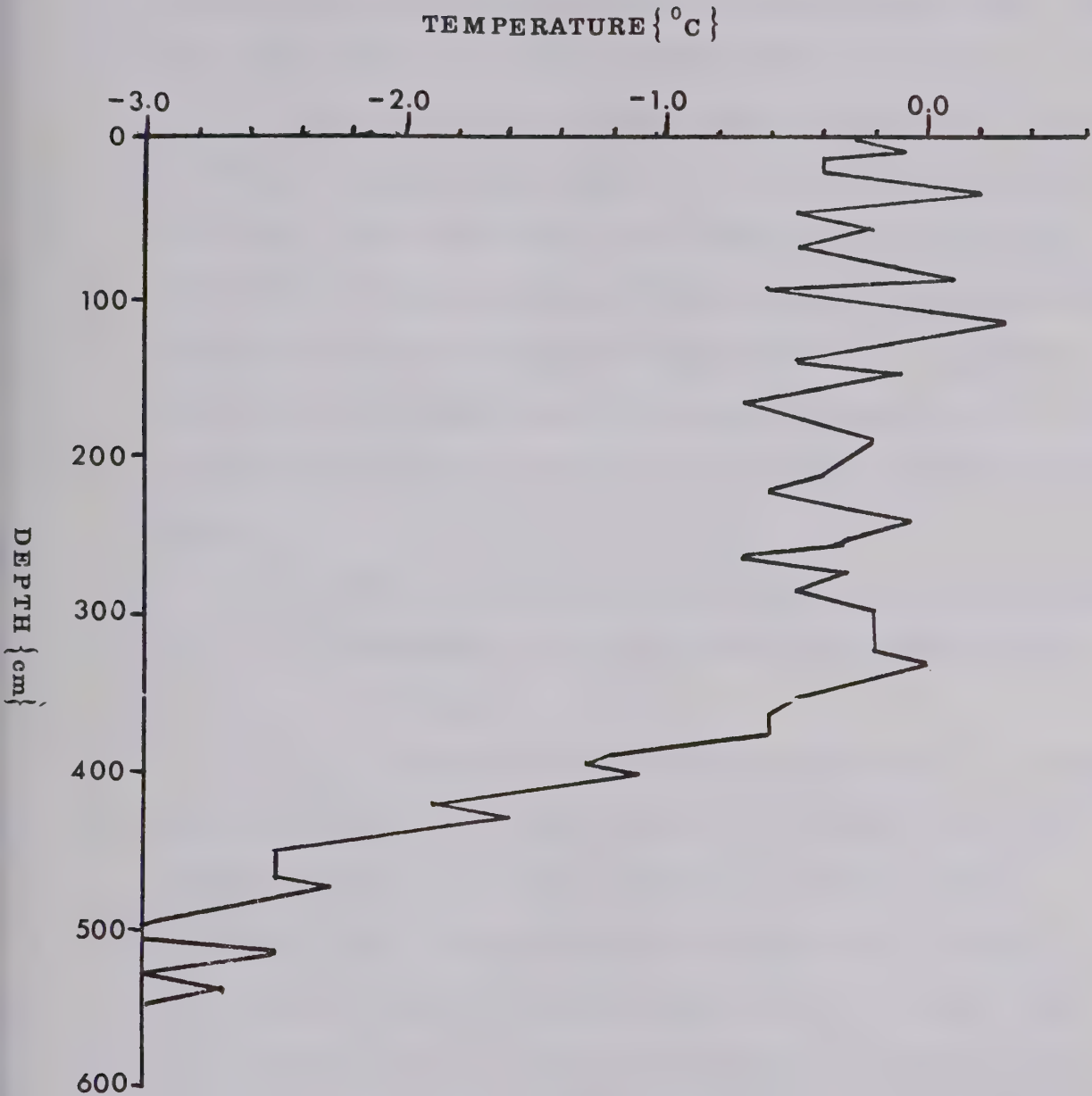


Fig. 9. Temperature Profile of Divide Pit

there was a steep temperature gradient which shows signs of stabilizing at -2.8°C between 490 to 540 cm.

For reasons that follow (density and δO^{18} determinations) the previous summer level, 1967, was placed at 360 cm. This means that the warming by mid June had removed all indications of temperatures to be identified with the previous winter's accumulation. Supposedly, this warming effect would penetrate deeper as the melt season progressed. The reasons for this warming effect are:

- 1) latent heat released by refreezing of meltwater;
- 2) penetration of heat from the warmer summer radiation.

On a basis of snow density, temperature, hardness, and stratigraphy, a snow cover is divided into four facies which reflect the variation of melt season intensity and duration with elevation on a glacier. The ablation facies which occurs below the firn line is characterized by complete removal of snow of the current budget year. The wetted facies extends from the firn line to the saturation line, located at the intersection of the 0°C isotherm with the top of the previous annual layer; all the snow in this facies is warmed to the melting point and becomes wetted. The density of this snow in the upper 5 m is usually

considered to be greater than 0.5 gm/cm^3 . In the percolation facies, only the top part of the annual increment of snow is wetted and warmed to 0°C . According to BENSON (1962), the density should be between 0.43 and 0.39 gm/cm^3 . The upper limit of the percolation facies is the dry snow line, located where the -5°C isotherm intersects the snow surface at the peak of the melt season. The dry-snow facies should have a density of less than $.37 \text{ gm/cm}^3$. The temperature profile of figure 9 would indicate that this pit is in an area of percolation facies. Observations by other workers (WAGNER, 1969; GREW and MELLOR, 1969) agree with this conclusion.

ii) Density:

The density measurements were taken with the C.R.R.E.L. designed equipment mentioned in II.1. Horizontal and vertical sampling was done. Vertical, i.e. putting the sample tube in from above was used for all of the pit. Horizontal, i.e. horizontal placement of the density tubes in the working wall, was used for a more detailed density profile of the transition to the previous summer layer.

The average density is $.478 \text{ gm/cm}^3$. This is heavier than expected for percolation facies ($0.43 - 0.39 \text{ gm/cm}^3$) but it is similar to the densities found by WAGNER (1969).

Wagner pointed out that although the difference in amounts of melt above and below the saturation line (the line between wetted and percolation facies) may produce groups of densities as stated in III.2, c), i), a definite gap or break between the groups is not necessary, i.e. the saturation line may be a zone of gradational density changes. Thus, density measurements on valley glaciers and their accumulation areas, i.e. Divide, may not show groups of densities, such as the ones found in Greenland (BENSON, 1962), due to the lack of range in elevation and physical size of the facies zone, i.e. the transition zones become significant in size when compared to the actual facies zone.

The density at the surface of the pit is low, with a sharp increase of density to a local maximum at 20- 40 cm (fig. 10). This density gradient was attributed to meltwater migration. Density usually remains low at the surface, for low body stress limits mechanical compaction, and grain growth reduces capillary retention of meltwater, thus allowing it to drain to lower layers.

Ice lenses were found at 60, 160, and 245 cm. It seems unlikely that direct solar radiation alone would cause melting at a sufficient rate to form these lenses, as the daytime heating periods are offset with nightly cooling periods. It seems more likely these lenses

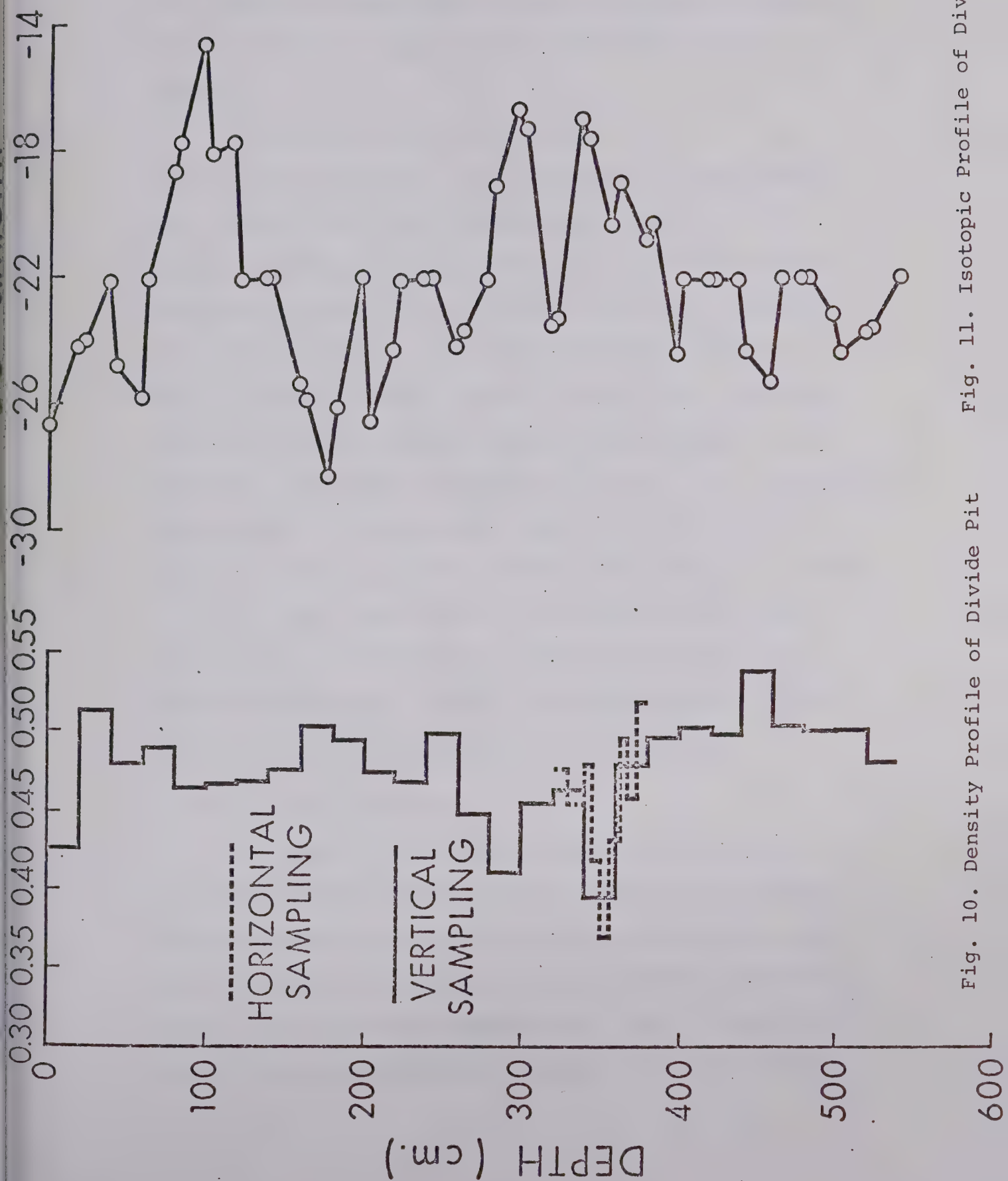


Fig. 10. Density Profile of Divide Pit

Fig. 11. Isotopic Profile of Divide Pit

were formed by sustained convective heating during warm spells of several days duration or perhaps from rain-water.

The two light density anomalies at 280 cm and 356 cm are depth hoar. This is formed in the Autumn when vapour, due to the latent heat released by re-freezing summer meltwater, contacts the cooler Autumn snows and freezes, forming a layer of large, loosely-packed snow crystals. The two anomalies indicate a sort of "Indian Summer" at 280-300 cm, with the cold spell from 300-340 cm and the end of the summer near to 356 cm. The heavy density at 440-460 cm is probably due to small, closely-packed firn crystals from the winter of 1966-67. Wind packing could also be a cause.

The small variation in the density shows that considerable homogenization has occurred due to percolating meltwaters, however little mechanical compaction seems to have occurred in the snow-pit.

iii) Oxygen Isotopes:

The oxygen isotope profile of the snow-pit is quite complicated. The classical profile of negative values corresponding to winter precipitation and more positive ones for the summer precipitation can be seen, if the first 60 cm are ignored (fig. 11). A positive peak at 350 cm corresponds closely to the end of the

melt season as suggested by the corresponding light density anomaly. Another positive peak at 300 cm corresponds to the density anomaly at 290-300 cm, attributed to an "Indian Summer".

Below 360 cm, there is evidence of another negative peak, representing the winter of 1966-67. However, due to homogenization, the spread of the δ -values is much less than in the 1967-68 samples.

Still ignoring the first 60 cm, one is able to compare these results favourably with those of a pit of MACPHERSON and KROUSE (1967), which was dug on June 30, 1963 near Divide camp (fig. 12). The Macpherson pit has a smaller range of δ -values and a slightly more negative average δ -value. This indicates that while the 1962-63 average temperature was colder than 1967-68, the winter minimum and summer maximum temperatures were greater in 1967-68. The relative positions of the minimum δ -values suggest 1962-63 had more snow in the spring than fall or early winter while equal amounts of snow fell after, and before the δ -minimum in 1967-68. This was probably due to snow caused by the warming spell around 270-300 cm. The density of the Macpherson pit is less uniform since it was sampled earlier in the melt season. This may also have been true of the δ -values if his pit had been sampled in more detail. Macpherson's

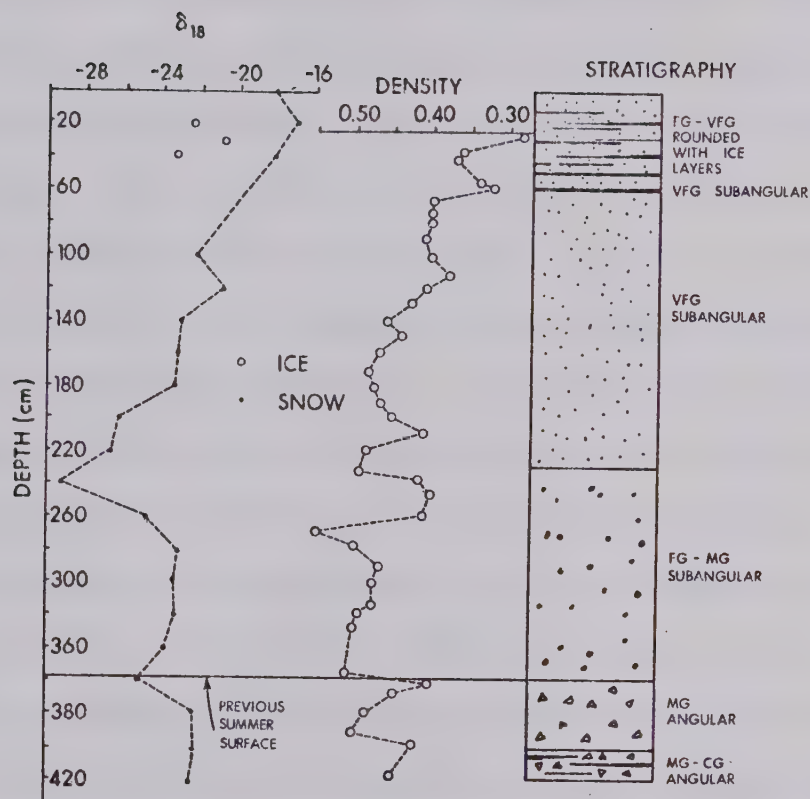


Fig. 12. Pit 1 of MACPHERSON and KROUSE, 1967
(June 30, 1963, alt. 8396 ft.).

data points between 20 and 40, attributed to ice layers, are similar in their δ -values to the snow of the present study between 0 and 60 cm. Unfortunately, samples of ice layers were not collected in the present study.

The relatively negative δ -values from 0-60 cm, (more positive δ -values would be expected from spring and summer snowfall) allow some interesting conjectures not alluded to in density, temperature or stratigraphic observations. As pointed out in III.2, b), Divide is an area of complex weather patterns, as it is located near or in a zone of a climatological divide between continental and marine weather. TAYLOR-BARGE (1969) has suggested that the oscillation of this climatological divide could place Divide in either of the weather patterns, marine or continental, or in the zone of change. Also Divide (fig. 8) lies in the rain shadow of Mt. Logan. FRIEDMAN and SMITH (1970) analysed the deuterium content of snow cores of several transverse of the Sierra Nevada divide (fig. 13). The altitude relationship was particularly well defined west of the divide, but was not well defined east of it. However, samples from east of the divide tended to be depleted by about 10 to 15 per mil relative to samples collected at the same elevation west of the crest. Therefore, if the climatological divide moved to the west of the Divide pit in the spring and early summer one would expect more negative δ -values as found by Friedman and Smith.

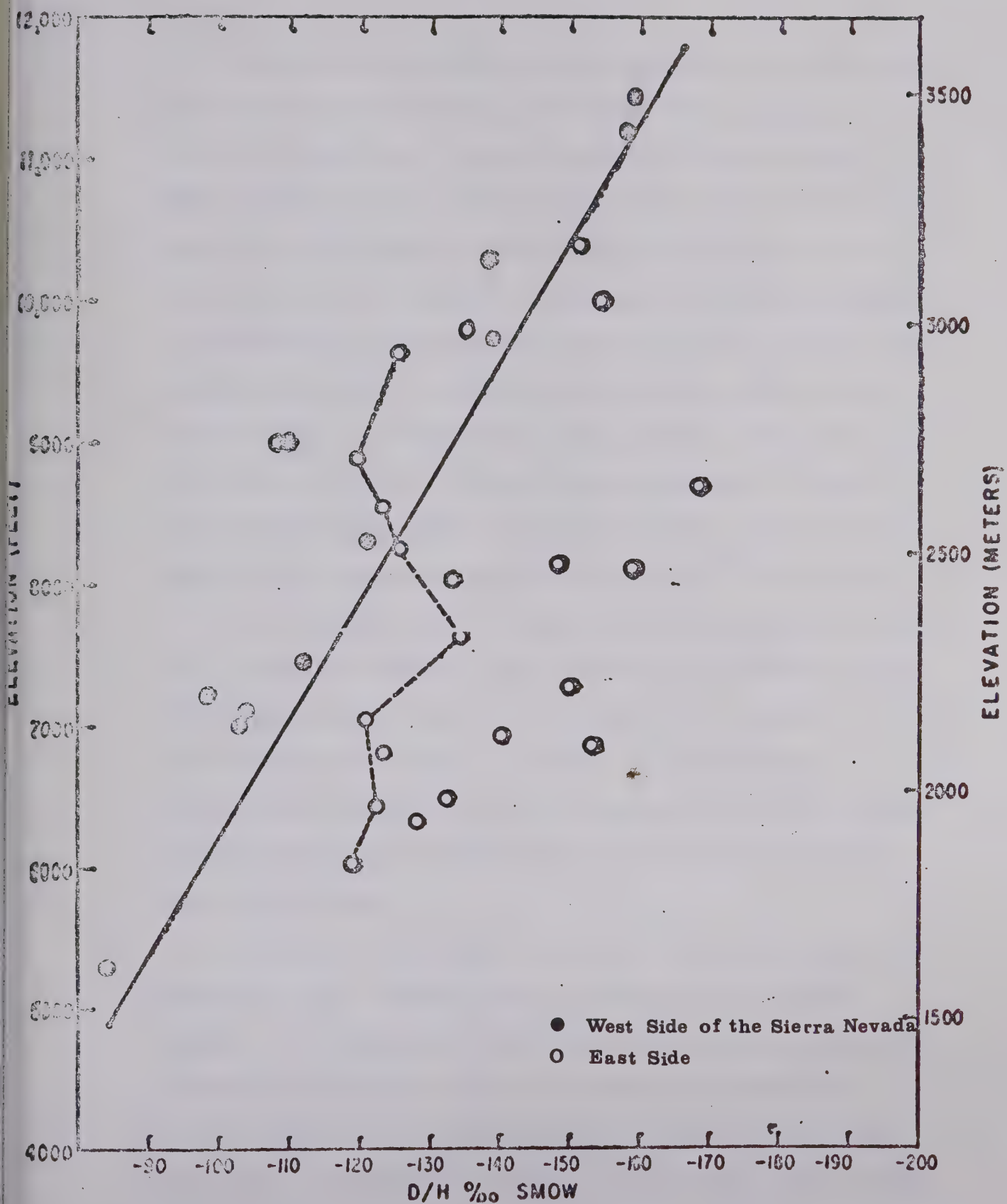


Fig. 13. Deuterium Traverse of the Sierra Nevadas (after FRIEDMAN and SMITH, 1970).

Another explanation of these data is the fact that most of the precipitation could have been brought, during this period, by westerlies which had to first pass over Mt. Logan. This again would place the divide west of Divide camp and also the pit would be in the rain shadow of Mt. Logan. However, the expected decrease in precipitation, because of the rain shadow, is not seen for this period. In the context of this explanation, Divide could not always be in the direct rain shadow of Mt. Logan, since the temperature dependence of $\delta\text{H}_2\text{O}^{18}$ would necessitate that the $\delta\text{H}_2\text{O}^{18}$ minimum for winter be significantly more negative than the $\delta\text{H}_2\text{O}^{18}$ for summer.

The phenomenon of an easterly flow although uncommon, is a third explanation. This might give Divide a simulated continental source, which would be expected to give more negative δ -values. Although cloud build up was visually seen in the east in mid-June, no weather observations were taken in the spring to confirm or refute this explanation.

Therefore, although the $\delta\text{H}_2\text{O}^{18}$ data points out meteorological complexities in the spring and early summer, not revealed by density, temperature or stratigraphic observations, more information is needed to discern the correct mechanism which caused these complexities. Depletion of $\delta\text{H}_2\text{O}^{18}$ by meltwater percolation, although a factor, was not considered a controlling factor,

since the δ -values around the ice lens at 60 cm were also relatively negative.

III. 3 Mt. Logan

a) Introduction

Mt. Logan, elevation 6100 m, is the highest peak of the St. Elias Mountain Range. It is approximately 90 km inland from the Gulf of Alaska (fig. 7). The meteorology of this area is dominated by the cyclonic storms associated with the low pressures in the Gulf of Alaska. The predominant storm tracks are from the W.S.W. Despite the fact that Mt. Logan is somewhat protected by a barrier range of peaks up to 5500 metres in height (Mt. St. Elias), it receives the majority of its precipitation from these maritime storms.

Accumulation on Mt. Logan is controlled by several factors, including topography, wind, elevation and temperature. In a dry-snow region such as Mt. Logan, the total accumulation is equal to the sum of the precipitation, the snow blown in and the hoar formation, minus the snow blown away and evaporation (MELLOR, 1961). It is often impossible to determine the relative contribution of each factor.

Previous work by ALFORD (1967), ALFORD and KEELER (1968) and KEELER (1969) has given insights into accumulation on the lower slopes of the mountain and the summit

plateau. KEELER (1969) found that above 2500 metres, elevation appeared to exert little control over precipitation amounts. He stated that the reason for this may be that precipitation on Mt. Logan is associated primarily with frontal, as opposed to purely orographic, processes, and that site-to-site differences in accumulation reflect local processes, such as redistribution by wind, rather than elevational control. From these studies there is also no evidence that precipitation increases with elevation to a maximum before declining, owing to a depletion in the moisture reservoir. This effect has been seen in Antarctica and Greenland where topography plays a minor role in determining accumulation.

b) Results

In the summer of 1968, two snow-pits were sampled, and in 1969 a 15 m snow-core was taken. Unfortunately, none were sampled in great detail, however valuable information may be deduced from the results.

i) Pit I

Pit I was located in a narrow pass called the Northwest Col at an elevation of 5400 metres (fig. 14). This was the one pit sampled by LA BELLE (in press) whose stratigraphy and density relationship seem to indicate an annual layer. The low density anomaly, usually associated with fall depth hoar, is at 130 cm

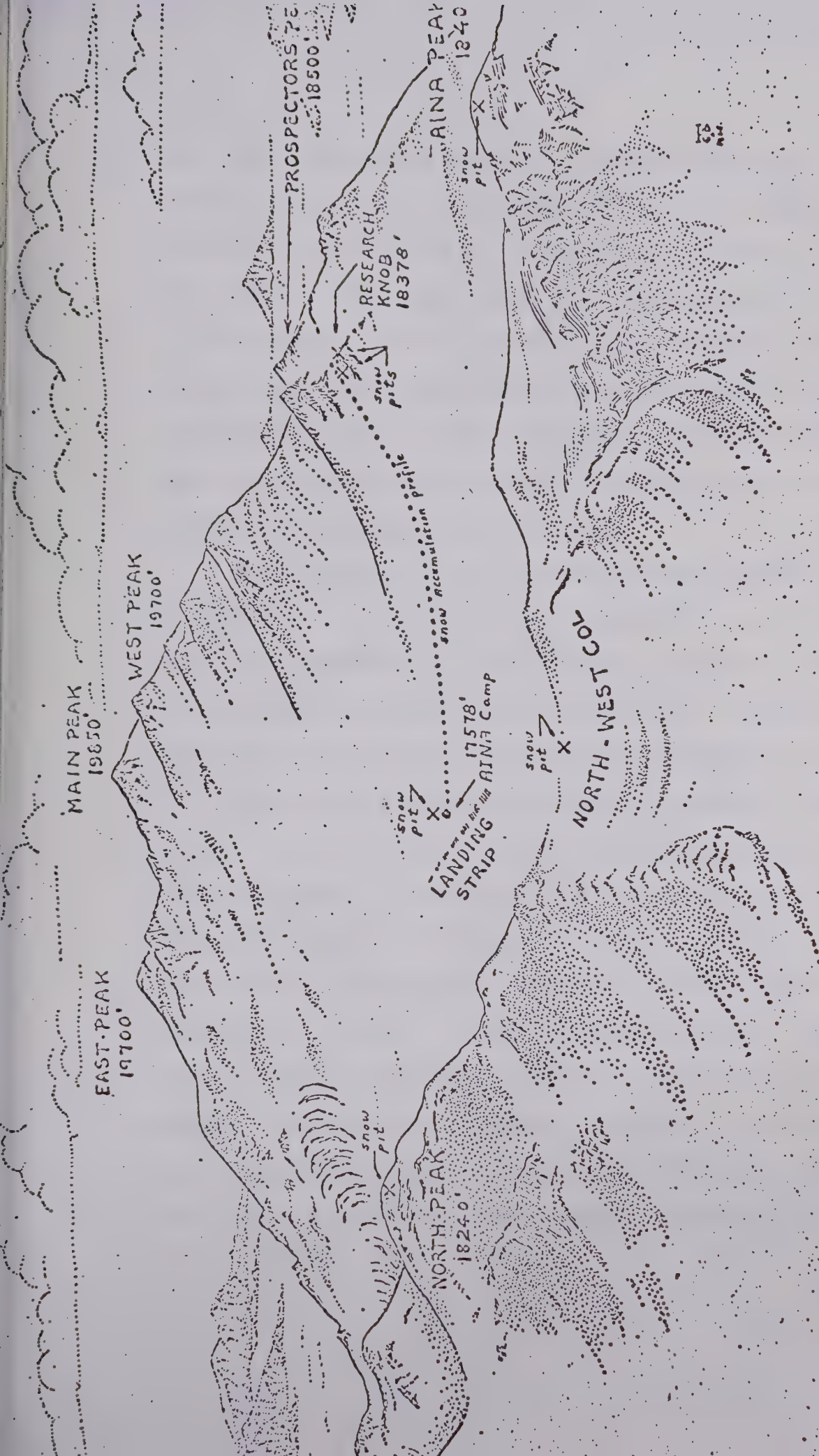


Fig. 14. MOUNT LOGAN — THE REGION ABOVE 17,000 FEET (5200 METERS) ON THE EASTERN HALF OF THE MASSIF. THE SITE OF THE RESEARCH CAMP IS SHOWN.

(fig. 15). The layer was also recognized by its friable appearance. This indicated a total annual thickness for the year of 1967-68 of 1.3 metres of snow, with a mean water equivalent of accumulation of 0.41 metres. This is considerably less than the accumulation that has been found on the summit plateau (up to 0.84 metres, water equivalent, KEELER, 1969). High winds which stream through the narrow pass were assumed to be responsible for this.

The temperature data establish this region as one of dry-snow facies (fig. 16). The density also indicates this. The temperature profile does not seem to stabilize or show yearly fluctuations, showing that summer temperatures penetrate deeper than the previous annual layer.

The oxygen isotope data show no seasonal trend. In fact, the profile is almost the inverse of what would be normally expected, with the positive peak in mid-winter instead of summer (fig. 17). This is probably due to mixing, depletion, and replenishment from other areas by high winds. It is interesting to note that a negative peak, similar to the one in the Divide pit appears just below the surface. However, the pit has not been sampled in enough detail to make any assumptions from this coincidence. The average δ -value of the pit is $-31.7 \text{ }^{\circ}\text{oo}$.

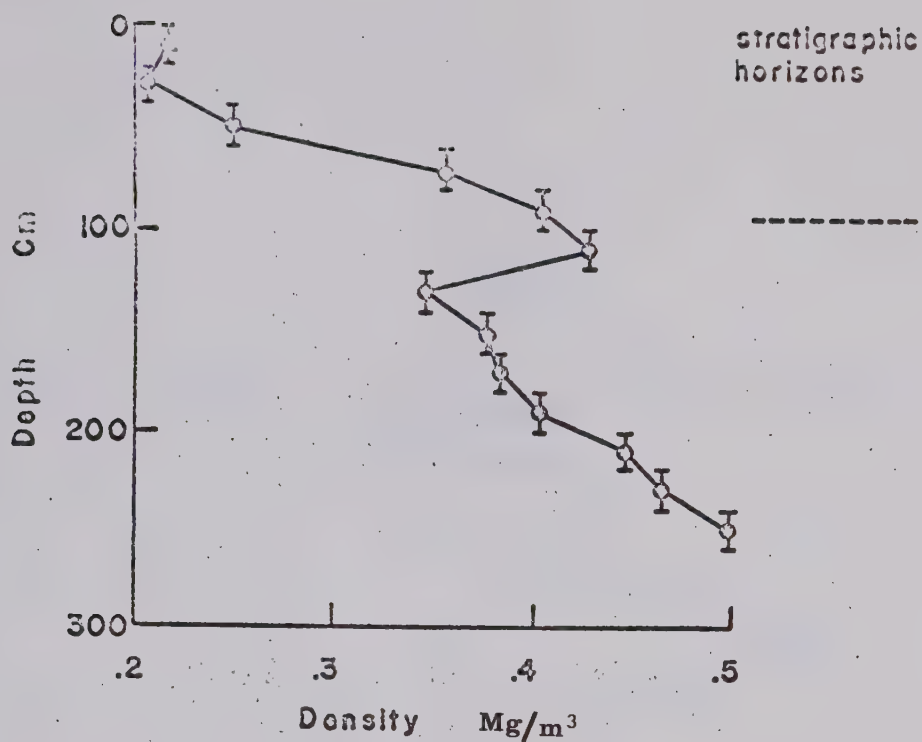


Fig. 15. Density of Pit I (Mt. Logan, Northwest Col, elev. 5400 m.).

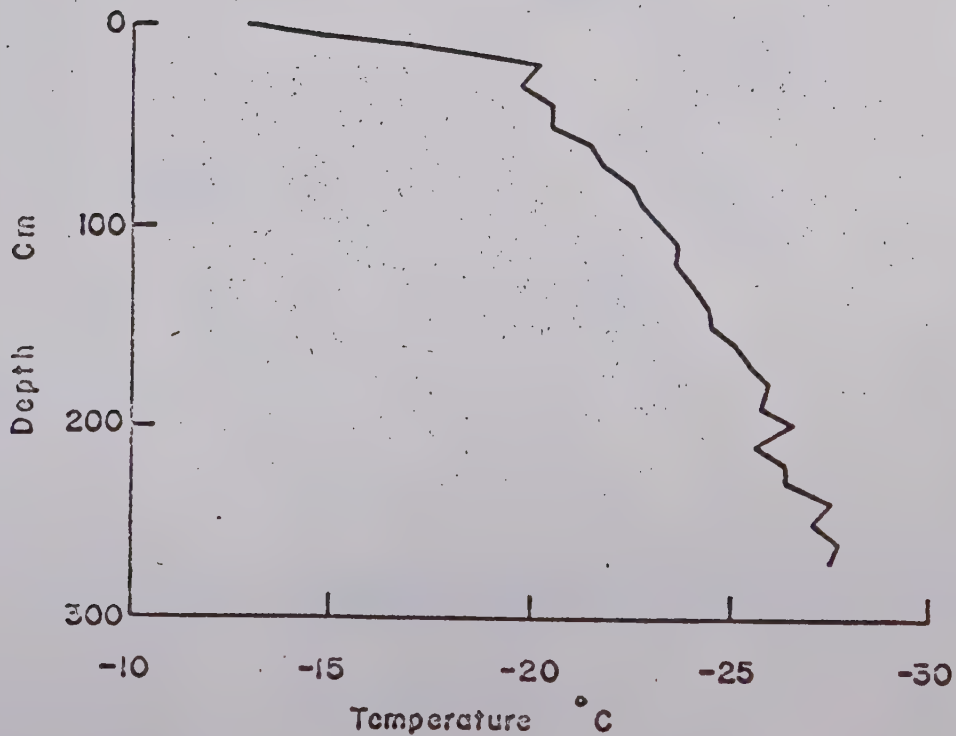


Fig. 16. Temperature of Pit I (Mt. Logan, Northwest Col, elev. 5400 m.)

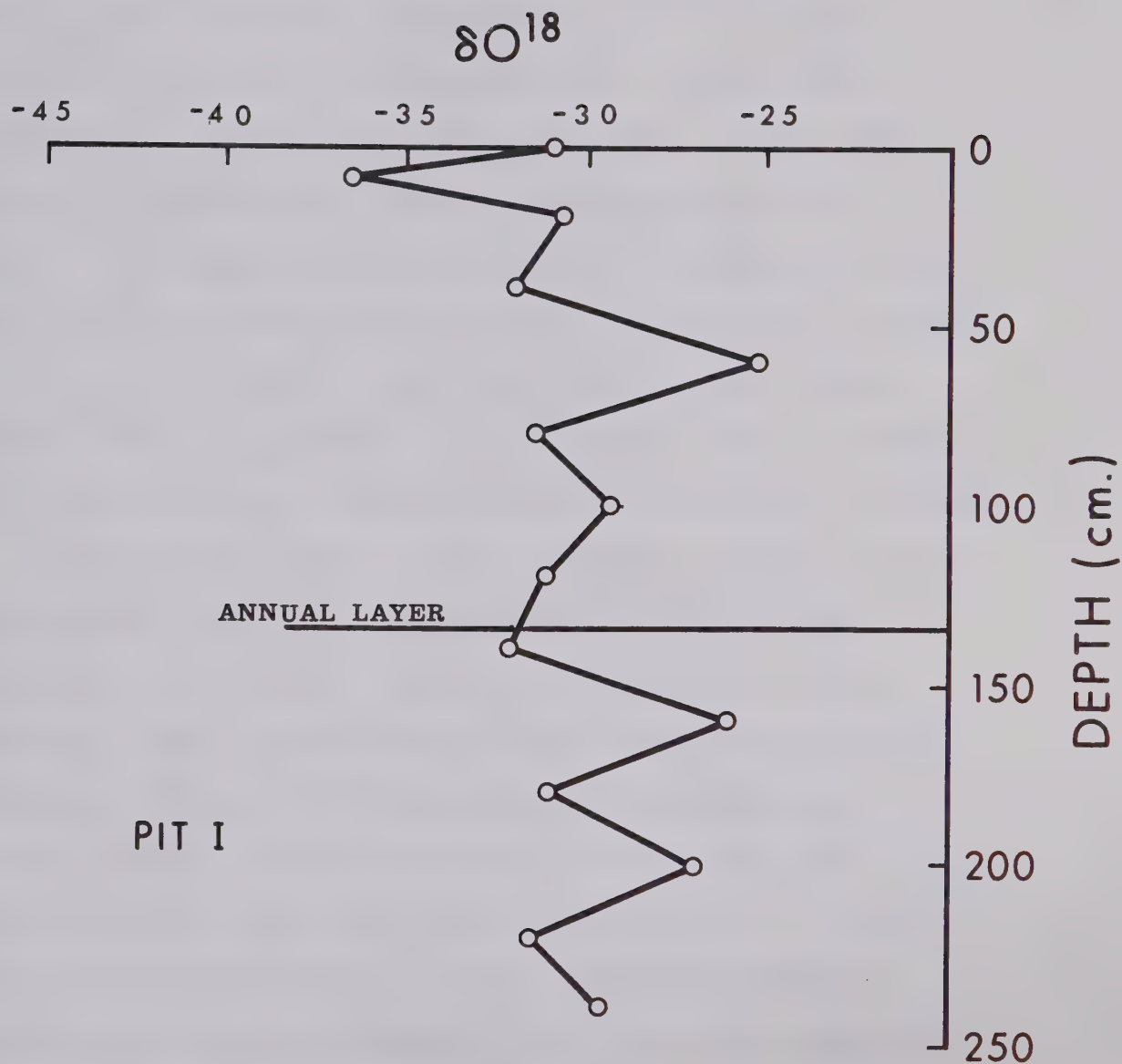


Fig. 17. Isotope Profile of Pit I (Mt. Logan, Northwest Col, elev. 5400 m.).

ii) Pit II

The location of pit II was in the snow-dome, elevation of 5680 metres, on the Arctic Institute of North America (A.I.N.A.) Peak (fig. 14). There were many layers of varying composition in the pit, but between 140 cm and 163 cm depth was a layer of low density and more friable snow (fig. 18). Below this, layers of considerably greater hardness were found. If the low density anomaly indicates the previous summer horizon, the accumulation of 1967-68 would be 1.5 metres of snow or 0.6 metres water equivalent. This figure seems high for a summit, but this summit has no windward rocks to control or cause wind-scour (LA BELLE, in press).

The isotopic data shows a definite negative trend with depth (fig. 19). Unfortunately, the pit was only sampled to a depth of 120 cm, so there is no way of knowing if the δ -values would have become more positive between 120 cm and 160 cm, giving the normal annual isotopic profile. The most striking thing about both pit I and pit II are their minimum δ -values, -38.6 ‰ and -45.1 ‰ respectively. These values are normally associated with the extremely cold, and arid regions of Northern Greenland and Antarctica. The average δ -value of pit II is -33.9 ‰ which is more negative than the average of pit I (-31.7), but this would be expected because of the change in elevation.

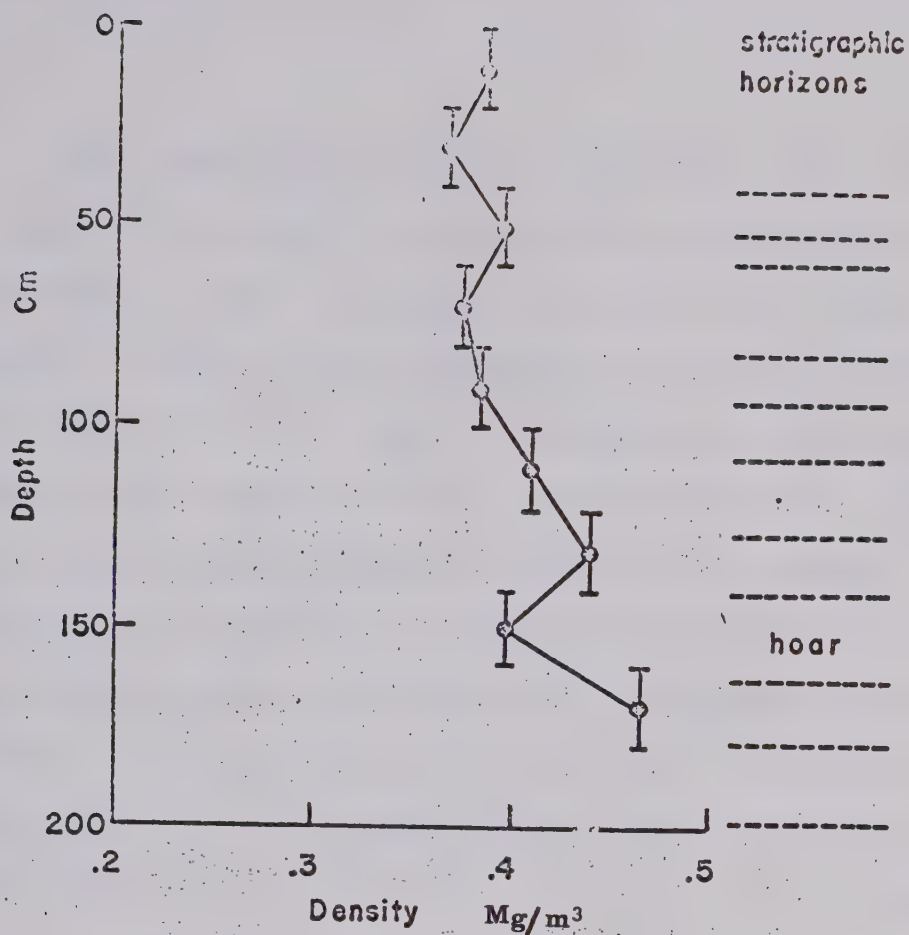


Fig. 18. Density of Pit II (Mt. Logan, A.I.N.A. Peak, elev. 5680 m.).

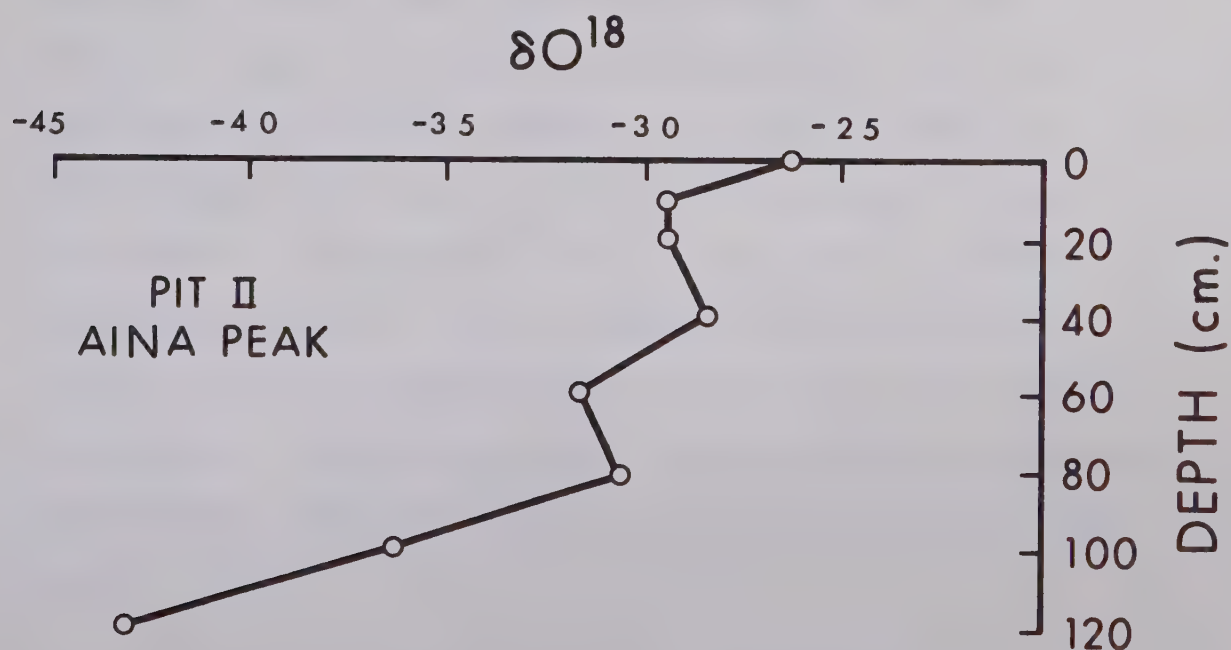


Fig. 19. Isotope Profile of Pit II (Mt. Logan, A.I.N.A. Peak, elev. 5680 m.).

The temperature profile again shows that this is a region of dry-snow facies and that summer heating has penetrated beyond the previous annual layer (fig. 20). However, little or no information is given by this or other data as to why snow accumulates on this particular peak. When compared to the other peaks on Mt. Logan it can only be described as an accumulation anomaly, caused by peculiar topographic or orographic conditions, which will require more detailed studies in order to be understood. It is assuring, however, that the presence of the isotopic trend with depth implies negligible wind mixing, the very condition necessary to retain snow on this peak.

iii) The Snow Core

The snow core was taken from the summit plateau (elevation 5400 m) near the A.I.N.A. Camp (fig. 14). Figure 21 shows the oxygen isotope profile, with the depth converted to water equivalent (W.E.). Two low density anomalies, one at 1.0 m and the other 2.5 m, were found. The one at 2.5 m or .96 m (W.E.) indicates the summer of 1968. This was positively identified by KEELER (personal communication) by using the 1968 spring surface as a reference horizon. Density and stratigraphic observations offer no further interpretation of the snow core.

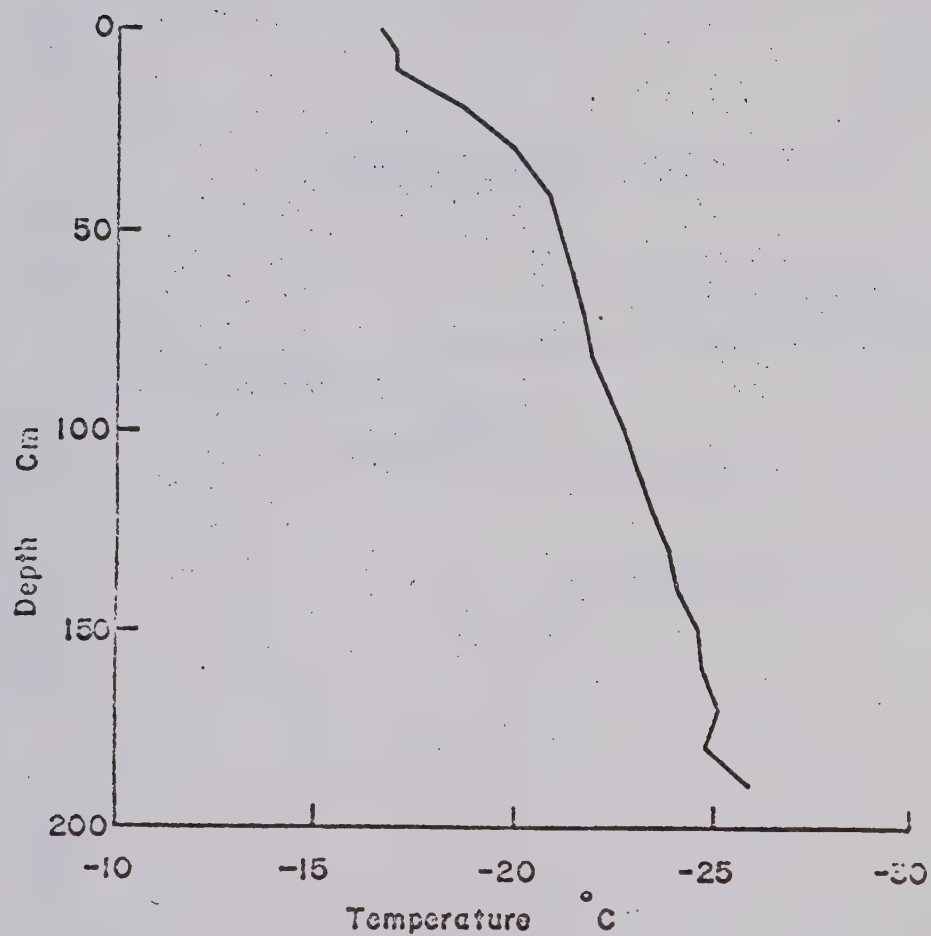


Fig. 20. Temperature of Pit II (Mt. Logan, A.I.N.A. Peak, elev. 5680 m.).

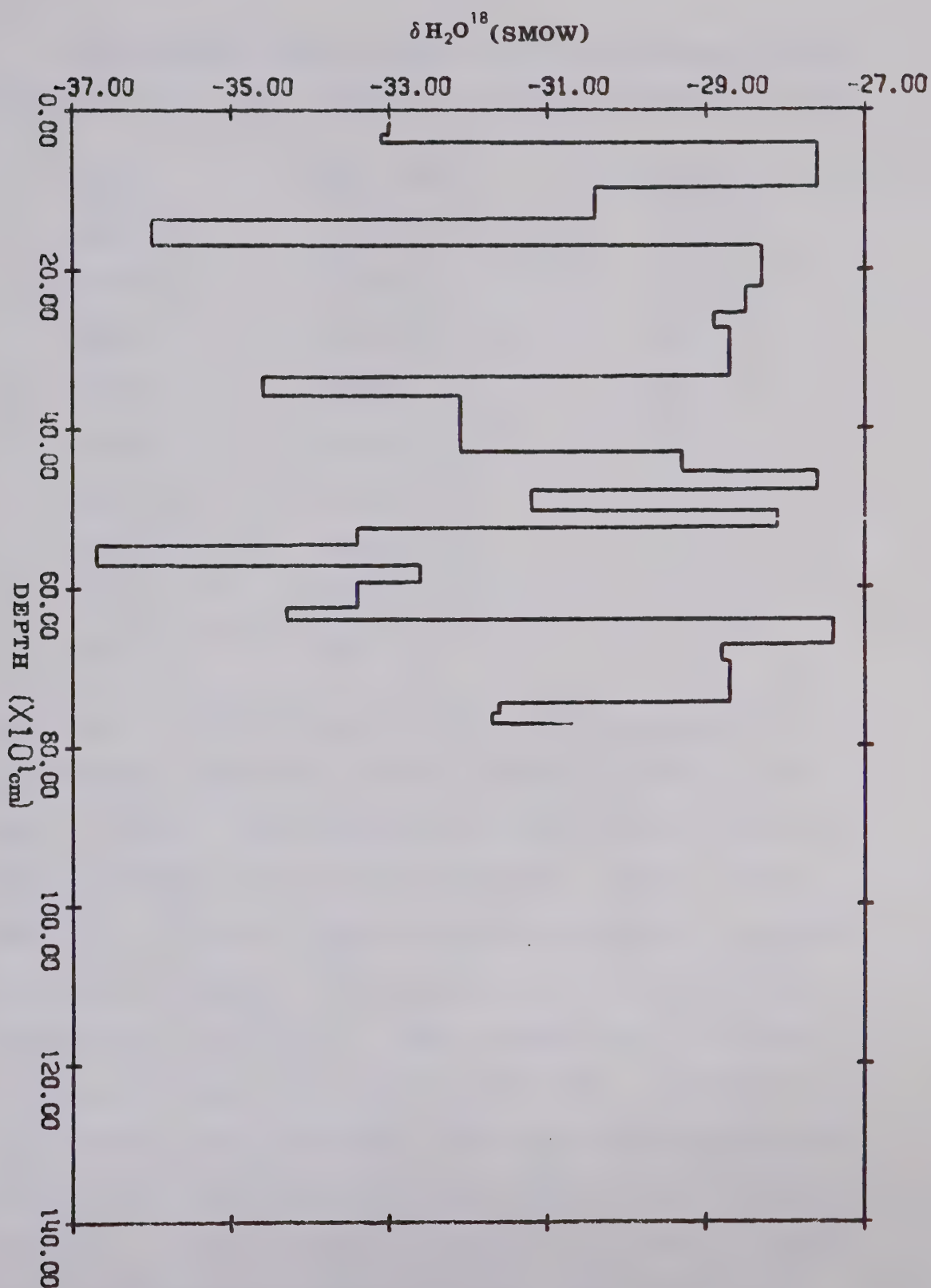


Fig. 21. Snow-Core from the Logan Plateau (elev. 5400 m.).

If we assume that a normal seasonal isotopic trend dominates, then the profile can be interpreted as below:

Years	Depth (W.E.)	Accumulation (W.E.)
1968-69	0-96 cm	96 cm
1967-68	96-178 cm	82 cm
1966-67	178-303 cm	125 cm
1965-66	303-442 cm	139 cm
1964-65	442-524 cm	71 cm
1963-64	524-593 cm	69 cm
1962-63	593-665 cm	72 cm
1961-62	665-742 cm	77 cm
1960-61	742- —	—

The 82 cm for 1967-68 agrees well with the amount of accumulation measured by KEELER (1969) in 1968 on the summit plateau. His measurements varied from 60-84 cm with an average of 70 cm for the year 1967-68. The summer of 1967 was a high accumulation period, according to personal accounts, and therefore 125 cm may not be unreasonable for 1966-67. The accumulation for Divide in the snow budget year 1965-66 was low. Therefore 139 cm would seem to be much too high since both Divide and Mt. Logan experience the same major meteorological patterns. If this depth was actually the sum of 1965-66 and 1964-65 precipitations, it would make more sense since 1964-65 was also a low accumulation year for Divide.

This would mean that the summer isotopic maximum had either been erased by wind or missed because of sparse sampling. The latter case seems the most likely and points out the need for detailed sampling to obtain a complete isotopic profile. 1962-63 was a year of high accumulation at Divide but this does not seem to coincide with the core data from Mt. Logan even if both interpretations of the 1964 to 1966 time span are considered. The expected winter minima of 1961-62 and 1966-67 are missing. This should not be surprising when one considers the dynamic mixing and wind-scour arguments which were invoked to explain the results of pit I. It may also have been that small snowfalls occurred in these winters because of extreme cold. Isotopically this would result in thin layers with relatively negative δ -values, which could be easily missed during sampling.

The average δ -value of the core, -29.8 ‰, is more positive than the average of pit II (-33.9 ‰). This is expected on the basis of the elevation difference between pit II and the core location. On the other hand when we compare the average δO^{18} values for two locations at the same elevation (the core and pit I) for the same year (1967-68), the agreement is remarkable (-31.6 and -31.7 ‰ respectively). Therefore, although elevation does not seem to affect the amount of precipitation on

Mt. Logan (KEELER, 1969), it does alter the δ -values significantly.

c) Discussion

If one plots the Mt. Logan results on a δO^{18} versus latitude graph, he readily ascertains the importance of altitude in determining the isotopic composition of precipitation (fig. 22). The bars in the graph show the range of δ -values of each of the cited locations. The Divide δ -values are in the same range as those of the Fox Glacier and thus fit the general trend. Therefore, although accumulation studies show no depletion of the precipitation reservoir in the area of Mt. Logan, isotopic values do. In order to find the δO^{18} depletion with altitude, it would be necessary to do a traverse from the Gulf of Alaska to the summit plateau of Mt. Logan, along the path of the predominant precipitation storms. Just using the theoretical Rayleigh distillation model (see fig. 2) it would seem that the cloud systems have lost over 95% of their initial vapour. Dansgaard calculated the amount of vapour left if isobaric cooling from 20°C to -20°C had occurred. His calculation, using formula (10), gave 5.2 % of the vapour left with the condensation (snow) having a δ -value of -28.2 ‰. Seeing the mean yearly temperature, recorded in a bore

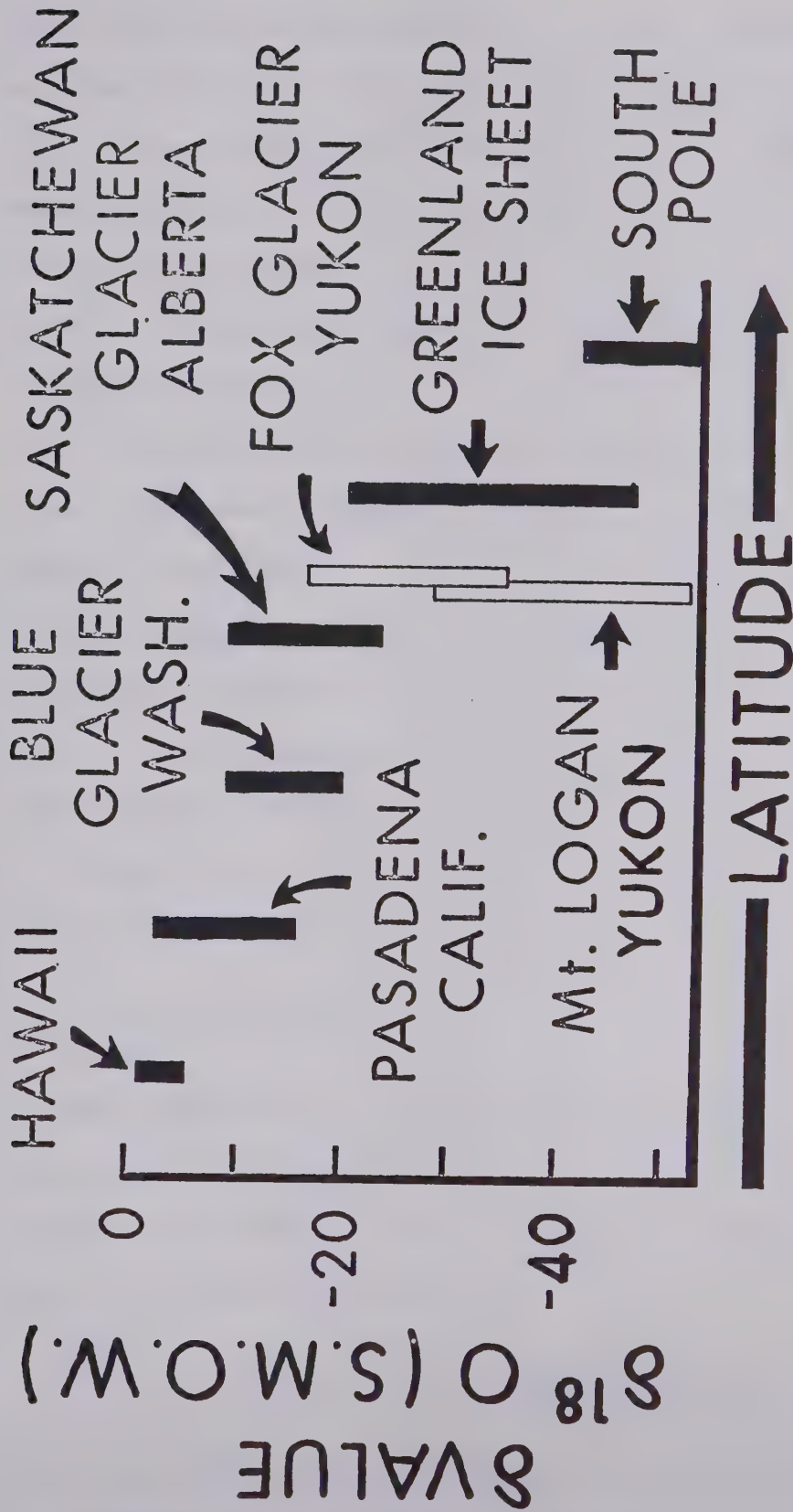


Fig. 22. $\text{H}_2^{18}\text{O}/\text{H}_2^{16}\text{O}$ composition of Fox Glacier and

Mt. Logan in relation to locations at other latitudes (after SHARP, 1960).

hole, of the summit plateau is -25.4°C (KEELER, 1969) and the average δ -value of the Mt. Logan core was -29.8 ‰; this precipitation model of straight isobaric cooling from 20°C , according to the Rayleigh condensation formula, seems to fit the Mt. Logan results. However a completely analysed traverse would be necessary to see if this was true.

To check for kinetic effects due to orographic or other processes, samples from Mt. Logan, Divide and Fox Glacier were sent to the Environmental Research Branch, Atomic Energy of Canada Ltd., Chalk River, Ontario for deuterium analysis. The results are plotted in figure 23, against their respective δO^{18} values. The prefixes on the samples represent the following: ML - Mt. Logan, A - Divide, T and B - Fox Glacier snow and rain respectively. The resulting formula;

$$\delta\text{D} = 8.2 \delta\text{O}^{18} + 6.5 \quad (19)$$

is very close to the northern hemisphere results of the International Atomic Energy Agency and the World Meteorological Organization world survey of isotopic concentration in precipitation:

$$\delta\text{D} = (8.1 \pm 0.1) \delta\text{O}^{18} + (11.0 \pm 1.0) \text{ ‰} \quad (12)$$

This means that the snow found in the St. Elias Mountains was formed on later stages of an equilibrium condensation

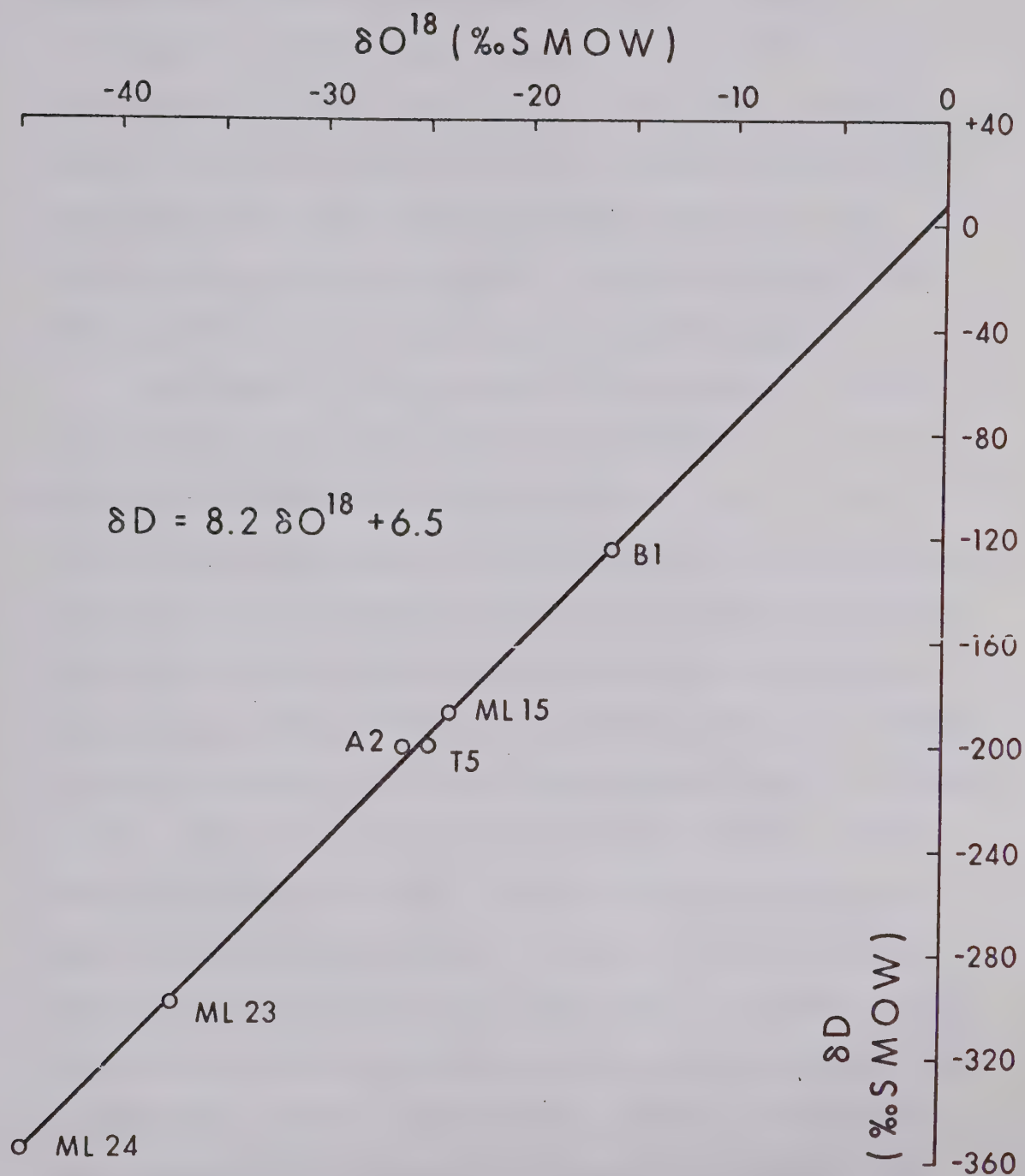


Fig. 23. δO^{18} vs. δD for Mt. Logan, Divide, and Fox Glacier Samples (ML - Mt. Logan, A - Divide, T - Fox Glacier Snow, B - Fox Glacier Rainfall).

from ocean vapour, which has been evaporated in a non-equilibrium process fast enough to give a surplus of deuterium, $d = +6.5 \%$, as compared to the world survey surplus of 11% (see Chap. I.2). This lower kinetic isotope effect contribution in the vapour source would seem consistent with the quasi-stationary lows that build up in the Gulf of Alaska (The vapour would have more opportunity to equilibrate with the ocean).

The slope of 8.2 in figure 23 indicates that the snow at these altitudes has been condensed in a near-equilibrium condition and has suffered few, if any, fractionational processes, such as uplift. Even though previous visual studies had established that precipitation was formed at these altitudes, they were unable to state whether most of the precipitation had been formed at lower altitudes and then blown up (as formerly thought) or not. The δO^{18} values, the deuterium values, their interrelationship and the latitude anomaly of the Mt. Logan samples, all present strong evidence that snow actually forms at these high altitudes. Although snows from lower altitudes may be blown up, this does not seem to represent a major contribution. There is no doubt that snows at this altitude can be very dependent on wind conditions for their deposition as witnessed by the data from the Northwest Col.

The author feels that more sampling in this area is warranted to clarify many of the situations indicated by this preliminary study. A traverse of the mountain range would be of particular benefit. It must be pointed out that stratigraphy, density temperature, climatic and if possible other forms of isotopic investigation, such as tritium, should be done as well as the oxygen and/or deuterium analyses to achieve a complete picture.

III.4 The "Fox" Glacier

a) Introduction

The so called "Canine Glaciers", (Dingo, Vixen, Jackal, Hyena and the Fox) are located just north of the Hodgson and east of the Steele Glaciers, at the base of Mount Wood (fig. 7). Although the canine names have not been officially accepted, they will be used as the glaciers' proper names for the rest of the text.

The Fox Glacier is a small valley glacier that shares a common drainage basin with the Jackal and Hyena Glaciers. All three of these glaciers are believed to have surged in the past, with the Jackal being in active surge during 1967 and 1968. The term "surge" refers to a rapid advance of a glacier, generally followed by a quiescent period (see III.4, ii)). The Steele and Hodgson Glaciers are also surging glaciers, with the

Hodgson in active surge during 1968, while the Steele had just reached the end of one of its surges.

Early in 1967, glaciologists from Canada and the U.S.A. selected the Fox Glacier for study in an effort to explain the mechanisms of a surging glacier. The moraines and glacial surface features were found to have much in common with the Steele Glacier before its surge. The choice of the Fox for study was also ideal since ablation had smoothed the surface permitting easier travel. Recent investigations have included; surface flow surveys by S. COLLINS (1968), mass balance by T. BREWER (1969), seismic and gravity studies by CROSSELY and CLARKE (1970), hydrology by T. FABER, bore-hole temperatures (CLASSEN and CLARKE, 1971), and morainal geology by G. DENTON.

The mean daily temperature recorded at Fox Camp between 6 July and 18 August, 1968 was 44.4°F , with a low of 39.5°F on July 13th and a high of 48.7° on July 22nd. The dominant wind directions were from the south or south-east. However, the wind directions were determined on the glacier and may be representative of the katabatic winds off the glacier rather than the prevailing winds of the region, since a number of storms were seen to come from the north.

b) Glaciers

Glaciers may be classified according to ice temperature and the amount of surface melt. A temperate glacier is at the pressure melting point throughout, while there is no surface melting in a high-polar glacier. Polar glaciers have glacier ice with temperatures below 0°C and surface melting. However, these categories are very general. Glaciologists now favour a system of glacial zones, similar to the snow facies described in Chapter III.2 c) i).

The idea of zones was developed by BENSON (1962) and MÜLLER (1962). Very few glaciers will show the entire sequence and the zone boundaries will likely vary from year to year according to weather conditions. The zones are as follows (fig. 24):

- 1) Dry snow zone. No melting in this zone, winter or summer. It is divided from the next zone by the dry snow line.
- 2) Percolation zone. Area of percolation facies bounded by dry snow line on one side and 0°C isotherm meeting the previous summer level (Saturation line) on the other.
- 3) Soaked or wetted zone. The area between the saturation line and the firn limit. The firn limit is farthest point of firn ablation during summer.

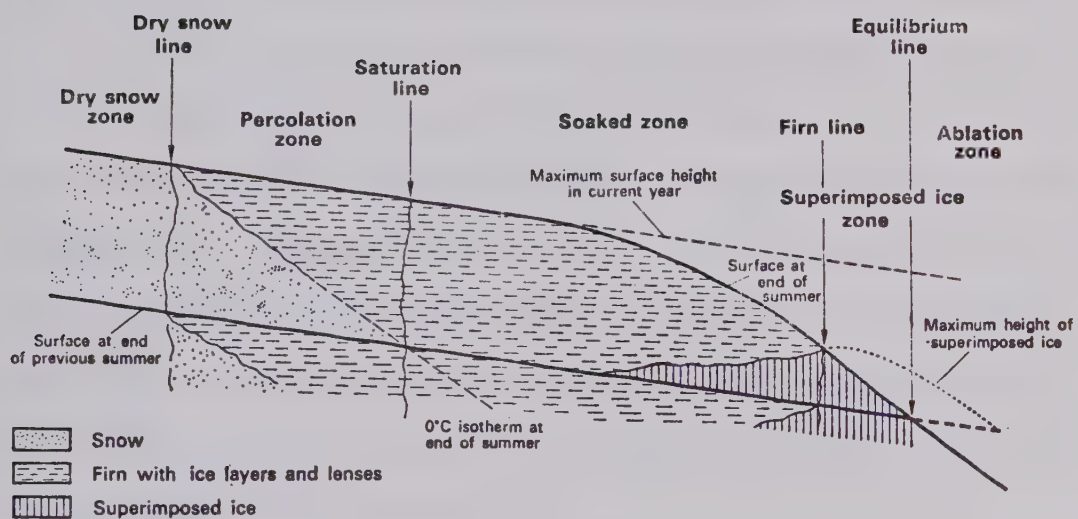


Fig. 24. Glacial Zones (after MÜLLER, 1962).

- 4) Superimposed ice zone. Superimposed ice is percolating meltwaters that have refrozen on contact with the previous years firn or ice. It is bounded by the firn limit and the equilibrium line (the line above which is positive accumulation, and below which is ablation, also called the firn line).
- 5) Ablation zone. From the equilibrium line to the toe of the glacier; the ablation zone is an area of negative accumulation.

The zones are not always distinct, as pointed out in the Divide case. A transitional zone between facies should be considered rather than discrete lines i.e. dry snow line, firn line, etc. The width of these transitional zones will probably vary with slope and general climatic conditions of the glacier.

The ice in a glacier is deforming plastically as a result of stress produced by its own weight. In addition, the ice mass as a whole may be sliding over the underlying bedrock. These processes, plus faulting in places, constitute glacier flow.

In Chapter I.3, e), the potential use of isotopes in elucidating glacier flow was discussed. The classic flow patterns of normal glaciers were first proposed by REID (1896). He suggested that snow from the top of the accumulation area submerges and eventually appears

down glacier, at the surface, near the terminus, while snow deposited just above the firn limit appears just below the equilibrium line as shown in figure 25a.

In the ideal case, this should give rise to an altitude dependence of isotopic composition below the equilibrium line which is reversed to that above (fig. 25c).

Figure 25b is a top view of an ideal glacier. The flow vectors show that if a traverse is taken the centre ice normally would have a more negative value, again due to the altitude effect. The centre flow vectors are faster, because movement near the edges of the glacier is retarded by the valley walls. In the longitudinal profile, the bottom motion is also slowed down by the drag of the bedrock.

Many theoretical studies of glacier flow have originated in the last 20 years. A good summary of this work has been compiled by W.S.B. PATERSON (1969). KAMB (1970) reviewed basal sliding, while some workers consider LLIBOUTRY's "Traité de Glaciologie" (1965) the glaciologist's bible. Isotopic studies have only been conducted to an extent sufficient to indicate very general trends in glacier flow. Hence, these works are not reviewed in this thesis.

ii) Surging Glaciers

Isolated examples of glaciers making sudden rapid advances have been known since at least the beginning

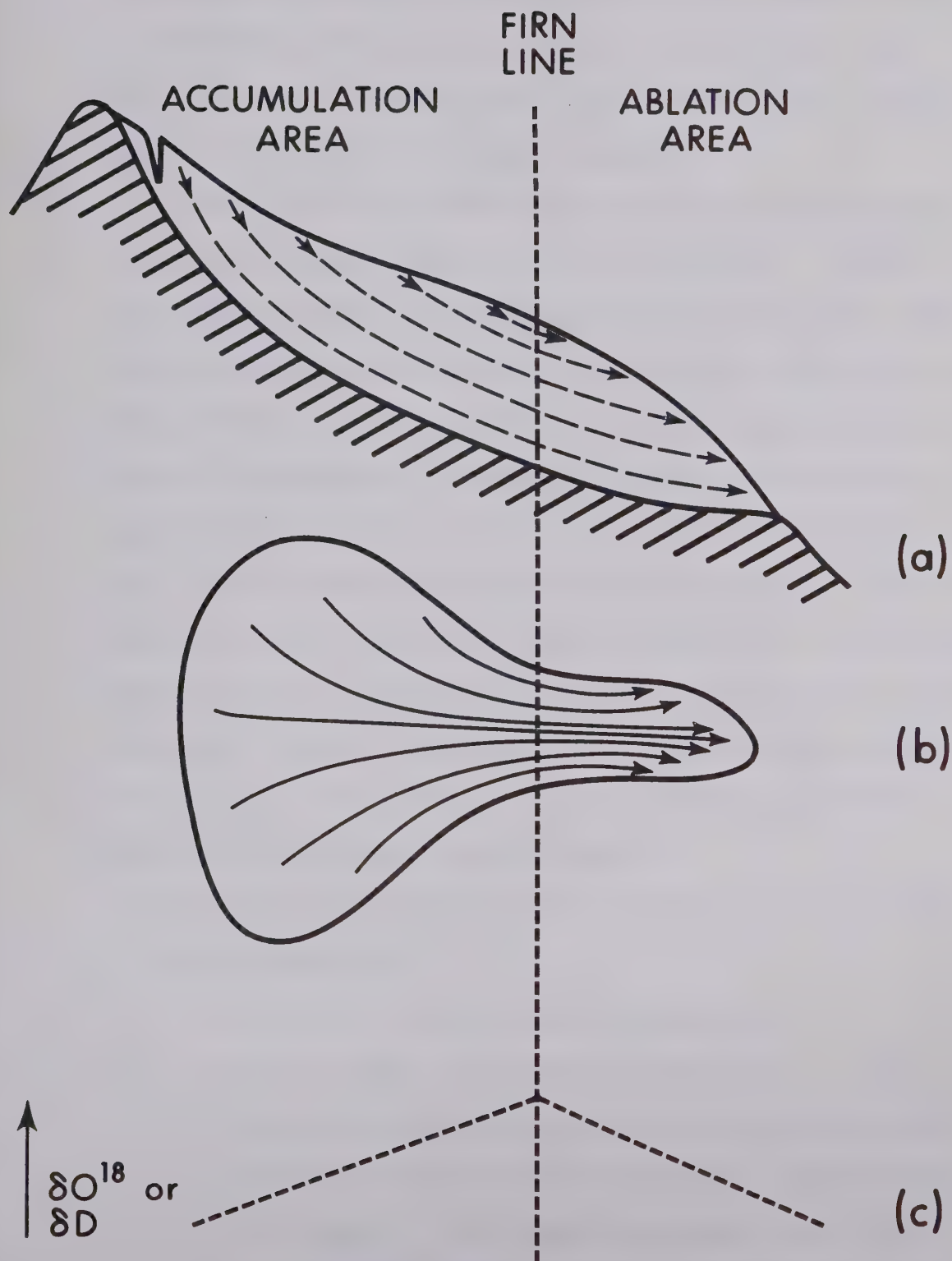


Fig. 25 a) Longitudinal Profile of Glacier Flow(after REID, 1896)
 b) Top View of Glacier Flow (after REID, 1896)
 c) Isotopic Variation of a Longitudinal Profile.

of this century. Typically, these glaciers move rapidly forward, transforming the surface into a chaotic mass of crevasses and pinnacles, then the rapid movement stops and the glaciers enter a quiescent stage. This type of behaviour is called surging.

MIER and POST (1969) outlined the characteristics and defined three types of surging glaciers. Type I are large to moderate-sized glaciers (>5 km long) with large displacements (>5 km) and very fast flow (>15 m/day averaged over a year, or >50 m/day for short periods). Type II are large to moderate glaciers with moderate displacements (2-5 km) and flow speeds of 2-8 m/day. Type III are small glaciers (2-10 km) with small displacements which are, however, large relative to the glaciers size ($10^{\circ}/\infty$ - $30^{\circ}/\infty$). Rates of flow may vary from 1-8 m/day. Almost complete stagnation usually occurs in the lower end of Type I and III during quiescence while slow flow may occur in Type II.

The following general characteristics are common to surging glaciers:

- 1) Surging glaciers surge repeatedly.
- 2) Most surges are uniformly periodic.
- 3) All active surges take place in a relatively short period of time (1-6 years, most commonly, 2-3 years). The quiescent phase lasts for a much longer time (15-100 years, commonly 20-30 years).

- 4) No abrupt bedrock sills or depressions are suggested by the profile of most surging glaciers.
- 5) So far, surging glaciers have been reported in restricted areas, especially in North America.

The Fox (length ~4 km) is believed to be a Type III surging glacier. The lower portion of the Fox seems to have been virtually motionless for a considerable period of time since at several locations, linear drift features extend from the valley walls into the ice in a direction transverse to the flow. These appear to have originated as crevasse fillings, deposited by ablation during a period of no forward motion. Using recent ablation rates and the height that these features extend up the wall, it is concluded that motion of the lower glacier ice during the last two decades was trivial, (BREWER, unpublished). The movement is only a few metres/year in the active portions of the upper glacier. This projected mass balance for the end of the melt season was positive and probably is near 2.5×10^9 grams. This is also consistent with "surging" since these glaciers reservoirs must build up for the next surge.

Although the Fox is generally a polar glacier, CLASSEN and CLARKE (1971) found a basal hot spot (near 0°C). They concluded that the surge behaviour of the

Fox Glacier must relate to this thermal regime, but whether the observed hot spot causes surge activity or is a consequence of it could not be determined. However, it is significant that the Fox Glacier satisfies the essential requirement of thermal surge theories.

Theoretical models of surging have been based on both basal sliding and internal motion. WEERTMAN (1969) has proposed a theory based on the premise that a glacier surge occurs when a water layer at the base of a glacier attains a thickness sufficient to drown the obstacles in the bed that offer the greatest hindrance to sliding. ROBIN (1969), and ROBIN and BARNES (1969) suggested that initiation may be accomplished by switching from compressive to extending flow in the ablation zone, or the opposite switch in the accumulation zone. This would cause a wave to move down the glacier. They showed that studies of deformation and sliding of ice under these conditions permit the high speed associated with surging glaciers. LLIBOUTRY (1969) proposed that glacier surges may result (1) from the warming of a cold glacier, which follows an unusual snow cover, with formation of a temperate basal layer, or (2) from the fact that instabilities in the perturbation equation of flow may be caused by two values of sliding velocity corresponding to a single value of the friction. NIELSEN (1969) assumed that a

stagnant ice block or dam developed in the lower region of a glacier. Ice gradually built up above the dam while the dam itself became thinner by ablation. Eventually the upper end of the stagnant ice block crumbled from the force above it and much of the glacier was changed from a state of compression to one of tension. The rupture of the ice dam resulted in the glacier rapidly becoming broken into a mass of blocks or powdered ice. The apparent viscosity of a broken-up glacier is much less than that of bulk ice, so high velocities of flow are possible.

All these theories have strong and weak points, but Nielsen's seems the most unpopular. This is because it differs considerably from normal glacial flow and many glaciologists believe that surges are just like fast flowing outlet glaciers that just "run out of gas". The other theories are extensions of normal flow theory. Perhaps the answer is some combination of various theories but many more experiments, especially at the bedrock interface, will have to be conducted before any are accepted or rejected.

c) Results

i) Upper Glacier

Seven snow pits and two cores were analysed from the accumulation area of the Fox Glacier. The two cores were located at stake 24 (see fig. 26) while the pits

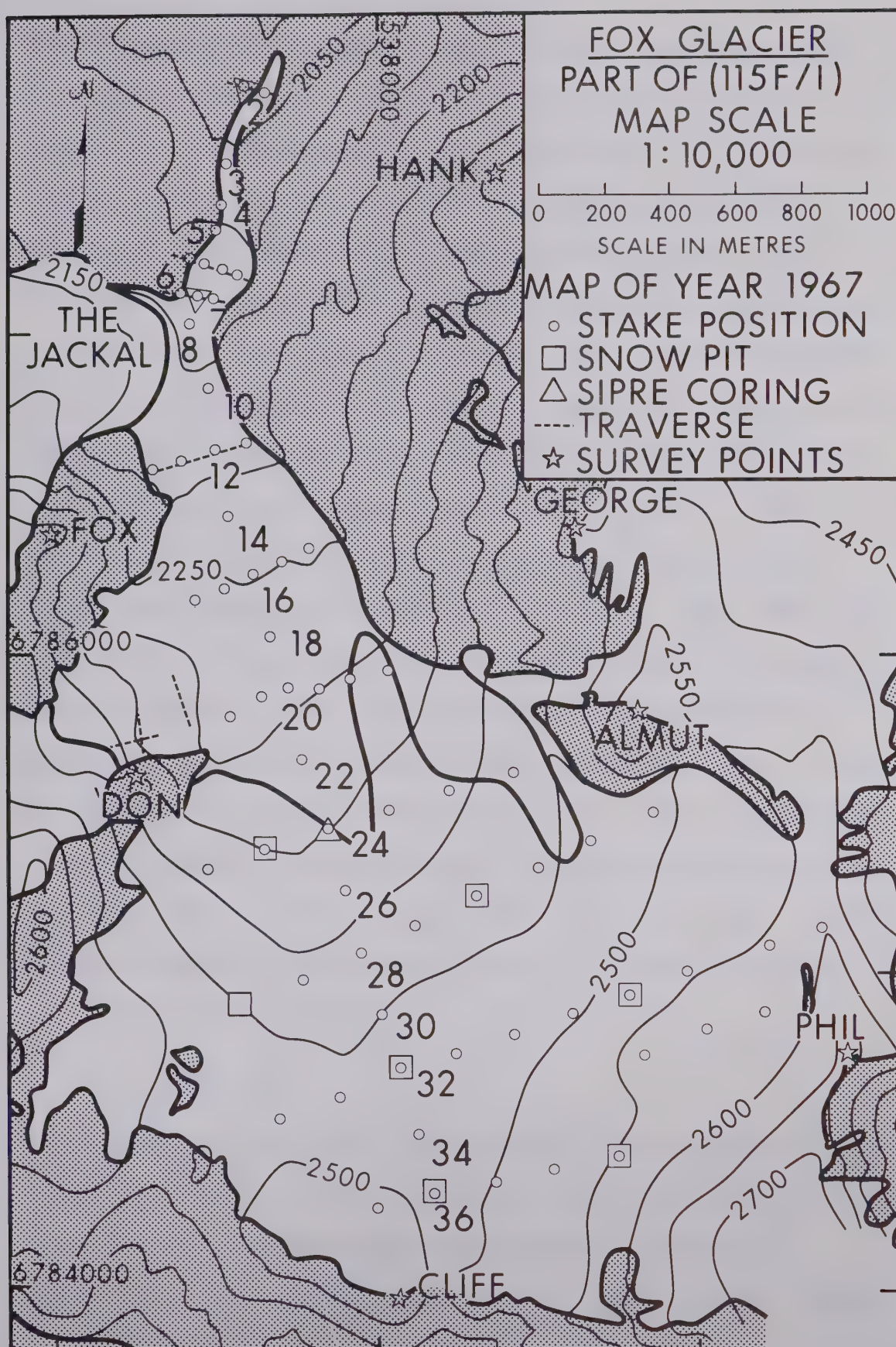


Fig. 26

were located near stakes, 24W2, 28W4, 28E4, 32, 32E8, 36, 36E8. The stakes system was set up so that the stakes were approximately in a 200 m grid. The central stakes were labelled by their distance away from the terminus, i.e. stake 32 is approximately 3200 m away from the terminus. The traverse stakes are labelled by distance and direction away from their respective central stake, i.e. 32E4 is 400 m east of stake 32. The elevation change from stake 20 (the lower limit on the firn line) and the top of the accumulation area is 400 m. The thick dark line passing through stake 24 is the firn limit from aerial photography in 1965. It was lower in 1968 but the melt season had not ended before the camp was abandoned. Just south of stake 36W2 a large melt water and slush pond was located. From this pond, a melt stream ran the whole length of the Fox. The stream was snow-bridged for the major part of the melt season above the firn line. However, near the end of the melt season, much of the snow collapsed or was not strong enough to hold a man or a snowmobile.

1) Snow Pits

Snow pit 36E8 was the highest (2550 m) and the last (Aug. 15) snow pit dug on the Fox. The densities range from 0.4 to .6 gm/cc with a low anomaly at 100 cm (fig. 27). Dirt bands appeared at 40 cm, 115-145 cm and

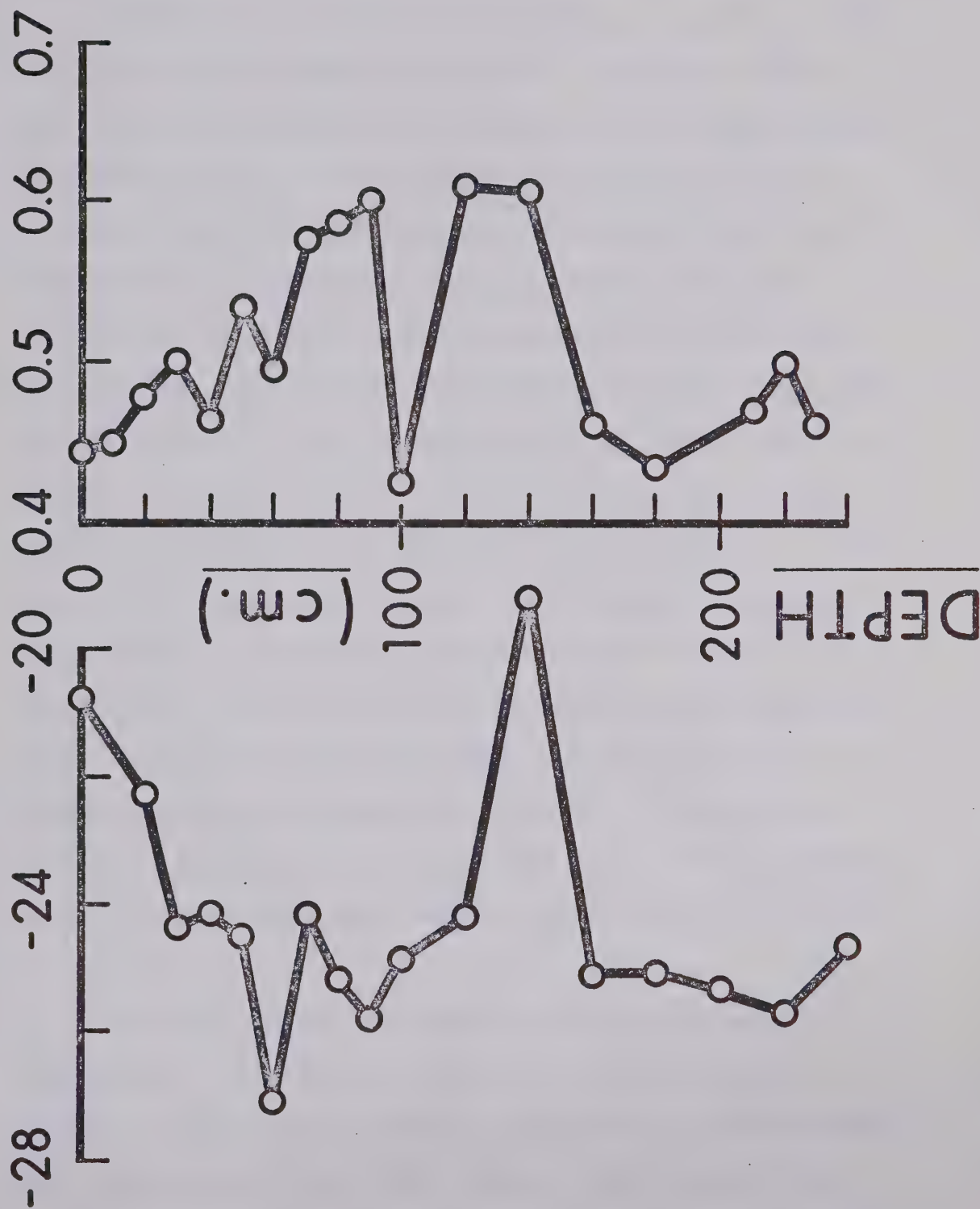
$\delta O^{18} S.M.O.W.$ 

Fig. 27. Snow-Pit 36E8, Fox Glacier.

185 cm while the only ice lens appeared at 60 cm.

The oxygen isotopes give a seasonal profile, which would locate the summer of 1967 at a depth of 140 cm. The discrepancy between the density and isotopic summer is probably due to the isotopic data indicating an unusually warm mid-summer period while the depth hoar (low density anomaly) is usually formed in the fall. The isotope data from 160-240 seems to be fairly homogeneous while the density is markedly lighter than that of the 1967-68. This indicates that meltwater percolation has homogenized the 1966-67 δ -values and at the same time has warmed up the snow when it refroze to the point that vapour was formed. This vapour then formed large crystals of loosely compacted firn similar to depth hoar. This explanation is supported by the fact that large amounts of dense snow and ice below 240 cm prohibited further sampling. However, it does seem almost no mechanic compaction took place. This probably occurs in the third year of the transformation from snow to ice.

The dirt bands occurred in either mid-summer or mid-winter. They most likely are from small dust tornadoes or just high southerly winds coming off the ridge near point Cliff (fig. 26). Small "dust devils" were often observed near point Cliff on a bright sunny day.

Therefore, these dirt layers may be indicators of periods of minimum cloud cover in this area.

The density values indicate that this pit is in a zone of soaked facies. However, one would expect, because of the proximity to the end of the melt season, that the isotopic values would be much more homogenized (MACPHERSON and KROUSE, 1967). It may be that the snow, because of loss of albedo due to the dirt cover, has been heated enough to allow faster compaction, thus giving the high density values. This would allow the pit to be in a percolation zone, yet explain the lack of homogenization of isotopic values and ice lenses.

Snow pit 32E8 is located at an elevation of 2525 m. The density data are very homogeneous, ranging from 0.4 to 0.5. Two light densities are located to either side of the isotopic winter minimum. Since they are not very prominent and are close to the isotopic mid-winter, neither seems to be a fall density (fig. 28a). Similarly, low density measurements can be seen in pit 36E8 at 40 cm and 60 cm. The isotopic profile of 32E8 is strikingly similar to that of 36E8, although the large positive value for the summer of 1966 was not found. This is probably due to faster transformation into extremely hard firn or ice, which was encountered after the 1967-68 budget year (110 cm depth). Again, because of the preservation of the isotopic data, the density values and

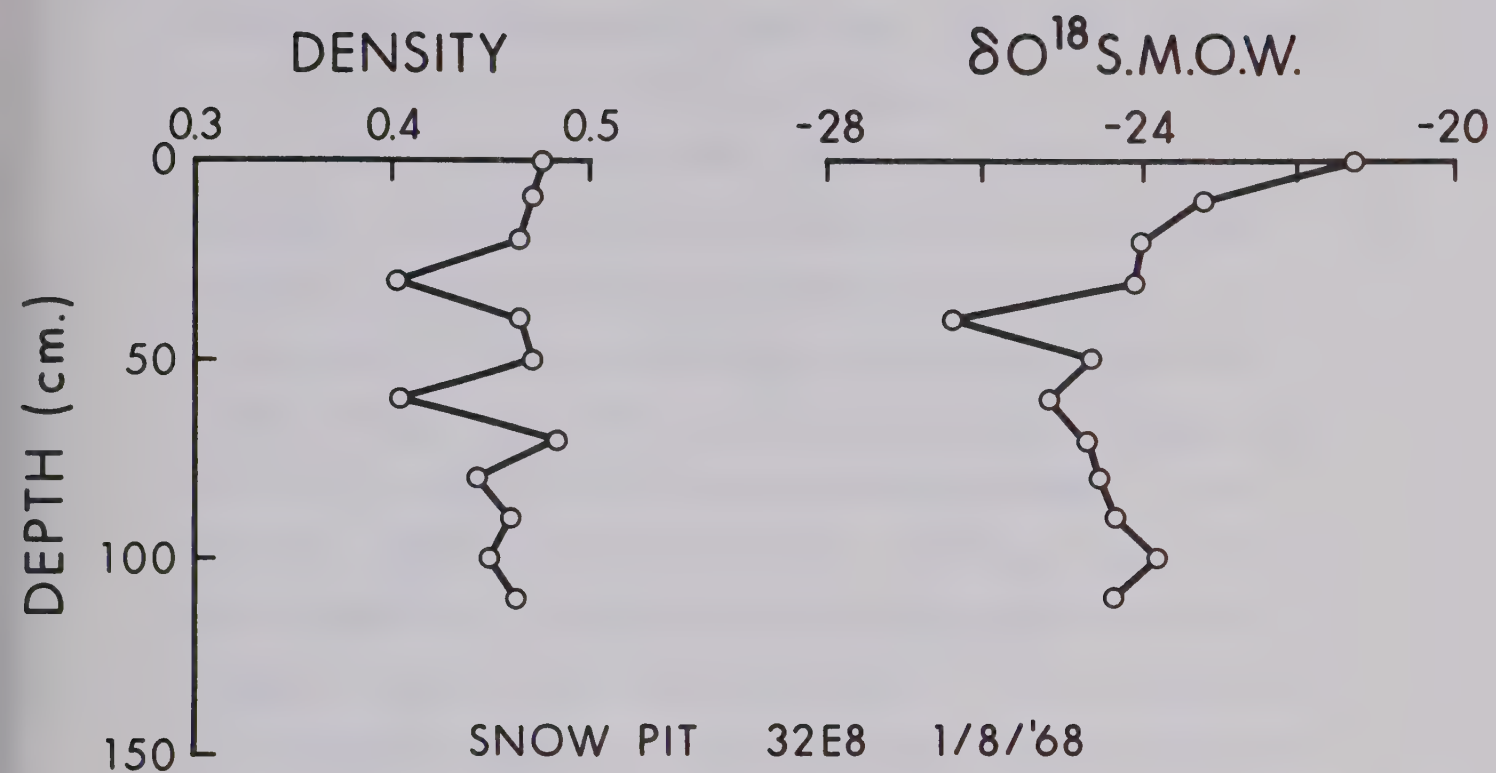


Fig. 28 a)

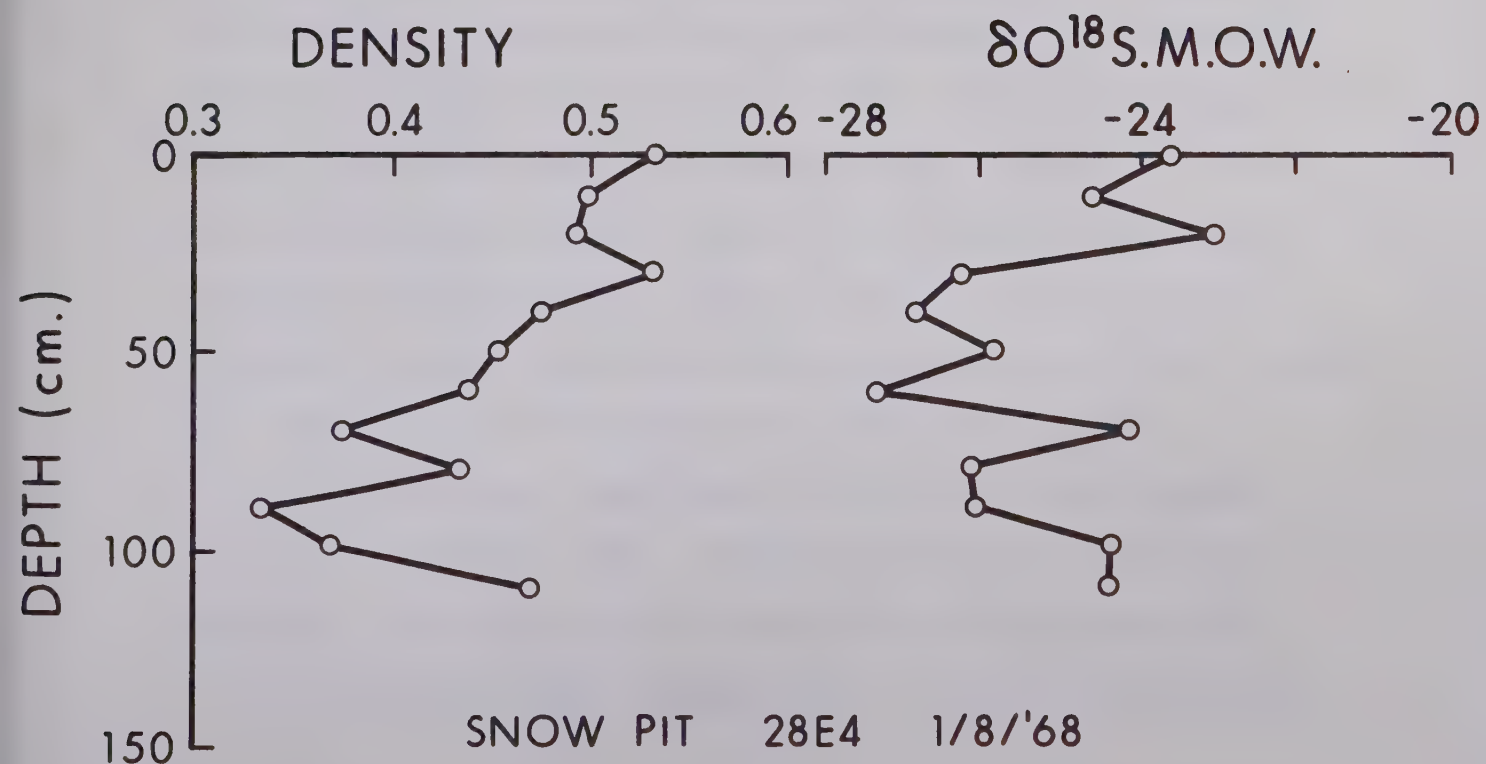


Fig. 28 b)

the general stratigraphic conditions, pit 32E8 was assumed to be in an area of percolation facies.

The snow pit near 28E4 (elevation 2425 m) was sampled on the same day, 1st August, 1968, as pit 32E8. However, homogenization has started and may have penetrated to the previous year by the end of the melt season (fig. 28b). The low density anomaly corresponding to the fall is at 90 cm and the isotopic summer is at 100 cm. Relatively high density at 80 cm and low δ -values at 80 and 90 may correspond to cool periods in the early summer of 1967. Ice was encountered at 110 cm. This pit is believed to be in a transition zone from percolation facies to wetted facies. The reason for the two facies in such a small area with very little elevation change is because of the angle which the northward facing slope of the Fox makes with the sun. Pits 32E8 and 36E8 were both located on steep, northward facing slopes and therefore had a high albedo. The rest of the snow pits were located in much flatter areas. This is consistent with BREWER's (1969) observation that "maximum snow depth occurs in 'pockets' at the bottoms of topographic hills".

The snow pit near stake 36 (fig. 29) was sampled on the 1st August, 1968. Although the recent snow fall gave the isotopic profile a positive peak, the rest of the pit was extremely homogenized. At a depth of 40 cm,

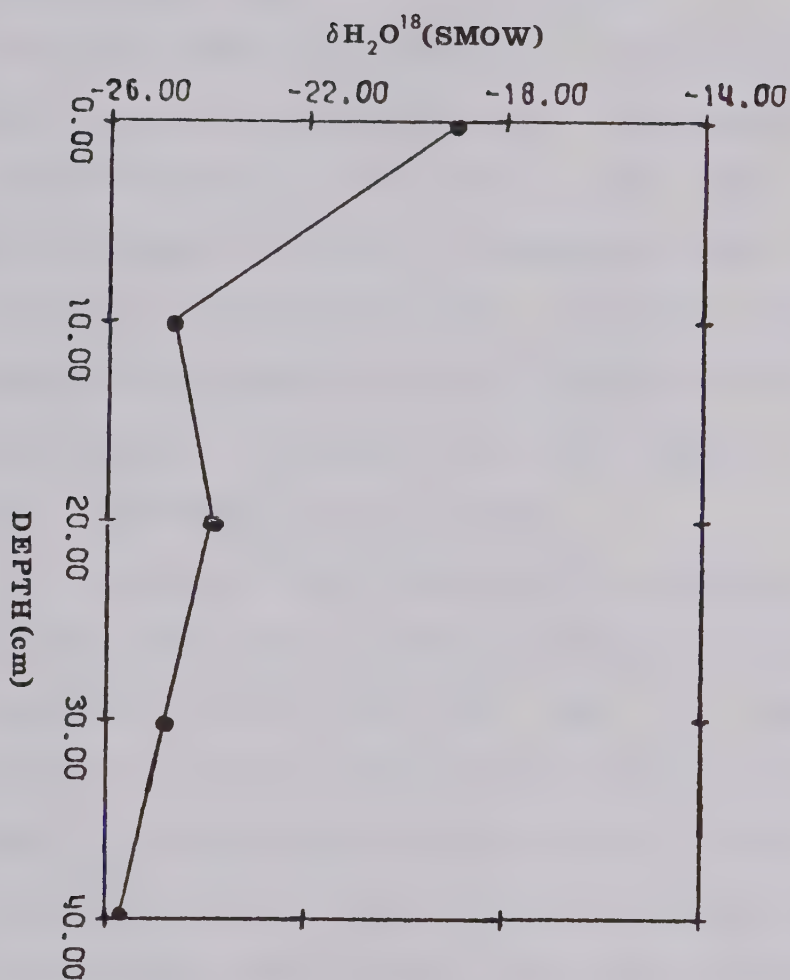


Fig. 29. Snow-Pit 36, Fox Glacier.

ice was encountered. The pit at 32 was similar, except slush had formed at 30 cm. This was as expected, since both pits are located near the slush pond at the top of the accumulation area.

Snow pit 28W4 has dirt layers at 65 cm and 100 cm. Below 100 cm, ice was encountered. The isotopic data show the 1967 summer to be at 90 cm (fig. 30b). Homogenization seems to be well in progress, since the δ -value range is from -21.5 to -26. Tentative temperature and density measurements suggest that this is in a zone of wetted facies. The dirt, as in pit 36E8 is probably from the ridge behind point Cliff.

The snow pit, 24W2, also seems to be fairly well homogenized, even though surface snow gives the isotopic data a definite summer peak (fig. 30a). No isotopic summer peak is obvious for 1967, but the ice at 80 cm is assumed to be the end of the 1967 melt season.

The accumulation area of the Fox Glacier then seems to be divided into two glacial zones with pits 36E8, 32E8 and perhaps 28E4 in the percolation zone, while pits 36, 32, 28W4, and 24W2 are in the wetted zone. The water equivalent accumulation at pit 36E8 is 55.6 cm at 100 cm and 73.0 cm at 140 cm depth. The water equivalents at 32E8 and 28E4 are 45.4 cm and 46.1 cm respectively. Using scanty density data at 28W4 the water

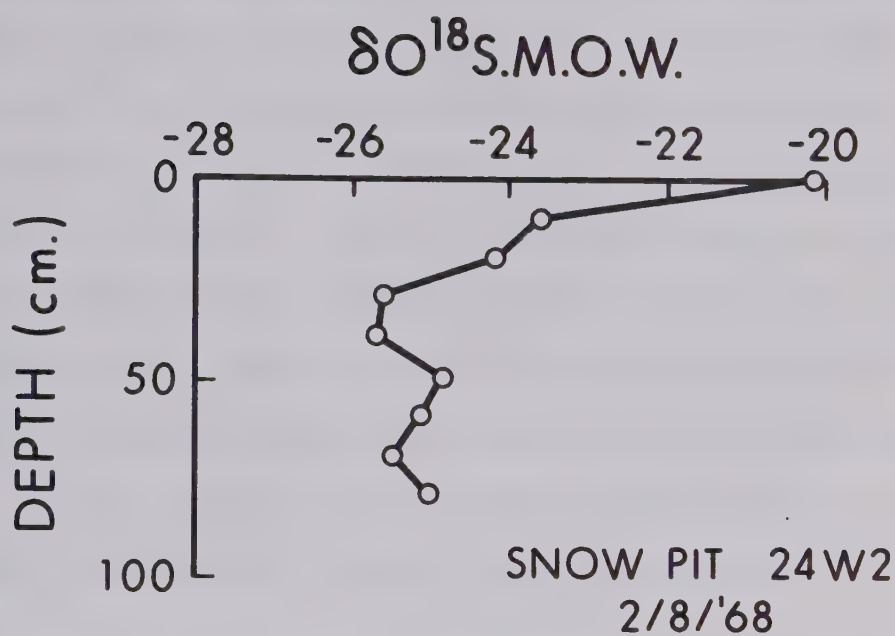


Fig. 30 a)

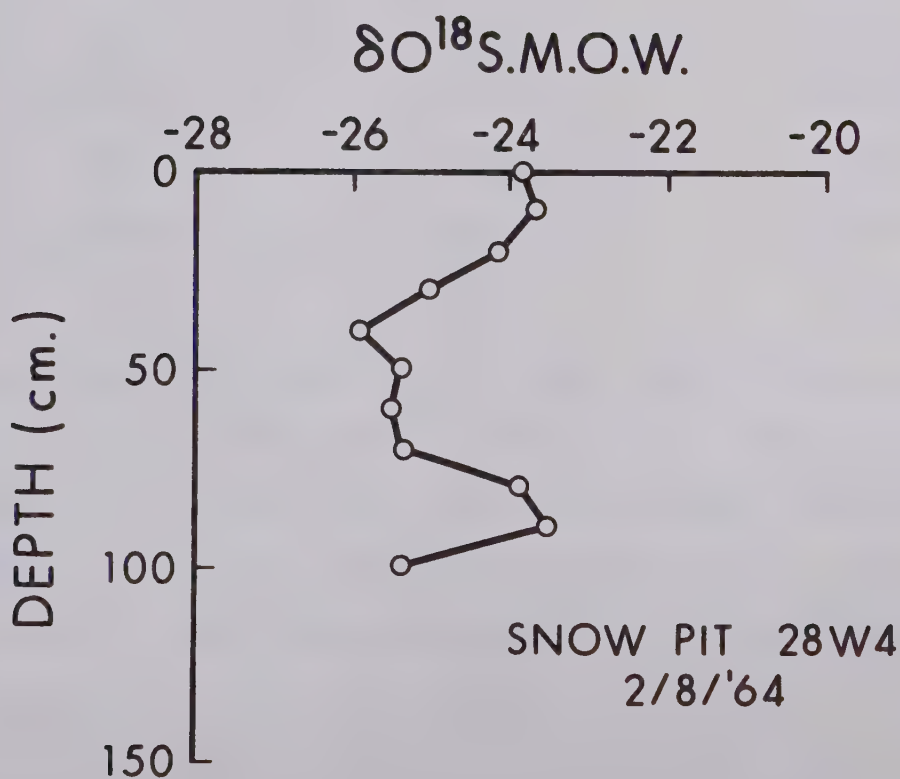


Fig. 30 b)

equivalent is 46.3 cm. Therefore the average accumulation in the wetted zone seems to be near 46 cm of water while in the percolation zone it may be slightly higher. The 73.0 cm (W.E.) at 140 cm in pit 36E8 strengthens the idea that the positive isotopic peak is a mid-summer peak and does not indicate the end of the melt season. Accumulation around stakes 32 to 36 is depleted, probably by drainage into the melt pond south-west of stake 32.

The isotopic average and elevations for all the snow pits except 32 and 36 are given below:

Pit	δ Average	Elevation
36E8	-24.4	2553 m
32E8	-24.1	2528 m
28E4	-25.0	2426 m
28W4	-24.7	2450 m
24W2	-24.3	2350 m

The elevation change on the west side of the glacier gives an isotopic change of $0.4 \text{ }^{\circ}/\text{oo}/100 \text{ m}$. SHARP, ET AL (1960) found $0.5 \text{ }^{\circ}/\text{oo}/100 \text{ m}$ on the Blue Glacier, Washington. However, the east side does not show this, which could be due to the change in glacial zone from wetted to percolation.

2) Cores

Two coring attempts were tried at stake 24. The first on 29th July, 1968 was frozen in at 1.5 m while the

other, which was drilled on 15th August, 1968, froze at 3 m. These freeze-ups were caused by meltwaters running into the holes and refreezing. Possibly because of this meltwater little information can be gleamed from the first core (fig. 31a). The summer positive peak for 1968 is evident, as well as the negative mid-winter peak at 40 cm. After that the results are very homogeneous. The second core shows positive isotopic peaks at the surface, 150 cm and at 300 cm; the negative peaks occurring at 50 cm and 200 cm (fig. 31b). This is far more accumulation than the snow pits indicate, especially since stake 24 is in the immediate area of the firn line. This high indication of accumulation is more than likely due to superimposed ice. Unfortunately, the core was broken up so that the ice in the core could not be identified as superimposed or glacier ice.

ii) Lower Glacier

Lower glacier sampling was done to elucidate the glacial flow patterns. The flow of the Fox Glacier is controlled by 4 factors (fig. 26);

- 1) It is a glacier with a presumed history of surging.
- 2) It apparently has not moved since its last surge.
- 3) An arm on the west side goes over the ice falls before joining the main stream.

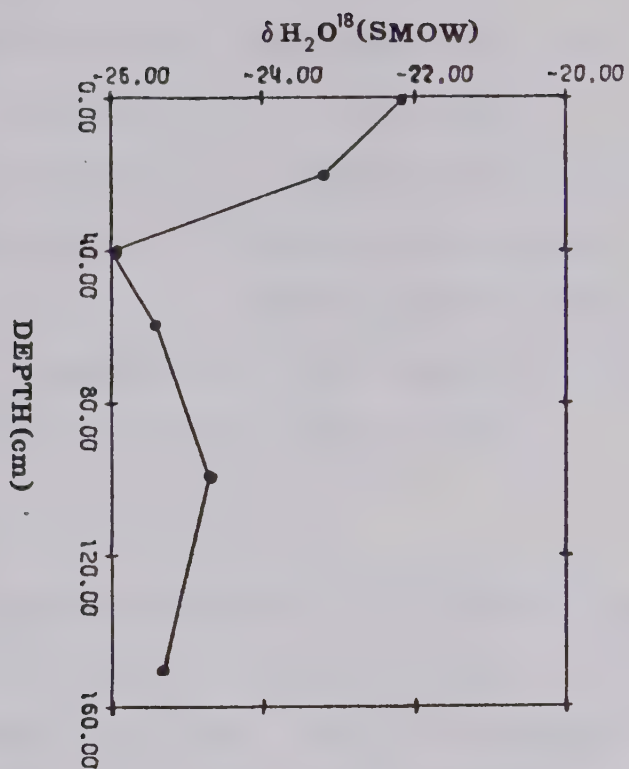


Fig. 31 a) Firn Core at Stake 24 (29/7/68)

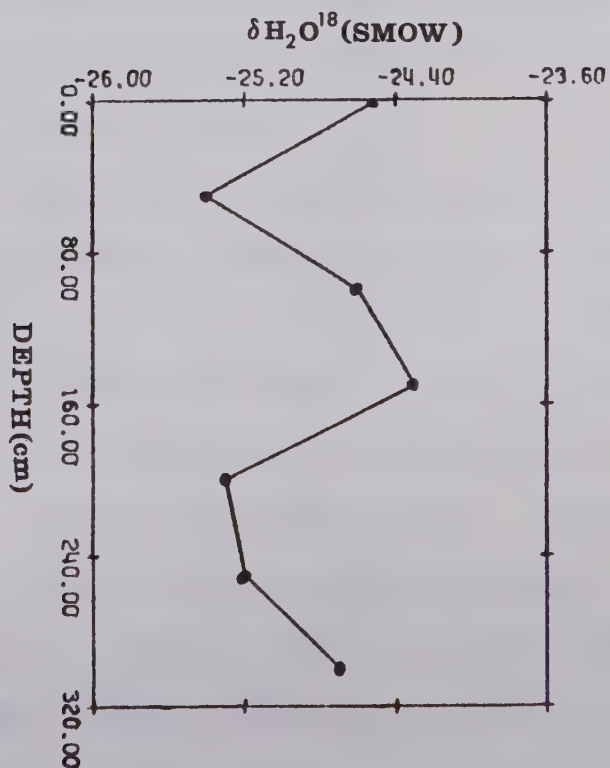


Fig. 31 b) Firn Core at Stake 24 (15/8/68)

- 4) The Jackal has surged over part of the Fox
(stakes 7 to 11, fig. 26).

Surface sampling of 4 traverses and a longitudinal profile was undertaken. Two cores were sampled at stakes 2 and 7 as well as snow and rainfall at the camp just west of stake 8. Sampling was also carried out on the ice falls of the west arm of the Fox Glacier.

1) Traverses

A peak in positive δO^{18} values (see * in fig. 32) in all traverses is assumed to mark the boundary of the Fox and its west arm. This is consistent with the flow lines which are evident in the aerial photograph of the Fox taken by the Canadian Defence Force in 1965.

The oxygen isotope data on the western portions of the traverses must be considered in conjunction with;

a) the ice falls.

b) distortion and contamination by the Jackal.

The moraine-covered samples at stake 6 are possibly superimposed ice. The rest of the δ -values west of the asterisk in figure 32 show no trends. This is expected since the flow had been perturbed by the ice falls. The traverse at stake 7 was terminated at 7W0.6 because of the presence of the melt stream and the Jackal.

The east sides of the traverses show that the edges of the main stream have more positive δ -values than the

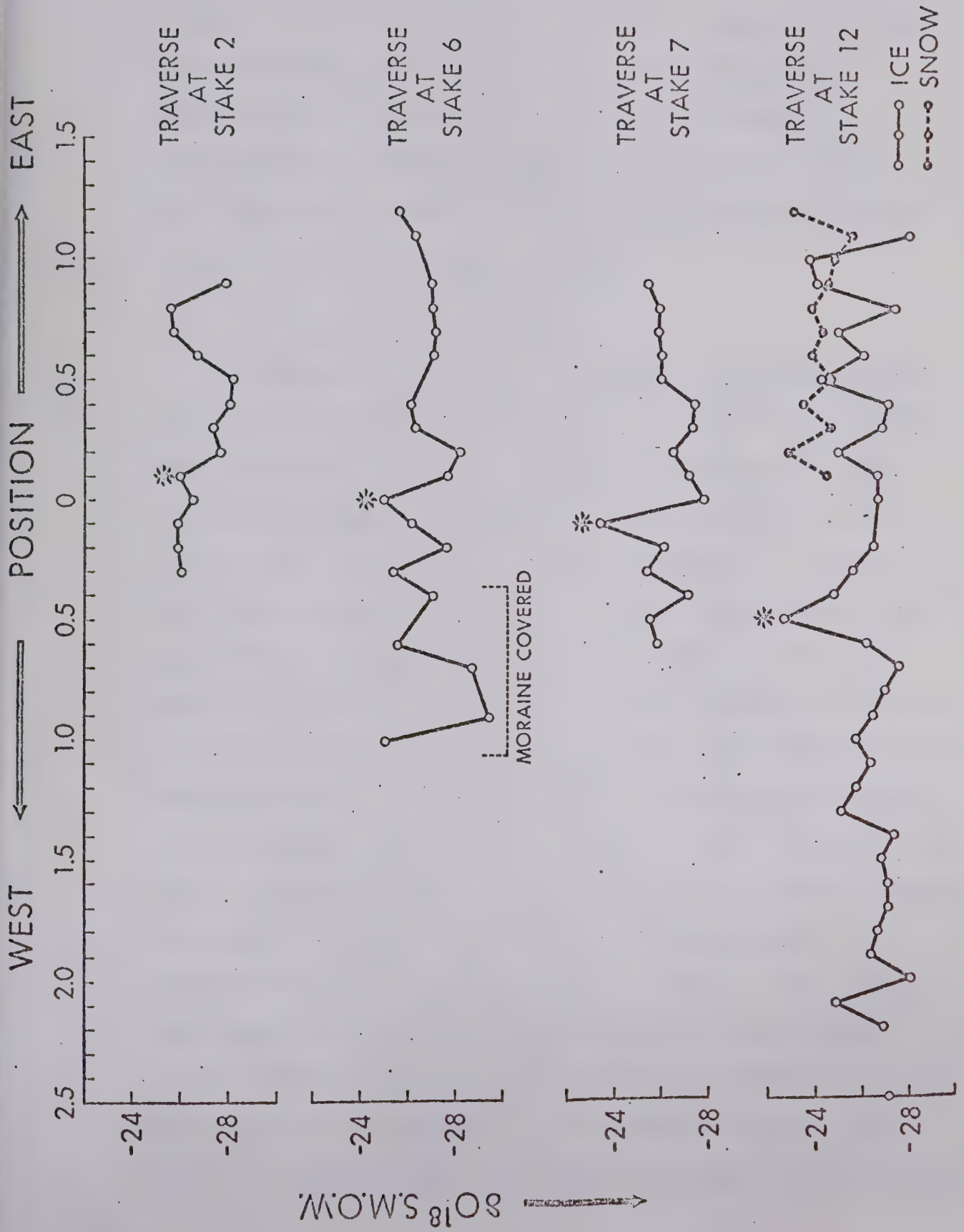


Fig. 32. Isotopic Traverses of the Fox Glacier.

centres, which is consistent with the centre ice moving faster than the sides (fig. 25b). The inconsistent variations in δ -values below the snow at stake 12 is probably due to varying degrees of meltwater contamination, while the δ -value at 2E0.9 is attributed to superimposed ice from the lateral moraine.

2) Longitudinal Profile

A longitudinal profile was made by sampling at the centre survey stakes from 1 to 12. The δO^{18} results are given in figure 33. From surface observations on the Fox Glacier, this longitudinal profile appeared to be in the centre of the main arm of the glacier. However, from the results of the traverses, one can see that such a profile goes from the main arm at stake 12 into the west arm by stake 2 (fig. 32). It was therefore necessary to apply a position correction so the longitudinal profile would not cross several flow lines. The criterion chosen was an average of the minimum values of δO^{18} found to the east of the asterisk in figure 32, i.e. the centre of the main arm, for stakes 7, 6, and 2. Unfortunately, no sampling was done east of stakes 3, 4 and 5. The values near stake 8 are possibly contaminated by the terminus of the Jackal. The rest of the δ -values, because of their position, were considered to be representative of the centre of the main arm. The corrected longitudinal profile

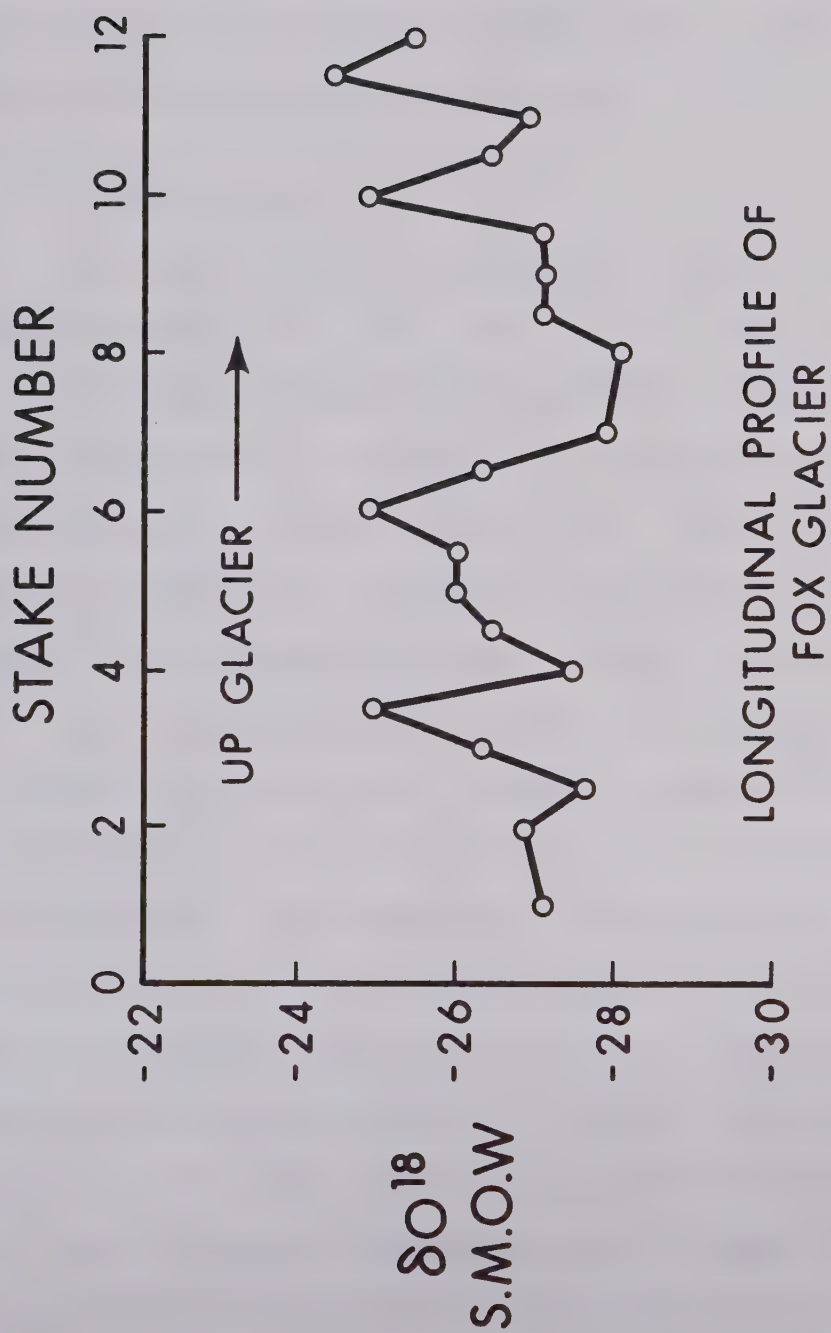


Fig. 33. Uncorrected Longitudinal Profile of the Fox Glacier.

gives a positive slope (fig. 34). This indicates that this particular surging glacier's flow is similar to the general mechanism proposed by REID (1896). Although this general observation cannot distinguish between Robin's, Weertman's or Lliboutry's theories, it does cast doubt on the ice dam, powder flow theory of NIELSEN (1969) for this particular glacier.

3) Ice Cores

Ice coring was made practical by the chain saw motor adaption (see II.1, b)). The core at stake 7 was drilled until it became physically impossible to retrieve the core, while coring at stake 2 was stopped because of meltwater entering the hole at 5 m. Unfortunately, these cores, according to figure 32, are located on opposite sides of the boundary between the west and main arms.

The variation found in the core at stake 7 (fig. 35) is almost as great as the variation found in the longitudinal profiles (fig. 33 and fig. 34). (A discussion as to whether the trend observed in figure 34 is significant is given near the end of this chapter). It is difficult to assess whether these variations are remnants of seasonal variation or general climatic changes. However, because of the size and surging properties of the glacier, this ice is probably not more than 300 years old. Further interpretations are rendered impossible by the unknown

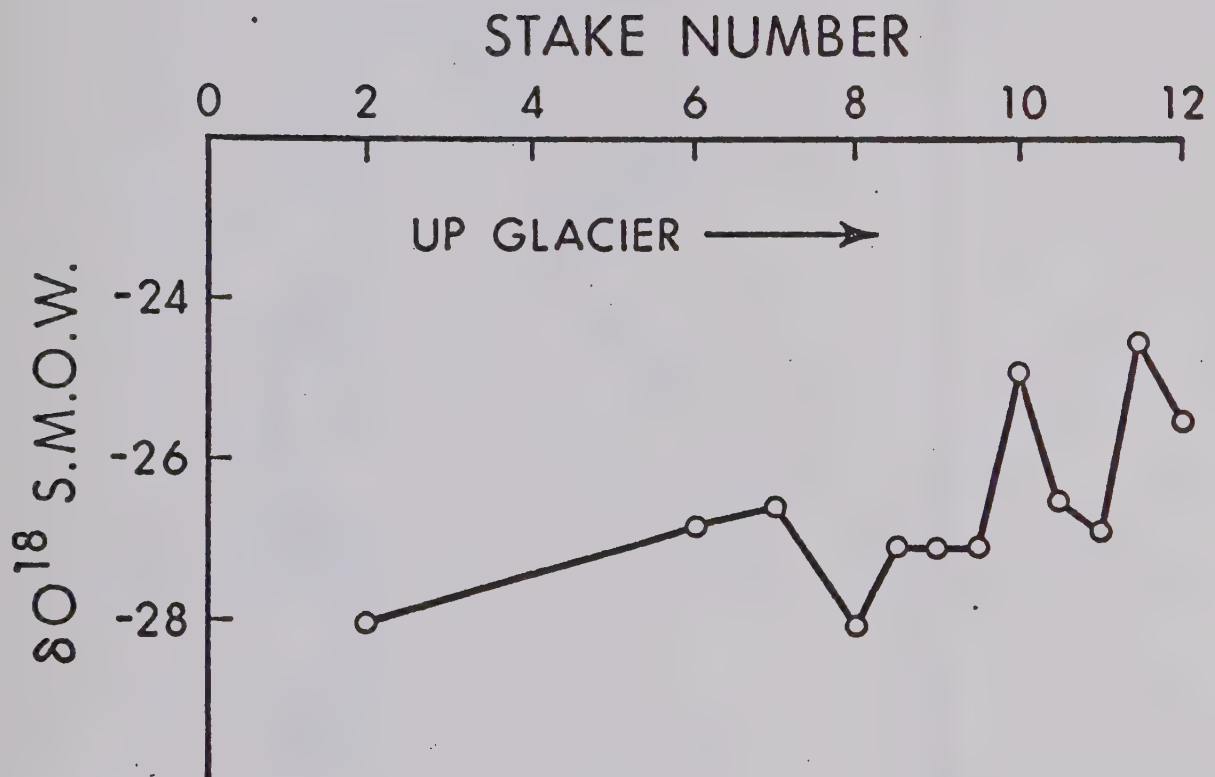


Fig. 34. Corrected Longitudinal Profile of the Fox Glacier.

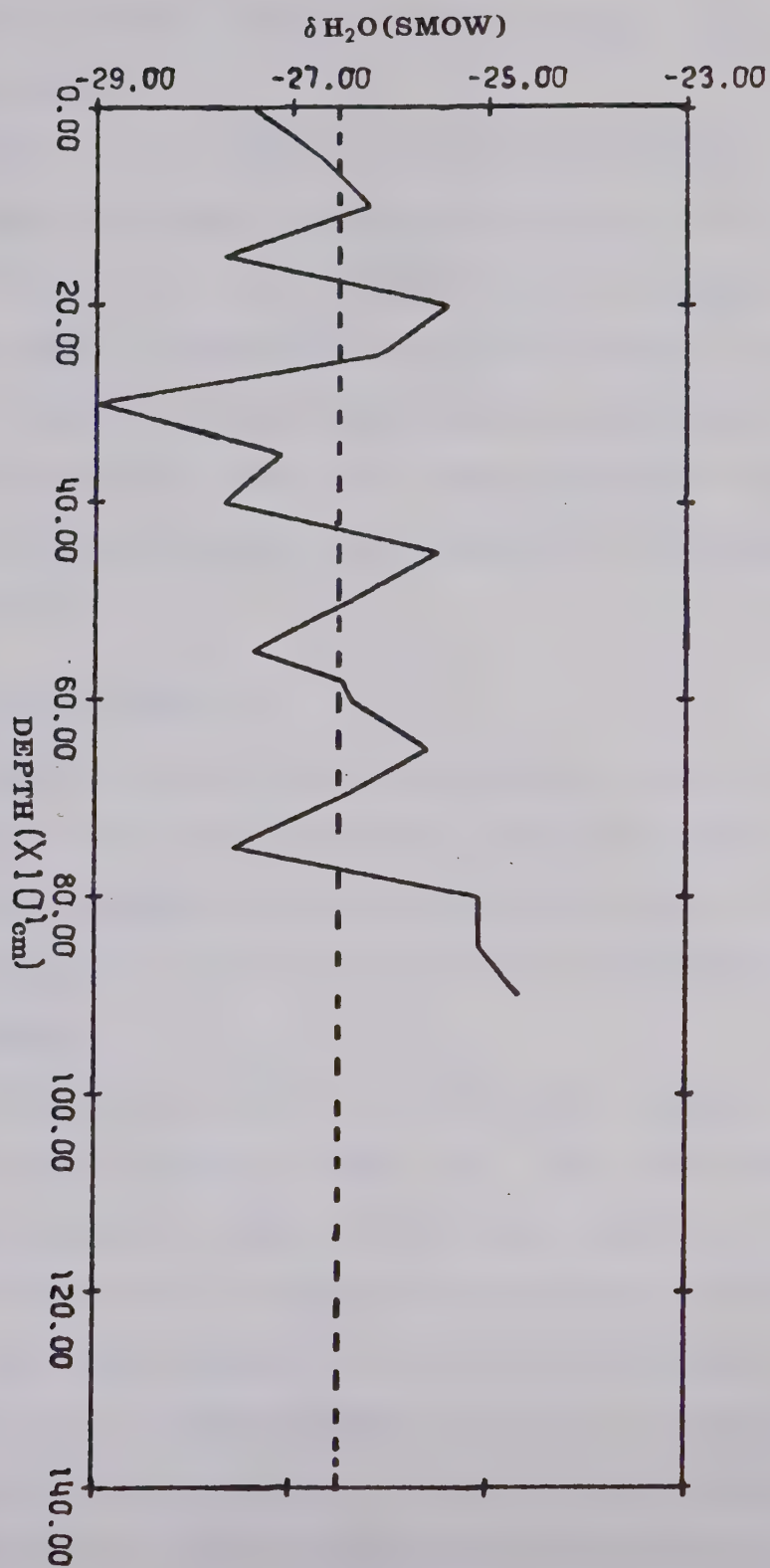


Fig. 35. Ice Core at Stake 7, Fox Glacier.

parameters of this glacier's flow history, i.e. the period of surge, etc.

The core at stake 2 was more homogeneous. The only large deviation from the average δ -value (-25.8 ‰) was at 50 cm (fig. 36). Whether this corresponds to the negative peak at 300 cm of the core at stake 7 is impossible to say. Correspondence between the cores is not expected, however, since the cores probably experienced different histories by being located in different arms of the Fox.

4) The Icefalls

Icefalls are formed by glaciers going over cliffs or areas of very steep descent. The ice tends to break apart, into blocks, forming a giant staircase riddled with crevasses. Two traverses and a longitudinal profile were sampled.

The traverses were located at the bottom and on top of level, or step, 1 (fig. 26). The two traverses are very similar except for the very negative δ -value at 15 m north of Pt. Don in the traverse at the bottom (fig. 37). This sample was covered by moraine and therefore may be superimposed ice and not representative of the body of the glacier. They are also similar to the traverse at stake 12 from 12W0.5 to 12W1.5.

The longitudinal profile gives more positive δ -values the higher the level (fig. 38). This, like the

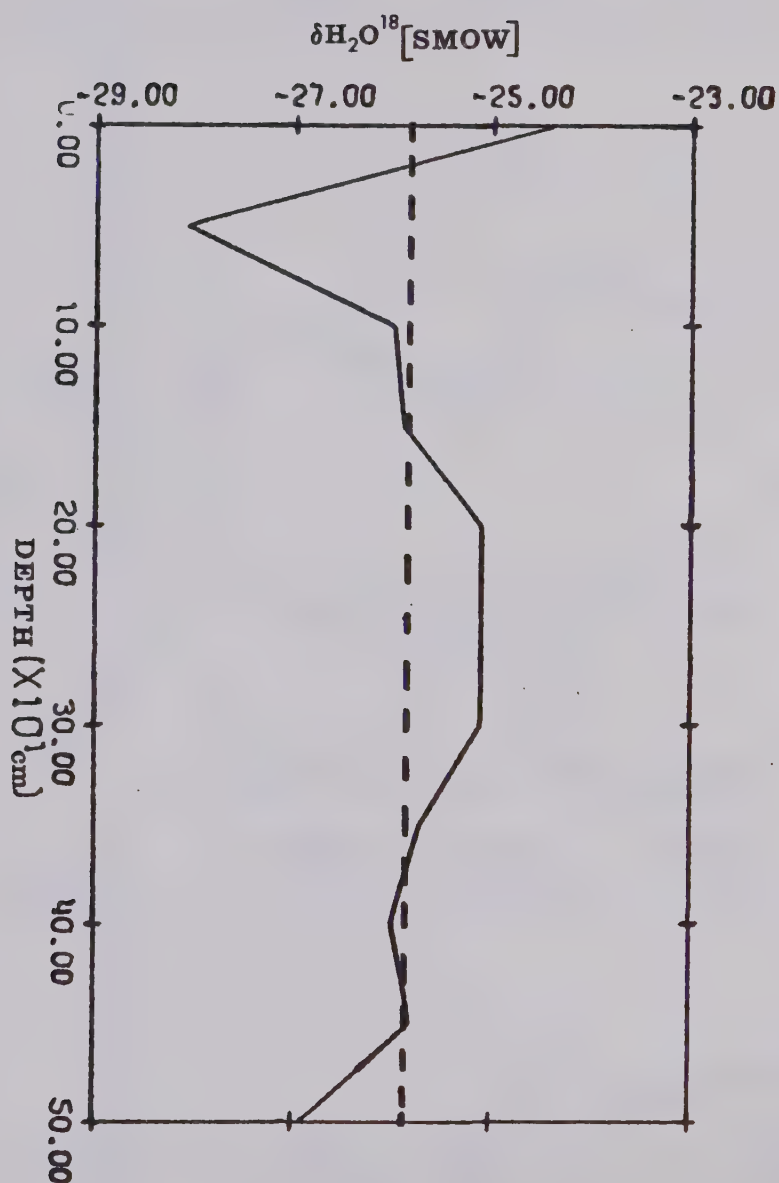


Fig. 36. Ice Core at Stake 2, Fox Glacier.

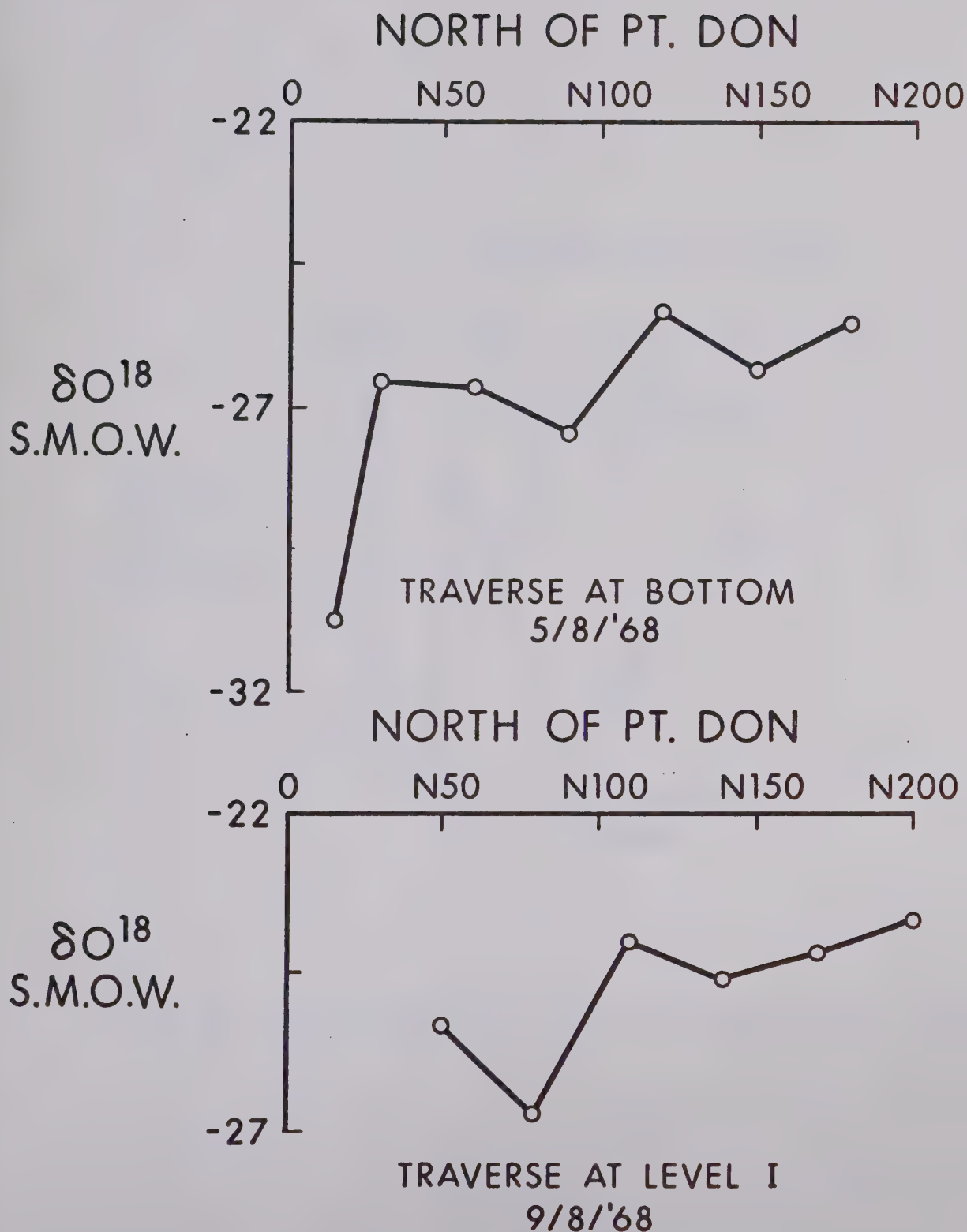


Fig. 37. Icefalls Traverses on Fox Glacier.

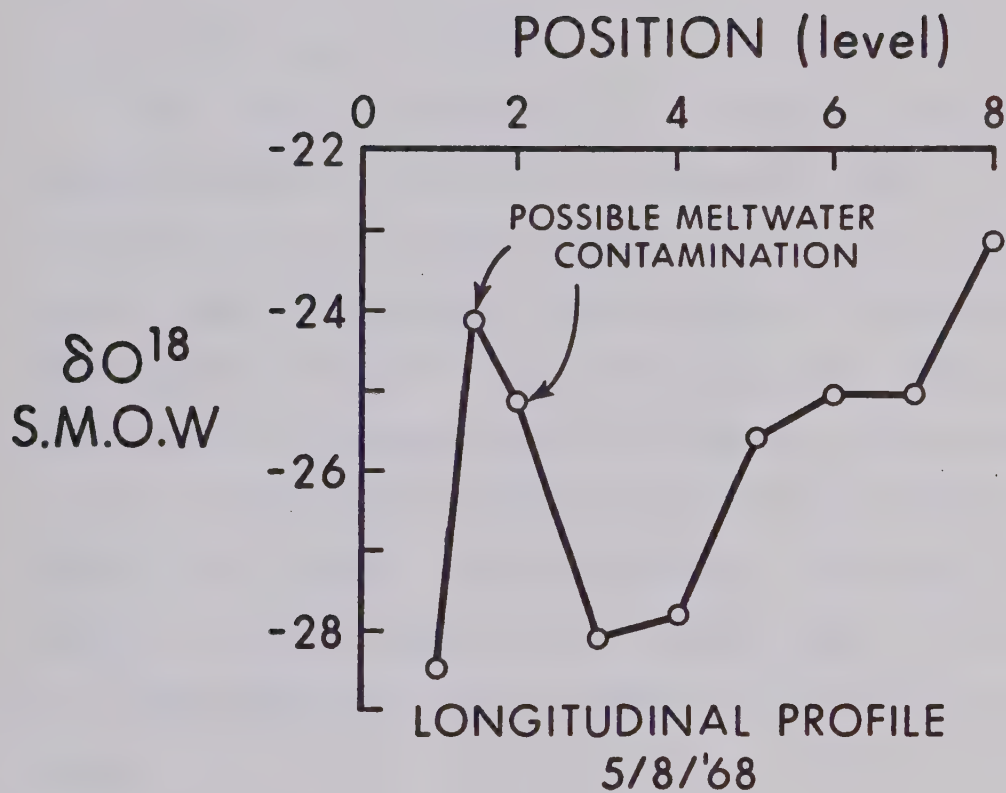


Fig. 38. The Fox Glacier Ice falls' Longitudinal Profile.

longitudinal profile of the main arm, is consistent with a flow similar to REID's (1896). This trend is not seen below the icefalls, which probably represents the re-orientation of the blocks of ice by the time they reach the bottom of the icefalls.

5) Snow and Rainfall

The snow and rainfall at Fox Camp was very sparse during the period of 6 July to 8 August, 1968. A total of 9.3 cm (W.E.) of precipitation fell in the form of rain or snow. Relatively large amounts of precipitation fell on July 25 and 27. On both days, snow samples were collected on a traverse from the Fox Camp (near stake 7) to Point George (an elevation difference of 350 m). However, no altitude trend was found. Also rain and snowfall samples were collected at Fox Camp. The average δO^{18} and temperatures at the time of deposition are given below:

	Temperatures ($^{\circ}\text{C}$)	δO^{18} ($^{\circ}/\text{oo}$)	Description
July 25	2.5	-14.8	rain
	3.2	-16.5	snow (traverse)
July 27	1.3	-20.9	snow (traverse)
	0.3	-20.0	snow (from south)
	1.6	-18.0	rain (from north)

All of the $d\delta O^{18}/dt$ values range from -0.9 $^{\circ}/\text{oo}/^{\circ}\text{C}$ to $+2.43$ $^{\circ}/\text{oo}/^{\circ}\text{C}$, with the average being 1.27 $^{\circ}/\text{oo}/^{\circ}\text{C}$.

These values are not very consistent with the values found by DANSGAARD (1964) and PICCIOTTO, ET AL (1960) of $0.69 \text{ }^{\circ}/\text{oo}/^{\circ}\text{C}$ (equation 13) and $0.95 \text{ }^{\circ}/\text{oo}/^{\circ}\text{C}$ (equation 11) respectively. This inconsistency is believed to be caused by the glacier's moderating effect on the air temperatures, since all temperature measurements were taken directly above the glacier surface (MARCUS, 1965).

Two storms on July 27 were sampled hourly. The results were as follows;

	Time	$\delta\text{O}^{18} \text{ (}^{\circ}/\text{oo)}$
1st	4 p.m.	-17.0
	5 p.m.	-17.2
	6 p.m.	-21.9
2nd	8 p.m.	-17.8
	9 p.m.	-18.8
	10 p.m.	-20.7
	11 p.m.	-21.2
	12 p.m.	-21.6

Both storms' δ -values became more negative as the storms progressed. In order to determine whether this effect is due to reservoir depletion, temperature changes or a combination of both, a detailed temperature regime would have to be known. However, if one applies isobaric cooling to the Rayleigh condensation formula (equation 10), from an initial temperature of 20°C , the above δ -

variations would correspond to a depletion from 18% of the original vapour reservoir to 10% of the original vapour reservoir. Since small amounts of precipitation were observed, and this area is directly east of Mt. Wood, i.e. perhaps in Mt. Wood's rain shadow, these depletion figures do not seem unreasonable.

d) Discussion

Applying equation (13) to the average δ -value of the snowpits of the Fox Glacier (-24.5%), gives an average yearly temperature of -15.8°C . Applying the lapse rate of $.65^{\circ}\text{C}/100\text{ m}$ (GREW and MELLOR, 1969) to the yearly average temperature of Bethel, Alaska, a maritime station and Whitehorse, Yukon, a continental station and averaging the results, one gets a temperature of -15.2°C for an elevation of 2460 metres (the average snow pit elevation). This agreement suggests that the isotopic composition of precipitation on the Fox Glacier is due to a mean yearly temperature near -15.8°C and a combination of marine and continental weather patterns, such as found at Divide.

The rapid transformation of snow to ice (one year in wetted facies, 2 to 3 years in percolation facies) seems to be an effect of both the surging and temperature properties of the Fox Glacier. The last surge has lowered the slope of the accumulation area, allowing heavy melting from direct radiation, while the sub-

freezing temperatures of the Fox refreeze much of this percolating meltwater into ice when it makes contact with the previous annual layer. Dirt layers, from the surrounding ridges, also seem to play an important role in this transformation by lowering the albedo of the surface snow.

The lower glacier results are very similar to the results of SHARP, ET AL (1960) on the Blue Glacier, Washington. Their longitudinal profile also showed a small "inversion" of the δ -values below the firn line. However, in this case a core taken below the firn line was extremely homogeneous. Since the Blue Glacier is about the same size as the Fox, one might expect to see similar paleoclimatic variations in both glaciers. Accepting the Blue Glacier's homogeneous results as proof of little or no paleoclimatic trends in glaciers of this size, two explanations of the δO^{18} variations in the lower glacier cores of the Fox are as follows;

- 1) These variations may be preserved seasonal variations. However, this seems unlikely because of the homogenization of the δO^{18} observed on the Fox in the wetted facies and on Divide in percolation facies (MACPHERSON and KROUSE, 1967) by the end of the melt season.
- 2) These variations may be due to firn and snow recently incorporated into the crevasses caused by the surging of the Fox Glacier.

If the latter explanation is correct, then the longitudinal profile of figure may be significant, since most of these samples should represent old glacial ice.

A peak in δO^{18} corresponding to a boundary between 2 arms (marked by a medial moraine) was also found on the Blue Glacier. However, MACPHERSON and KROUSE (1967) and EPSTEIN and SHARP (1959a) found no such peak, but both of these studies based their traverses on very few samples. It would seem that if a traverse is sampled in enough detail, boundaries between arms of glacier may be identified. The identification of boundaries may have important applications in the interpretation of glacier dynamics. In the case of the Fox, this information elucidates the basal hot spot reported by CLASSEN and CLARKE (1971) at stake 16W2. The isotope data would identify this feature with the west arm. Since the basal hot spot is just below the icefall, it may be a consequence of the icefall rather than the surging properties of the glacier as suggested by CLASSEN and CLARKE (1971). This interpretation does not exclude this temperature regime from being a contributing factor to the surging properties of the Fox; rather it allows for another mechanism to create the temperature regime.

CHAPTER IV

PEYTO GLACIER

IV.1 Introduction

a) Description

The Peyto Glacier, a temperate glacier, is situated approximately 40 km northwest of Lake Louise in Banff National Park (lat. 52°N , and long. $116^{\circ}30'\text{W}$). It is the northernmost outlet from the Wapta Icefield and drains through Peyto Lake to the North Saskatchewan River. The Peyto has a surface area of 13.7 km^2 and is 60 % ice covered (STANLEY, 1970). The terminus has retreated about 1 km since this glacier was first observed in 1897 (ØSTREM, 1966). Although the Peyto had a positive mass balance of 0.09 metres in 1965, negative mass balances (ranging from -0.11 m to -0.80 m) have been recorded from 1966 to 1969, the 1969 mass balance being -0.65 metres (STANLEY, 1970).

The maximum accumulation is slightly greater than 200 cm (W.E.) whereas up to 350 cm (W.E.) is removed from the lowest part of the glacier tongue by ablation. The mean summer temperature at 2200 m elevation ranges between 0°C and 15°C with 7°C being the mean, compared with a 3°C for the Fox (2150 m elevation).

Sampling was carried out between 2200 m and 2350 m elevation, on the tongue of the Peyto Glacier. The

equilibrium line was at approximately 2600 m in 1969 (YOUNG, 1970). Unfortunately no sampling was done above the equilibrium line.

b) Other Investigations

As part of the Canadian contribution to the International Hydrological Decade, glaciological studies of the Peyto Glacier were begun in 1965. As stated in section IV.1 a), mass balance studies have been conducted since 1965 with an average result of -0.33 metres (W.E.). DERIKX and LOIJENS (1970) studied the hydrology of the Peyto. Topographical and radiation studies have also been carried out on the Peyto Glacier.

YOUNG (1970) has tried to relate the shape of the glacier surface to the patterns of accumulations and ablation. Unfortunately this study is not yet completed, but mapping of the slopes, azimuths, accumulations, net losses and concavities versus convexities has been achieved.

GOODISON (1970) measured the total global radiation at many points over the glacier. Correlation between azimuth and slopes, and the measured radiation could be seen, however, these correlations alone did not dictate any statistically meaningful relationship between radiation and ablation.

IV.2 Isotopic Data

A total of 86 surface samples were analysed. They ranged in value from -19.1 ‰ to -25.4 ‰ (S.M.O.W.) with the average δ -value being -20.7 ‰ (S.M.O.W.). Using equation (13), the mean annual temperature for these δ -values would be -10.7°C . Applying the lapse rate of $0.6^{\circ}\text{C}/100$ m to Banff and Edmonton one gets mean annual temperatures for Peyto of -6.0°C and -9.1°C . The warmer temperature predicted by the Banff data may be due to the chinooks experienced at Banff (which may not be experienced at Peyto). Also, the more negative temperature given by equation (13) could be a result of the glacier δ -values being representative of a colder climatological period, such as the 18th century. $\text{H}_2\text{O}^{18}/\text{H}_2\text{O}^{16}$ analyses of the snow in the accumulation would clarify these alternatives.

The surface samples were taken from thirteen traverses between 2180 m and 2350 m. The averages of these traverses show no trends. However, the average δ -values at 10 metre elevation spacing do show the δ -values getting more negative, figure 39, as the altitude decreases, which is an indication of a flow such as proposed by REID (1896, see fig. 25c). The δ -value at elevation 2180 is the ratio of a single sample and therefore may not be representative of this altitude.

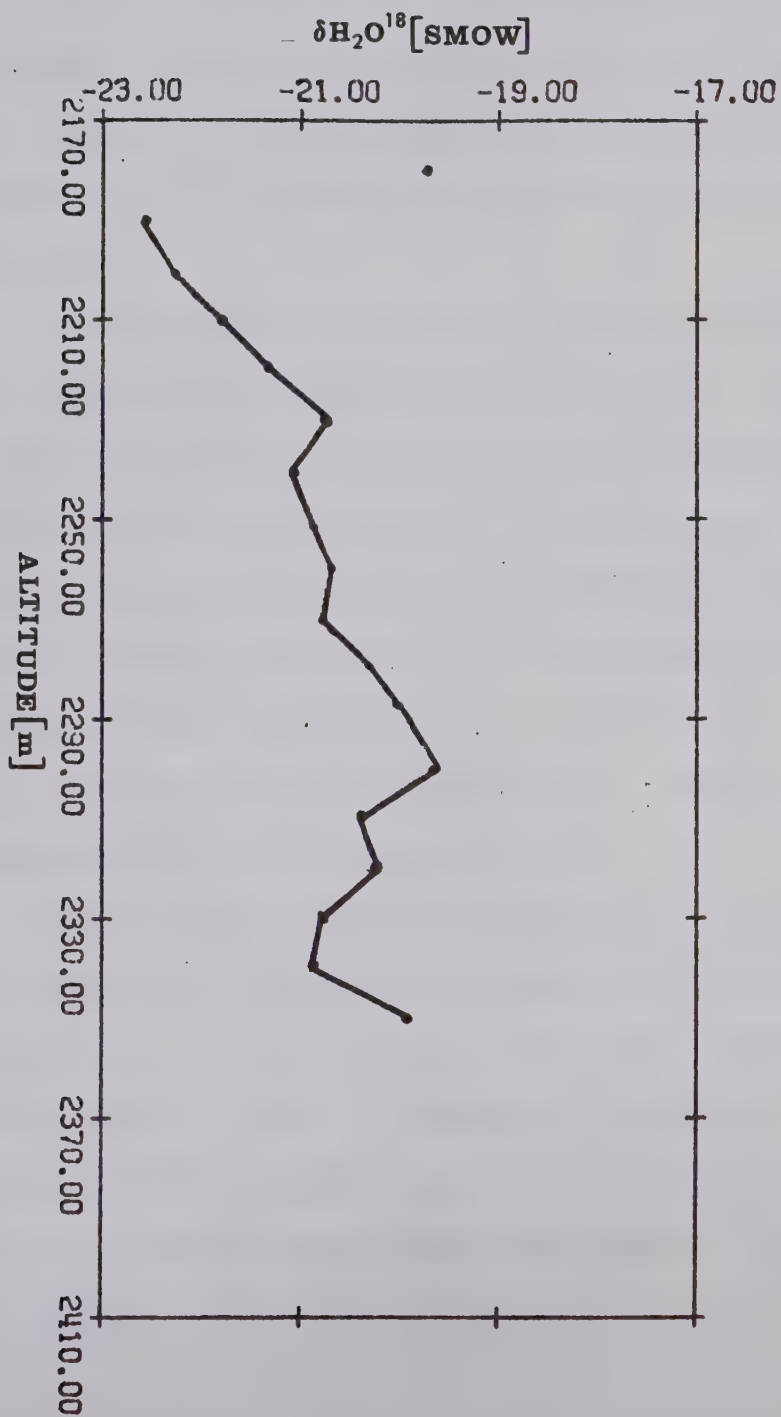


Fig. 39. Longitudinal Profile, Peyto Glacier.

This "inverse" trend is very similar in magnitude to the results at the Fox Glacier and therefore is subject to the same criticism considered in section III.4, ii), 2). However, due to the larger number of Peyto samples the result reduces the speculative aspect considerably. The Peyto data were sufficiently numerous to permit iso- $\delta^{18}O$ contouring. A computer program was used to rule out human bias.

This program plots three types of contour diagrams; a raw data contour map, a polynomial fit (up to degree 8) to the data which is called a trend surface and a residual contour map, which is a map of the differences between the observed data and predicted values obtained by the trend surface fit. The original program was written by D.B. McIntyre, D.D. Pollard and R. Smith of the Kansas State Geological Survey. Details of its operation are given in Appendix A.

The contour map of the raw data, figure 40, does not reveal much information about the pattern of distribution of the $\delta^{18}O$ isotopes. The very negative anomaly between the 2nd and 3rd traverses from the left is a function of the computer program and probably would not appear if sampling had been done there. The thick black line is the outline of the glacier.

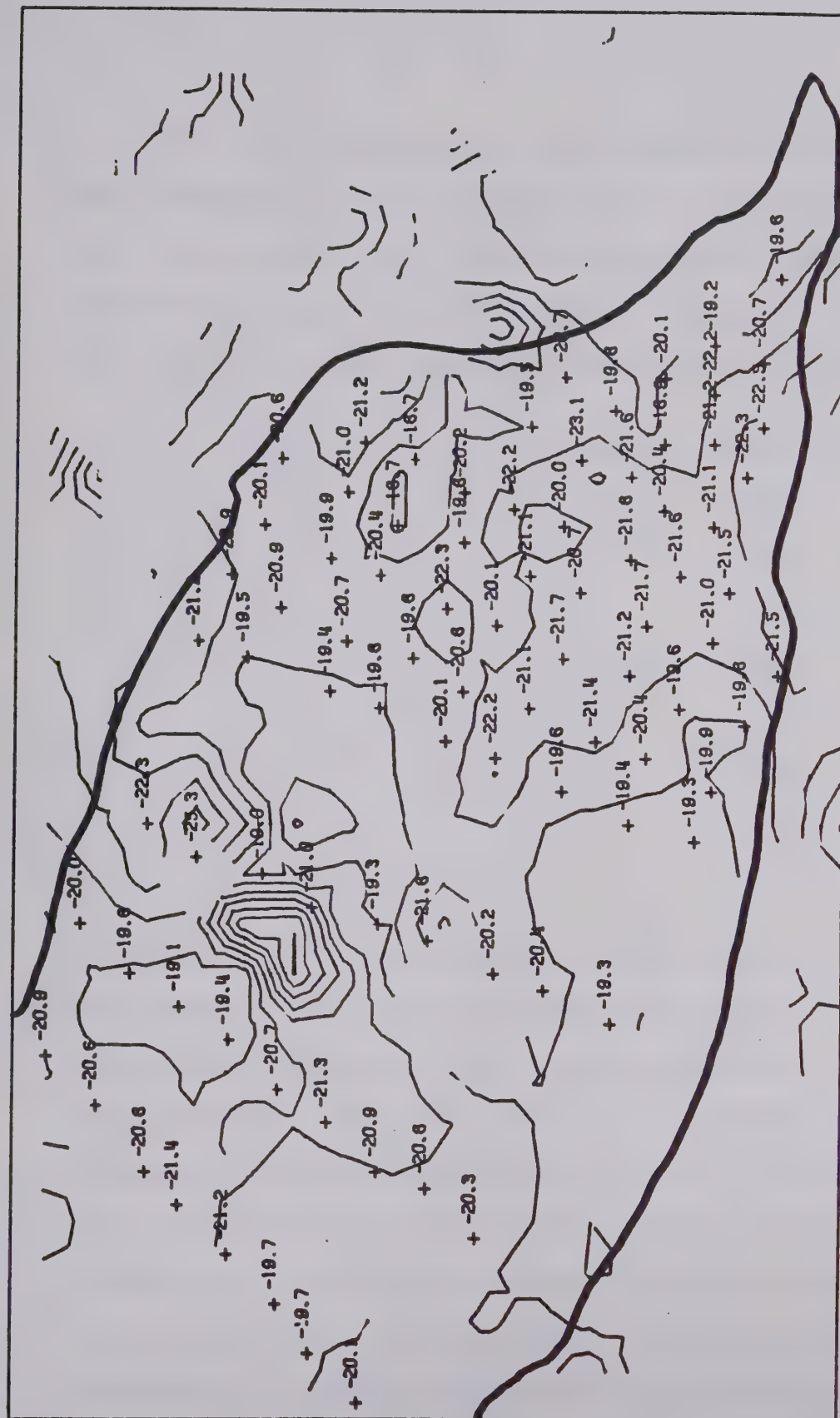


Fig. 40. Raw Data Plot, Peyto Glacier.

```

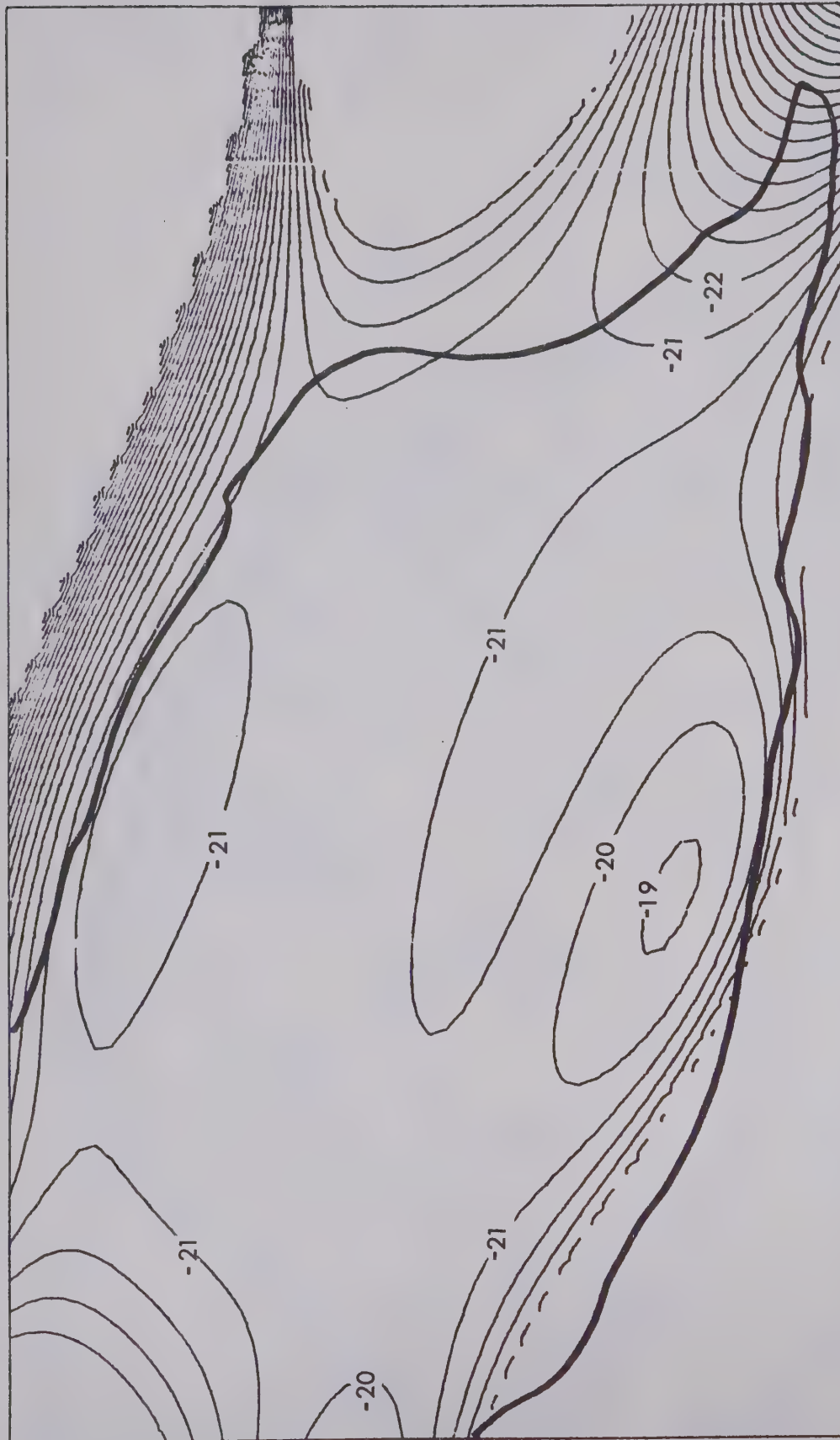
      PCTO      GLACIER
      RAW DATA

```


The trend mapping was then applied to see if a more coherent isotopic pattern could be seen (figs. 41-48). As expected, the higher the degree of the polynomial the more detail was revealed by the contours. However, the coefficients of correlations varied as follows:

Degree	Coefficient of Correlation
1	.00867
2	.04991
3	.14133
4	.19951
5	.30046
6	.40530
7	.13230
8	_____

Therefore the 6th degree trend surface seems to be the best overall fit. This, however, does not exclude some of the other polynomial fits from being better localized trend surfaces. The 5th, 6th, and 7th degree trend surfaces show similar patterns (figs. 41, 43, 45). From these patterns the glacier seems to have a zone of minimum δ -values down its centre. To either side of this minimum zone, more positive δ -values are encountered. These zones in turn are surrounded by more negative zones which are near the edge of the glacier, except in the middle of the eastern edge. Here relatively positive contours extend right to the edge of the glacier.



TREND SURFACE 5 DEGREE
PEYTO GLACIER

Fig. 41. 5th Degree Trend Surface Plot.

Fig. 42. 5th Degree Residual Plot.



TREND SURFACE 6 DEGREE
PEYTO GLACIER

Fig. 43. 6th Degree Trend Surface Plot.

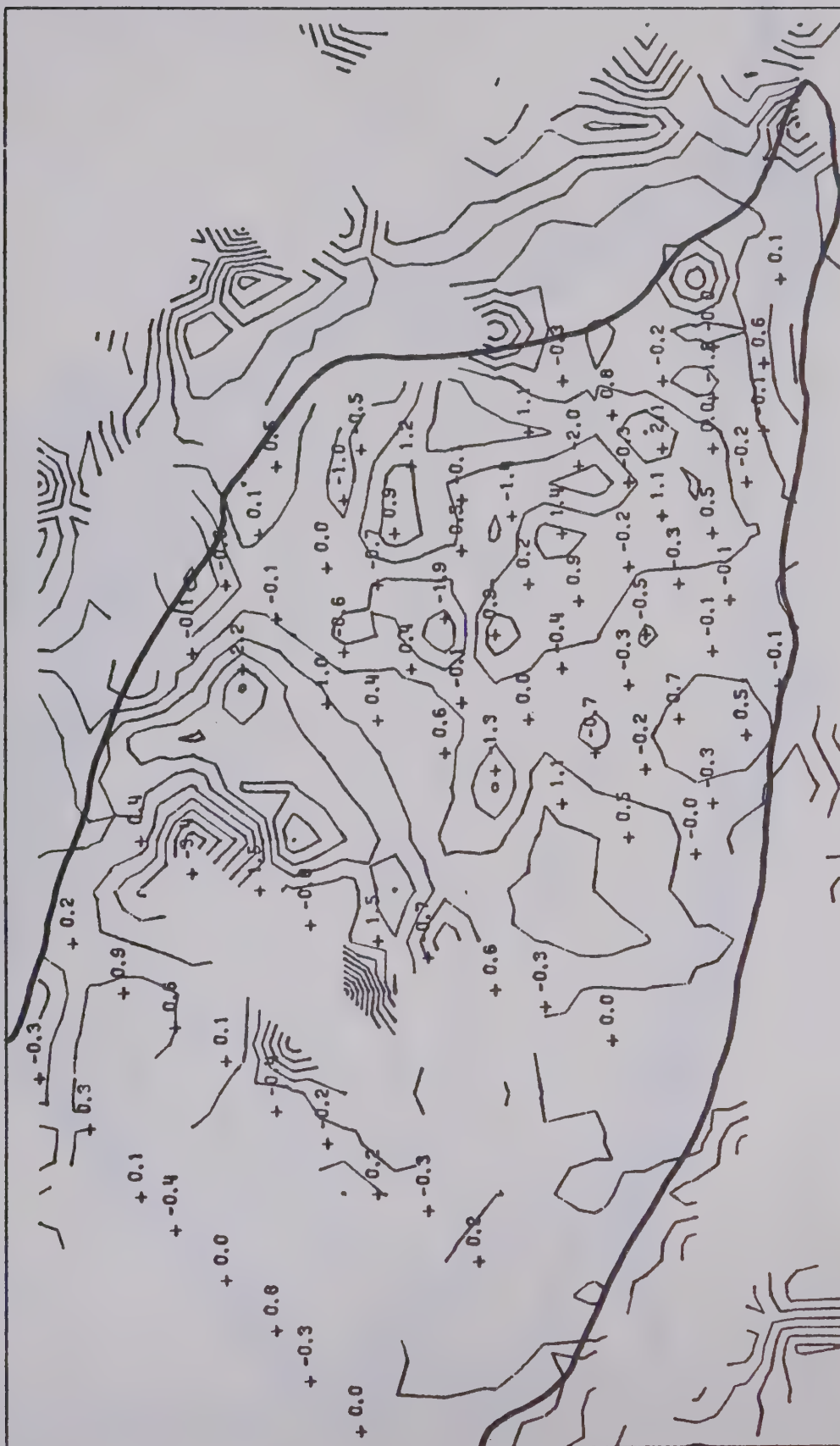
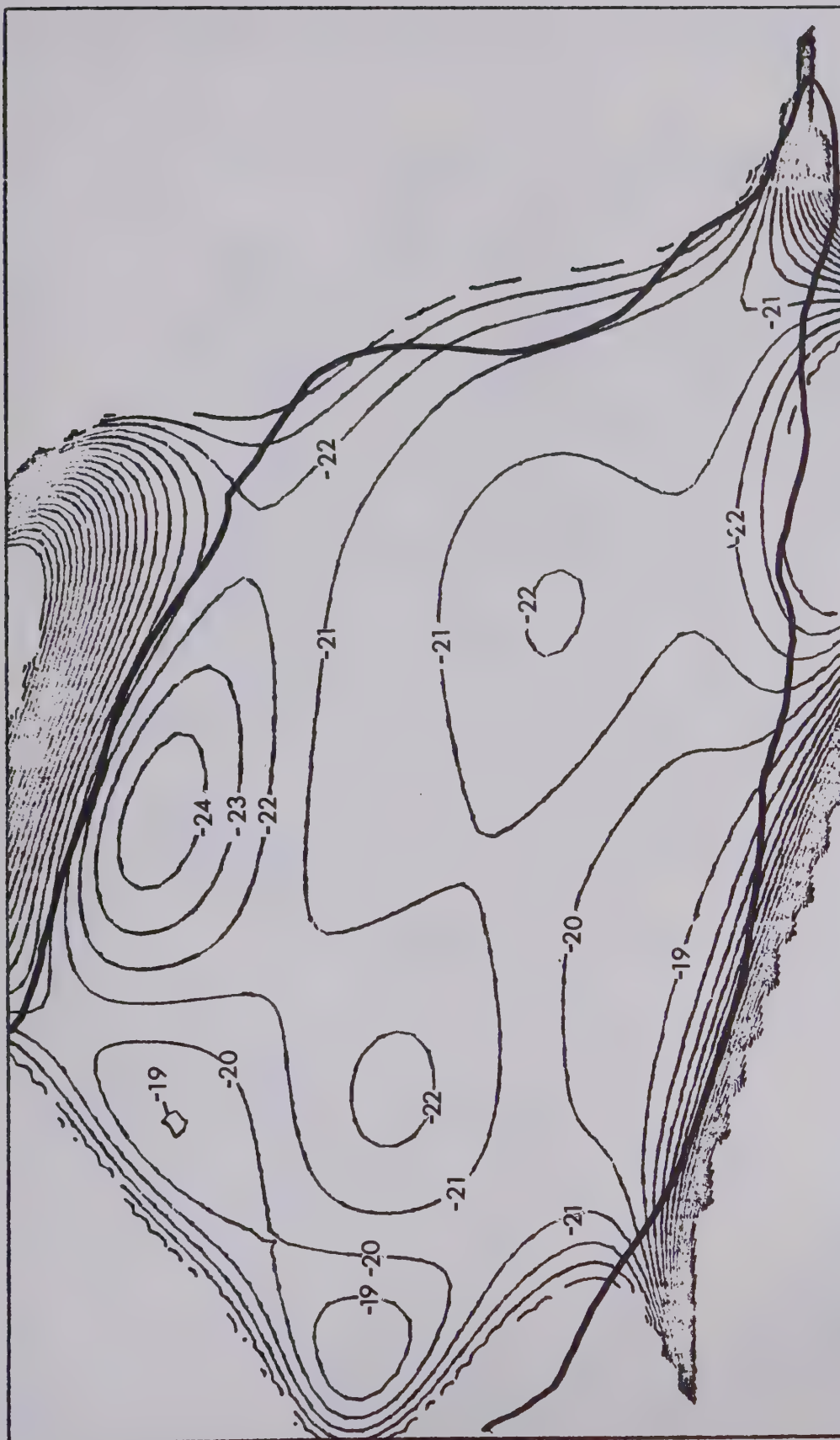


Fig. 44. 6th Degree Residual Plot.



TREND SURFACE 7 DEGREE
PEYTO GLACIER

Fig. 45. 7th Degree Trend Surface Plot.

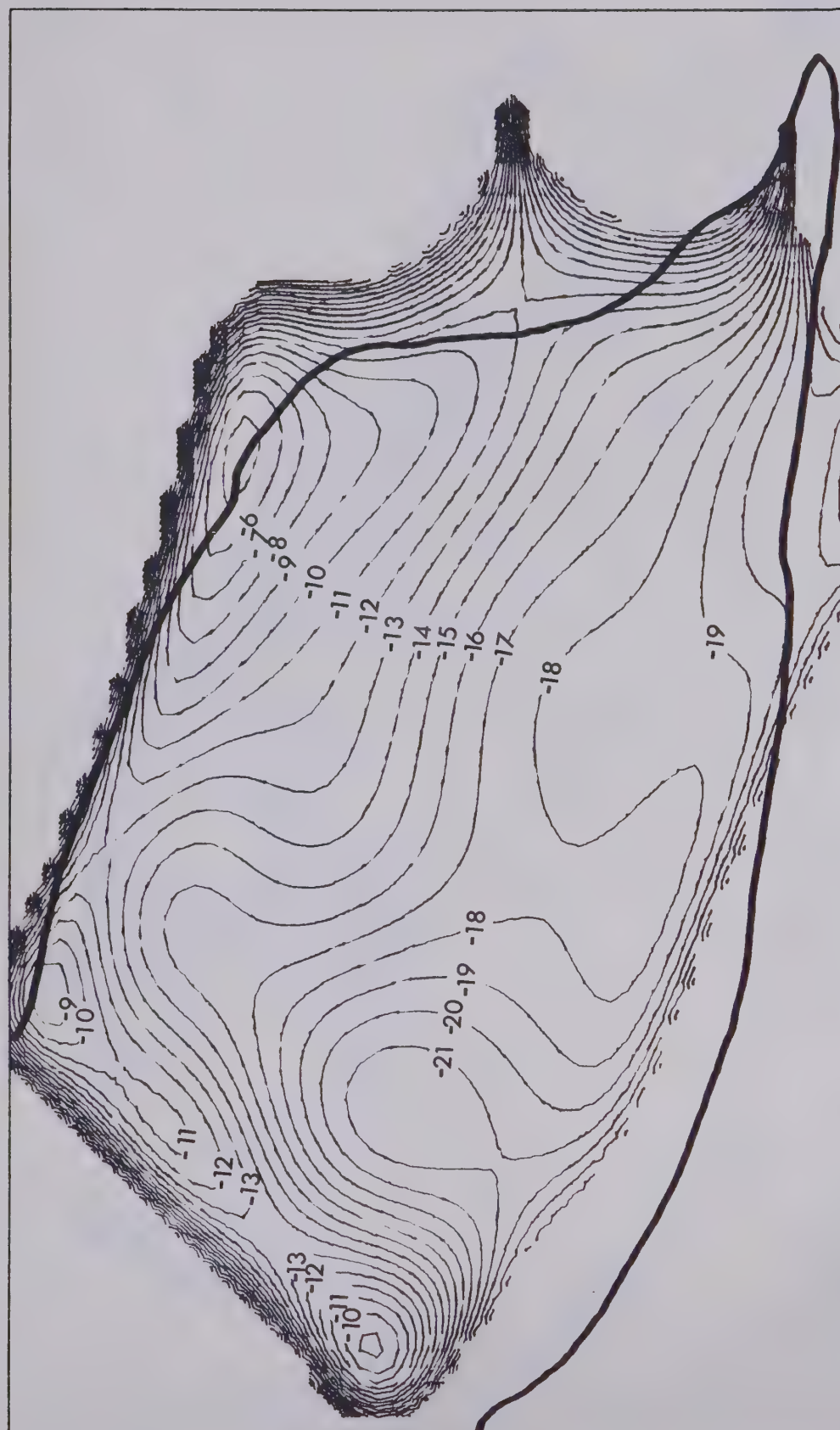


Fig. 47. 8th Degree Trend Surface.

TREND SURFACE 8 DEGREE

PEYTO GLACIER

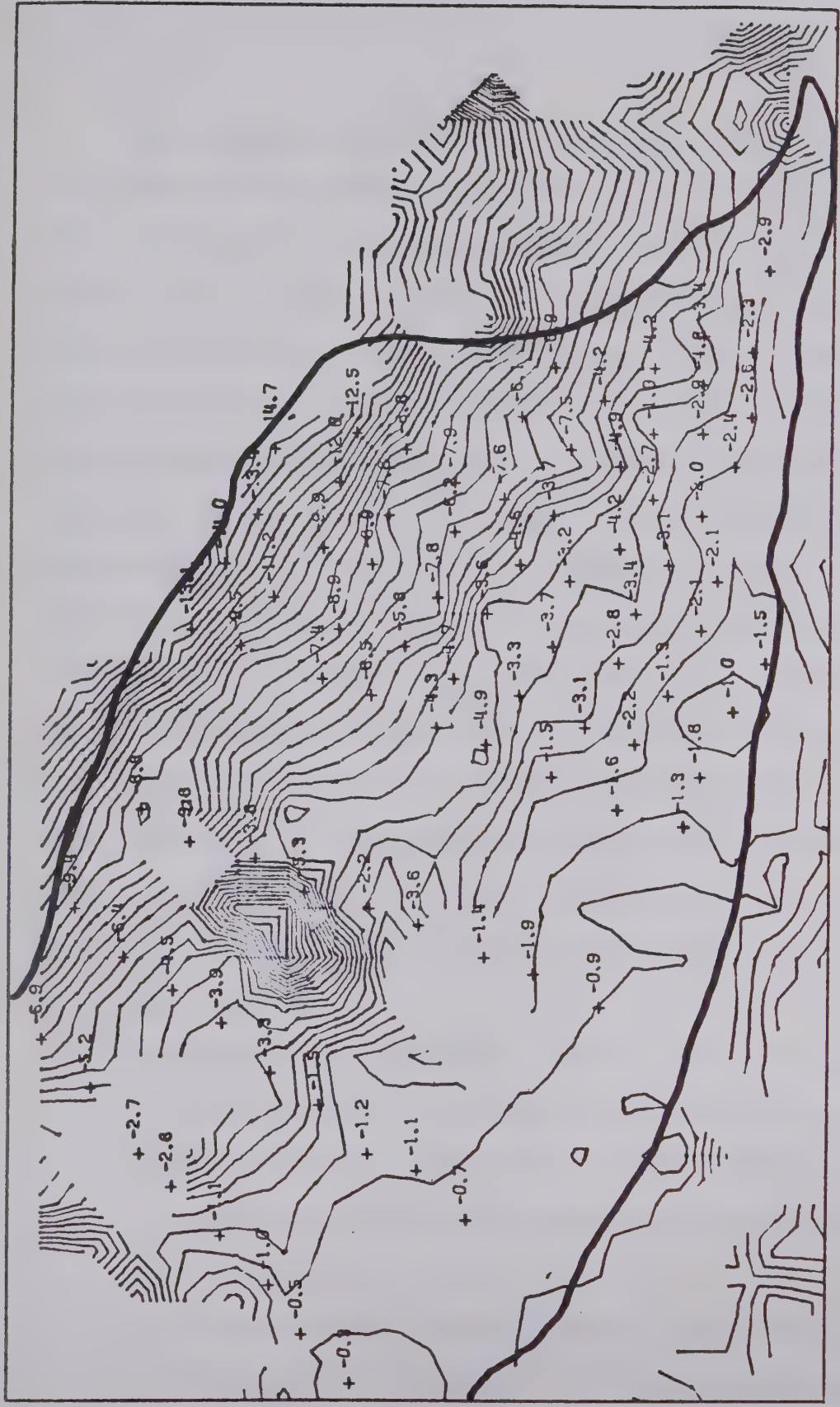


Fig. 48. 8th Degree Residual Plot.

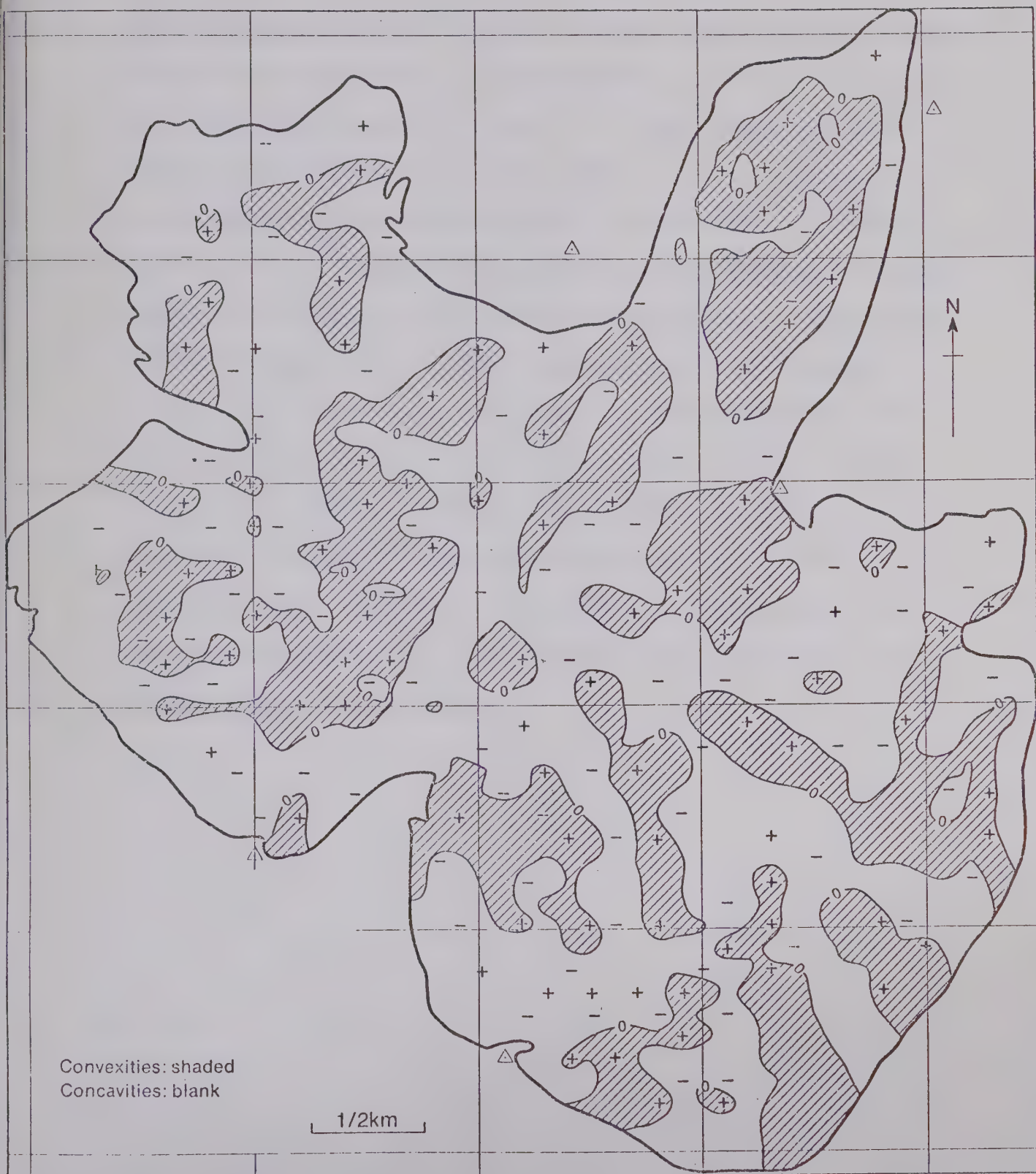
The shape of the accumulation area (fig. 49) would lead one to believe that three arms of ice would form the tongue. Considering REID's (1896) flow, as in the case of the Fox Glacier, one would expect relatively positive δ -values at the edges with two positive peaks to differentiate the arms. As stated above, this has not been found, but rather a negative, positive, negative, positive and then negative type of isotopic traverses has been indicated. EPSTEIN and SHARP (1959a) invoked the following argument to account for their isotopic data obtained from the transverse profiles of the Saskatchewan; severe ablation may expose deeper layers of ice which originated at higher elevations and hence the stream margins might have more negative δ -values than the stream centres. This explanation allows the glacier's isotopic pattern to be interpreted in the following manner:

- a) The central negative zone would be corresponding to the centre of the middle accumulation basin.
- b) The relatively positive zones on either side would be the positive peaks that differentiate the arms.
- c) The relatively negative zones occurring at the edges of the glacier would represent the northern and southern accumulation area's arms.

- d) No positive peak is recognized at the glacier's edge due to severe ablation (greater than 200 cm of water per year, YOUNG, 1970).

Another interesting correlation can be seen when the 6th degree surface trend (fig. 43) is compared to the concavities and convexities of the glacier's tongue (fig. 49, YOUNG, 1970). The convexities correspond very closely with the more negative δ -values position, while the concavities correspond to the more positive δ -values positions. This is what one would expect when one considers the reflective properties of these shapes and the preferential evaporation of the lighter isotope. This correspondence seems to warrant closer examination. It may be that sublimation (ice to water vapour) in areas of severe ablation plays a more important role than expected in the melting process. If this is so, isotopes in these areas would be a measure of sublimation as well as altitude. Extensive surface sampling of the accumulation area and then correlation with the surface shape would settle this question.

The altitude change on the Peyto is from 2200 m to 3000 m, however, the equilibrium line lies at about 2550 m. This leaves only 500 m of altitude to affect a change in the isotopic values of the snow and ice. Accepting SHARP ET AL (1960), and FRIEDMAN and SMITH (1970) values of $-0.5 \text{ } ^\circ\text{/}\text{oo}/100 \text{ metres}$ ($4 \text{ } ^\circ\text{/}\text{oo}/100 \text{ metres}$



PEYTO GLACIER

Fig. 49. Concavity/Convexity

for deuterium) for O^{18} , the variation due to the altitude effect alone should be approximately $2.5 \text{ }^{\circ}/\text{oo}$. This is the variation found in figure 40. This small elevation change coupled with the heavy melting is the cause of relatively homogeneous δ -values of the Peyto. It would seem that for smaller temperate glaciers, isotopic effects might be too small to be of any significance. The effect of the temperature on this homogenization of isotopic variations can be seen when the standard deviation of the isotopic values of Fox Glacier ($\pm 2.0 \text{ }^{\circ}/\text{oo}$), a small glacier (3.6 km as compared to 5.0 km), is compared to the Peyto Glacier's standard deviation ($\pm 1.2 \text{ }^{\circ}/\text{oo}$). However, even with the large amount of homogenization the identification of the general flow pattern of the Peyto Glacier is possible.

CHAPTER V

NORTHERN ELLESMERE ISLAND

V.1 Introduction

In May 1970, studies of annual accumulation were made in a 7 m deep snow-pit and 22 m corehole from the bottom of the pit to a total depth of 28 m, at an elevation of 1800 m on the ice cap northwest of Tanquary Fiord (fig. 50). The ice cap, centred on lat. $81^{\circ}30'N$ and long. $81^{\circ}W$ has an area of about 2000 km^2 and is one of the most extensive in Arctic Canada.

The field party was headed by G. Hattersley-Smith of D.R.B., Shirley Bay, Ottawa. The purpose of the trip was to study the ice cap, with the idea that a deep core might be drilled at a later date. (However, after evaluating data from radio echo sounding, Devon Island was chosen as the site for the deep core by the Polar Continental Shelf Project D.E.M.R.). However, since this was the first scientific field team to study the ice cap, the information gathered is still of great interest. Logistics and support were all supplied from Camp Tanquary at the northern end of Tanquary Fiord.

The weather pattern of the High Arctic is dominated by high pressure systems that build up during the winter, and reach their greatest intensity usually in April-May. When melting destroys the high albedo of the snow and

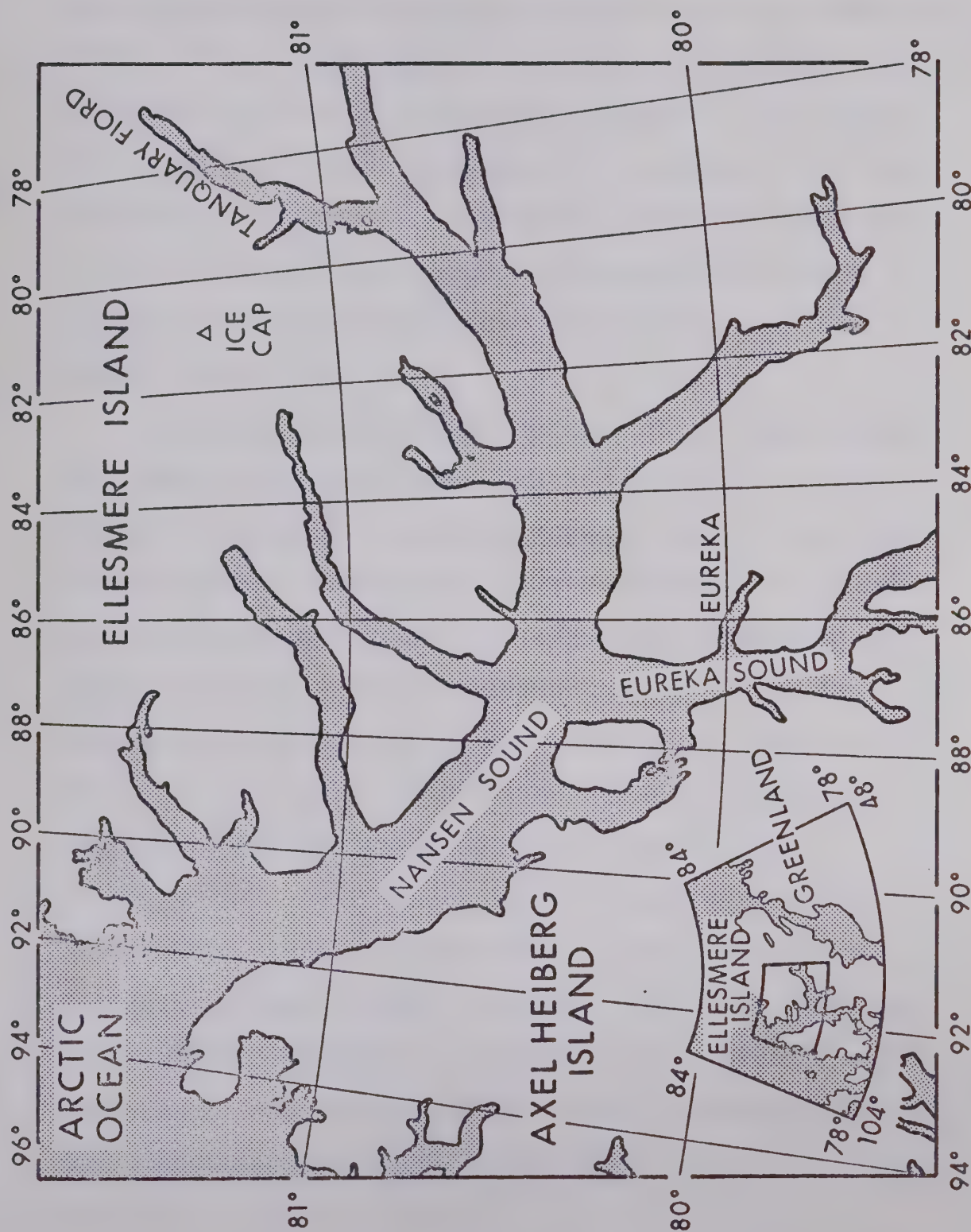


Fig. 50. Location of the Northern Ellesmere Island Snow-Pit.

ice surfaces, the "highs" begin to weaken. By the end of July the weather pattern is marked by weakly developed, diffuse "lows" and "highs", and generally slight pressure gradients, with only occasional intrusions from well developed low pressure systems, the Aleutian and the Icelandic. However, the variations from "normal" conditions in the High Arctic makes generalization about the weather of northern Ellesmere Island difficult (LOTZ and SAGAR, 1962).

The two Joint Weather Stations, Alert and Eureka, are located 200 miles N.E., and 125 miles S.W. of the snow-pit location. Therefore caution must be used when these stations' weather data are compared with the data from the ice cap. Weather data has been collected at Eureka since 1947 and since 1950 at Alert, with the average precipitations being 3.6 cm (W.E.) and 10.2 cm (W.E.) respectively. Alert data tends to reflect a "maritime" climate while data for Eureka is more "continental". However, since the snow-pit is on a topographic divide between these two weather stations, the United States Range, one might expect the location to be either "continental", "marine" or a combination of both, as in the case of Divide, III.2, depending on where the climatological divide is located.

Exploration meteorology has been carried out at Lake Hazen, Tanquary Fiord, the Gilman Glacier and the Ward Hunt Ice Shelf (HATTERSLEY-SMITH, ET AL, 1964; LOTZ and SAGAR, 1962; LOTZ, 1961a, 1961b, 1961c, 1959). Lake Hazen, the Gilman Glacier, Tanquary Fiord, like Eureka, seem to have a "continental" climate while the Ward Hunt Ice Shelf, like Alert, has a more maritime climate. These are consistent with the idea of the United States Ranges being a climatological, as well as, a topographical divide between the forementioned locations.

HATTERSLEY-SMITH (1963) found that the mean precipitation on the ice cap north-west of Lake Hazen (60 miles N.E. of the pit location of this study) was about 15.9 cm (W.E.) for the years 1916-1961 (18.6 cm for 1961) with values as high as 20 cm (W.E.) and as low as 10 cm (W.E.). The mean annual precipitation at Lake Hazen is unlikely to exceed 6.5 cm (W.E.). The precipitation at the Ward Hunt Ice Shelf seems to be comparable with the mean annual precipitation at Alert which is about 10.2 cm (W.E.) (LOTZ, 1961a).

V.2 Isotopic Data

a) Snow-Pit

The stratigraphic, density, and isotopic values for the snow pit are shown in figures 51, 52 and 53. The left hand column marks the stratigraphic annual layers as

chosen by Dr. G. Hattersley-Smith. It can be easily seen that stratigraphic designation and the isotopic designation of annual layers do not always agree. The following discussion assumes the isotopic designations to be correct. Reasons, for and against this assumption will be dealt with later in the chapter.

<u>Depth (m)</u>	<u>Description of Snow-Pit Data</u>
0-0.2	The presence of the thick wind crust would indicate small snow falls which were packed by high winds. The isotopic winter negative peak would be consistent since you would expect only small amounts of snow in the winter.
.2-.4	Loosely packed snow, as indicated by density, indicates "wetter" fall snow (layer crystals) which would be less affected by wind. This agrees with the isotopic data.
.4-.47	The depth hoar formed in "cooler" fall snow was caused by condensation of vapour from lower snow which was evaporated by the latent heat released when the summer melt-water refroze. Isotopically this would be expected to be more negative than summer values which it is, i.e. .4-.46 m. A light density anomaly is present as expected.

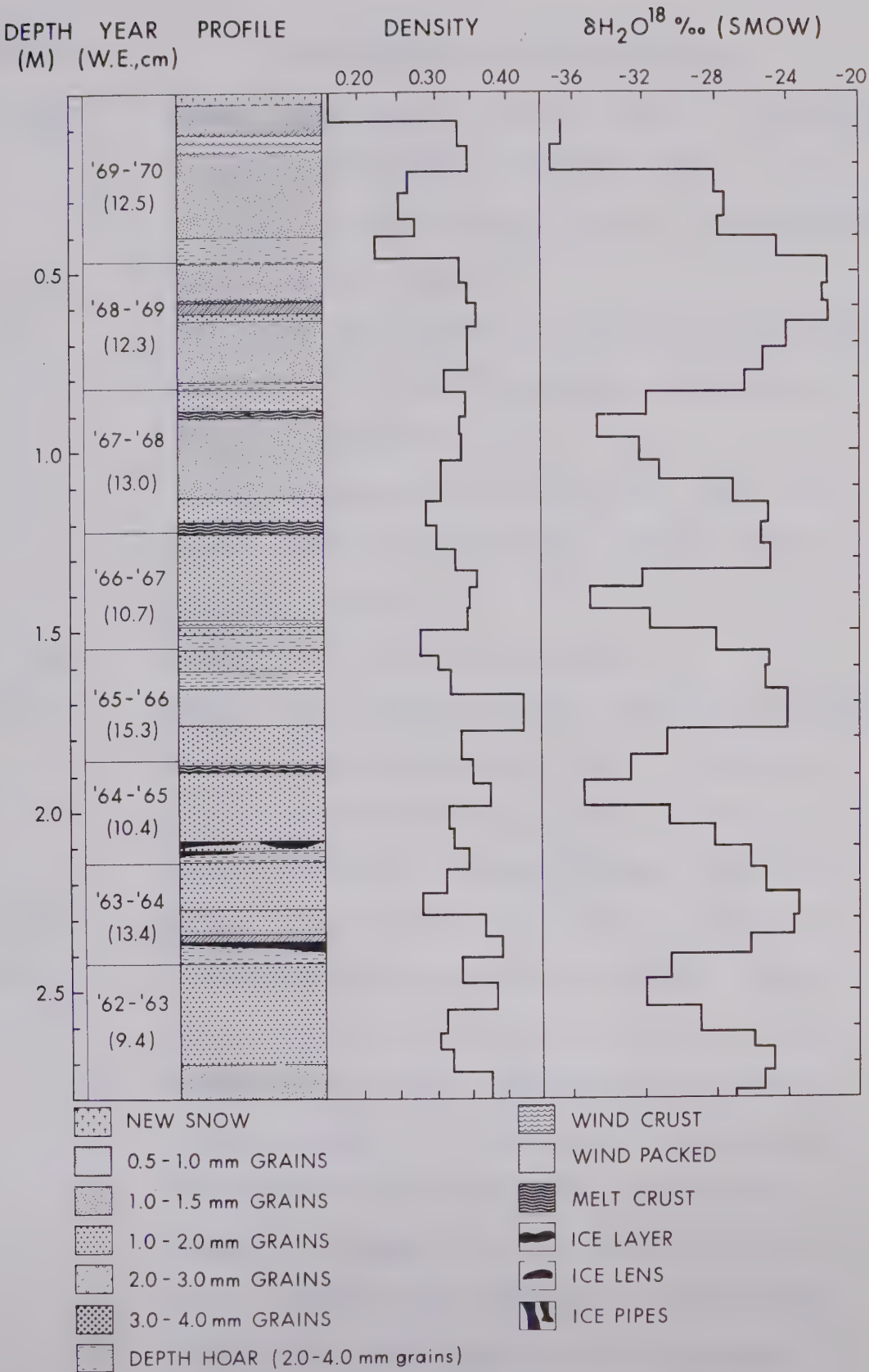


Fig. 51. Snow-Pit, 0-2.8 m., Northern Ellesmere Island.

<u>Depth (m)</u>	<u>Description of Snow-Pit Data</u>
.47-.64	Summer snow with the melt crust at .56 being isotopically slightly negative due to the melt effects on isotopic values. Summer 1969.
.64-.8	Spring snow of 1969.
.8-.9	The depth year, larger grains and melt crust may be due to the "warm" spells experienced at Alert and Eureka on 17, 18, 19 Dec. and 5 Jan. (temperatures up to 5 ⁰ F). The isotope values indicate this, rather than another summer.
.9-1.18	Winter and spring of 1968-69.
1.18-1.24	Depth hoar, melt crust and positive isotope values indicating summer 1968. The small amount of depth hoar as well as isotopic values indicate a cooler summer than 1969.
1.24-1.58	Winter of 1967-68 (also fall and spring).
1.58-1.78	Summer of 1967 by isotopic values. Depth hoar that usually occurs in early or late fall, in this case both may be due to an Indian summer. The isotopic values agree with this conclusion. Wind slab in mid-summer is unexpected, but perhaps it is just a drift feature formed in spring or winter and compounded on in the summer. The isotopic values indicate this is the warmest part of the summer.

<u>Depth (m)</u>	<u>Description of Snow-Pit Data</u>
1.78-2.2	Spring, winter and fall of 1967-66. The melt crust at 1.86 m again seems to be a winter feature from its isotope value. On 27 March 1967, the Alert temperature went up to 18°F. There seems to be heavy snowfall in the fall, by isotopic data from 2.04-2.2 with depth hoar forming at 2.12.
2.24-2.34	Mid-summer by isotopic values (1966). There is also a light density anomaly at 2.24-2.28 to support this as a summer, i.e. mild re-crystallization due to melting.
2.34-2.42	The wind slab and depth hoar seem to be spring features. The abruptness of the change from winter to summer peaks in the isotope data, perhaps, means little snowfall occurred in the spring, allowing the hoar to form at night after melting took place during the day.
2.42-2.66	Winter and fall of 1965-66.
2.66-2.79	Summer, 1965, with a light density anomaly occurring (at 2.62-2.66) in the early fall.
2.80-2.9	Large ice lenses occur at 2.81 and 2.88. This is isotopically the spring of 1965 so perhaps these lenses are formed by the melting during the summer of 1965. The depth hoar associated with the lens at 2.88 is probably due to

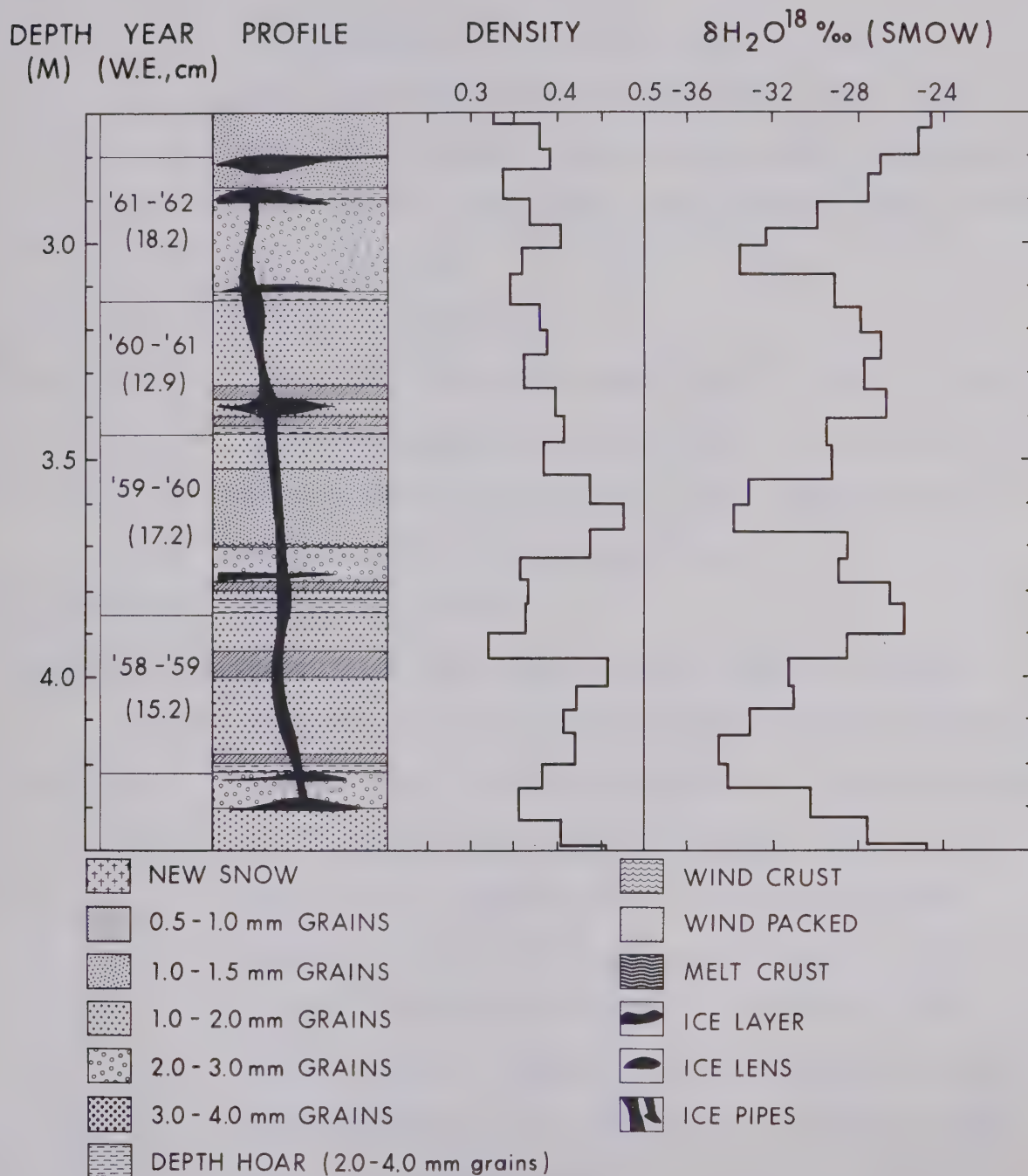


Fig. 52. Snow-Pit, 2.7-4.4 m., Northern Ellesmere Island.

Depth (m)Description of Snow-Pit Data

recrystallization, caused by the release of the latent heat of the melt-water when the ice lens formed. An ice pipe seems to connect the 2.88 ice lens with other lenses down to at least 4.6 m.

- | | |
|-----------|---|
| 2.9-3.12 | Winter of 1964-65. |
| 3.12-3.44 | Summer of 1964 with depth hoar at 3.14. Seems to be a relatively cool summer of fairly high precipitation with little fall, spring or winter (1964-65) precipitation. |
| 3.44-3.78 | Winter of 1963-64. |
| 3.78-3.9 | Summer of 1963 with a light density anomaly appearing at 3.92-3.96 for an unknown reason. |
| 3.9-4.39 | Winter, fall, spring of 1962-63, with wind pack, hoar, and an ice lens appearing at 4.0, 4.2, and 4.2-4.3 respectively. A light density anomaly is at 4.26-4.33. Isotopically these appear to have been formed in late fall or early winter. Some of the stratigraphy could be explained by the influence of the ice lens (i.e., the depth hoar). |
| 4.39-4.56 | Isotopic summer of 1962. The thick ice lens here seems to be due to percolation downward from above, i.e. along the ice pipe. The hoar underneath it is probably due to summer melt which seems to have been extreme in this summer. |

Depth (m)Description of Snow-Pit Data

(The summer of 1962 was unusually warm at Alert and Eureka.) The wind pack about the ice lens could be due to thawing and then re-freezing of snow around the ice lens under pressure, when the ice lens formed causing smaller crystals than normal for summer snow-fall.

4.56-4.76	Winter of 1961-62.
4.76-4.88	Summer of 1961 isotopically with light density anomaly at 4.82-4.88.
4.88-5.2	Winter of 1960-61.
5.2-5.5	The summer of 1960 isotopically with a light density anomaly at 5.12-5.18 or in the fall of 1960. Melt crusts were found at 4.8, 5.24 and 5.42. Depth hoar was located at 5.32. These all tend to indicate a warm spring, summer and fall, as found on the Gilman Glacier (LOTZ, 1961b).
5.5-5.62	Winter of 1959-60.
5.62-5.74	Summer of 1959, the more dense "summer snow" begins at 5.68.
5.74-5.9	Winter of 1958-59.
5.9-6.0	The summer of 1958 is not well defined isotopically. The light density anomaly at 5.88-5.94 coincides with the isotopic fall of 1958.

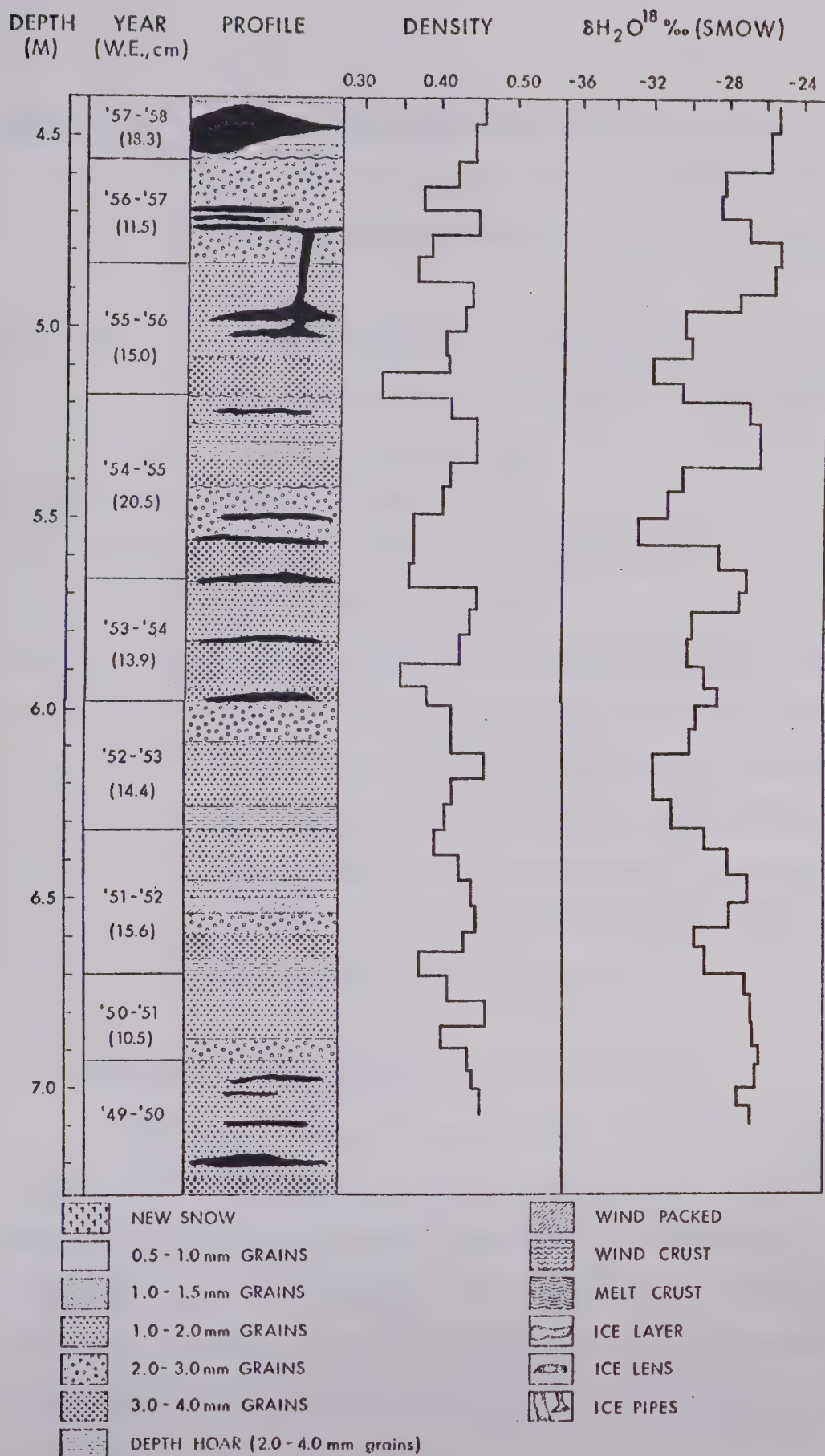


Fig. 53. Snow-Pit, 4.4-7.3 m., Northern Ellesmere Island.

Depth (m)Description of Snow-Pit Data

The lack of wind pack is consistent with the low wind velocities observed by LOTZ and SAGAR (1962).

6.0-6.32	Winter of 1957-58. Depth hoar at 6.28-6.32 indicates the fall of 1957. A large winter snowfall is indicated.
6.32-6.58	Summer of 1957.
6.58-6.7	Winter of 1956-57. Depth hoar at 6.7 indicating the fall of 1957.
6.7-7.0	Summer of 1956. The winter isotopic minimum seems to be disappearing. In fact, over the whole isotopic plot, the isotopic variation can be seen to get less and less extreme, i.e. homogenization by percolation, diffusion and packing is occurring, with the sparser winter snow tending to disappear.

b) Isotopic and Stratigraphic Discrepancies

The $\delta\text{H}_2\text{O}^{18}$ values ranged from -22 to -37 ‰ SMOW in the pit. The isotope variations show a striking periodicity with depth which are attributed to seasonal temperature fluctuations. However, in figures 51, 52, 53, only 15 winter minima in $\delta\text{H}_2\text{O}^{18}$ values are obvious whereas the stratigraphic data argue that 21 years of accumulation are

represented. Stating this discrepancy another way, stratigraphic data throughout the pit indicate a mean annual accumulation of about 140 mm H₂O/yr whereas the isotopic data accepted at face value would indicate a higher mean annual accumulation (~ 197 mm H₂O/yr). Therefore, while it is fortunate that summer melting and percolation activities have not totally homogenized seasonal isotopic variations, there is nevertheless the problem of resolving these discrepancies. One must determine whether the isotopic data failed to detect some winter minima or whether stratigraphic observations can falsely indicate additional years.

The stratigraphic annual designations are based upon the fact that the summer of 1962 was unusually warm and was therefore associated with the ice lens system in figure 52. The isotopic values place the summer of 1962 between 4.37-4.56 m (figs. 52, 53). The small winter peak for the winter of 1961 and the ice lens system between 4.7-5.0 m are consistent with this warm spell also.

It is assumed that, as is the case at Alert and Eureka, winter precipitation is very slight on this ice cap. Therefore isotopic minima represent very little snow and isotopic variations could be obscured by melt season activities. It is also possible that the sampling increment chosen was too long to resolve the winter minima during the years of sparse precipitation. This could be especially

true as one goes deeper into the pit (the density increases by compaction and a given sampling tube collects material over increasing time intervals). With these ideas in mind, a plot of isotopic values for the pit against the water equivalent depths (density corrected) were plotted down to a depth of 20 metres (after 20 m sampling was done every 50 cm.) The result is shown in figure 54.

A striking periodic variation is apparent, especially in the first 240 cm (W.E.). The 7 metre depth is at 268 cm (W.E.). To see how periodic this profile was the auto-correlation function was calculated (fig. 55). Although the correlation is not very high, it is extremely periodic up to about the 140 lag, where each lag corresponds to 1 cm depth in the snow-pit (W.E.). The period of this correlation is approximately 20 cm.

Power spectrum analysis of the figure 54 was also done. The computer programme required that the number of data points be an exact power of 2. The following power spectra were calculated;

<u>Range (cm)</u>	<u>Period (cm)</u>	<u>Power Spectrum Function</u>
8-135	8.0	0.44
	14.2	0.81
	18.3	2.84
	32	2.78

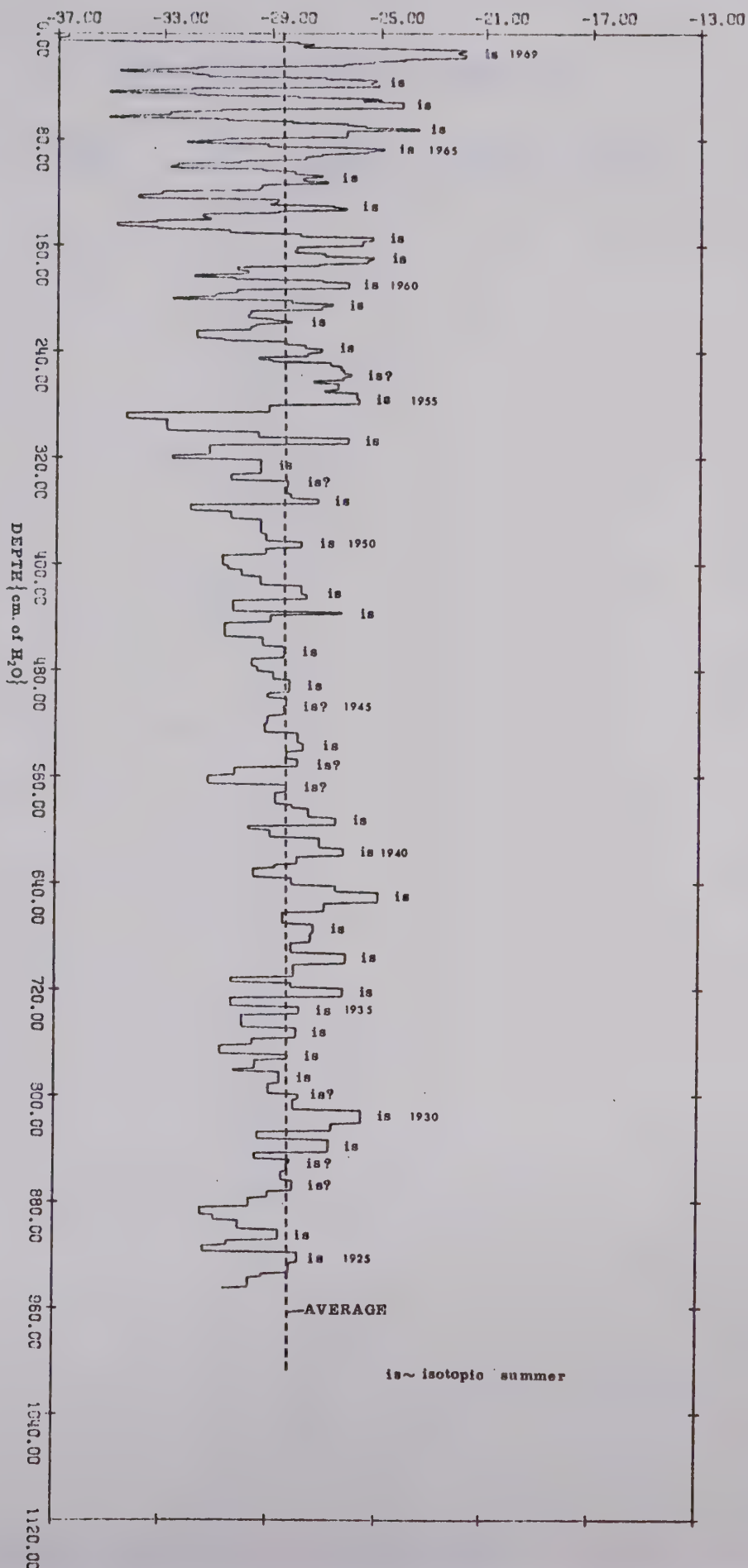


Fig. 54. Water Equivalent Profile of Northern Ellesmere Island Snow-Pit and Core.

AUTO-CORRELATION FUNCTION

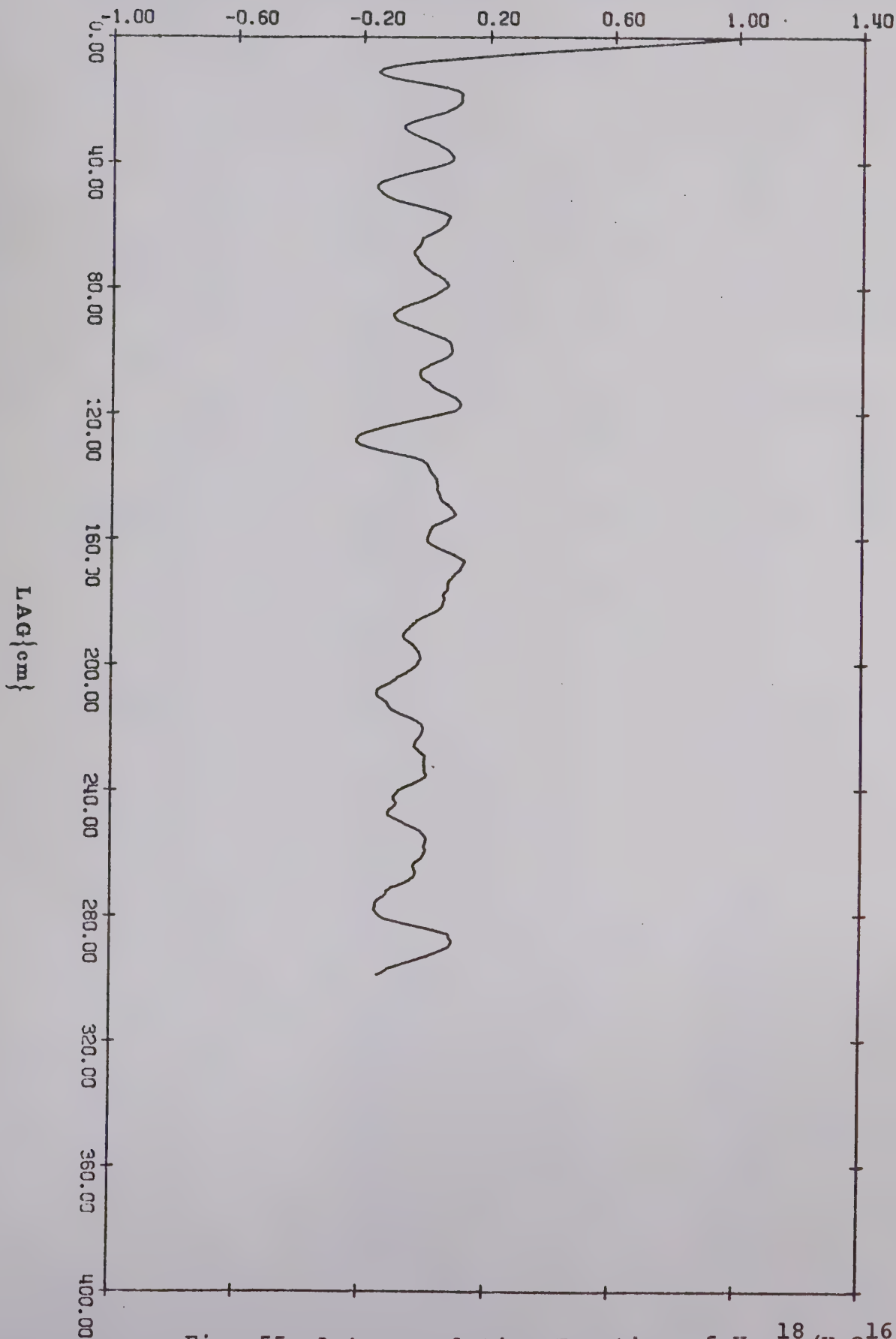


Fig. 55. Autocorrelation Function of $\text{H}_2\text{O}^{18}/\text{H}_2\text{O}^{16}$
Profile of Snow-Pit and Core (W.E.)

<u>Range (cm)</u>	<u>Period (cm)</u>	<u>Power Spectrum Function</u>
8-263	8.2	0.18
	13.5	0.38
	19.7	2.59
	28.4	0.87
	36.6	0.76
8-519	17.1	0.27
	19.7	1.01
	24.4	0.38
	28.4	0.42
	36.6	0.47
441-952	19.0	0.90
	26.9	0.13
	56.9	0.27
	102.0	0.14
8-1033	13.7	0.06
	15.1	0.06
	16.8	0.13
	19.7	0.33
	24.4	0.14
	28.4	0.26
	36.6	0.22
	48.8	0.10
	85.3	0.21
	204.8	0.09
	512.0	0.05
	1024.0	0.05

The power spectra are shown in figures 56, 57, 58, 59 and 60. The value of 19.7 cm seems to be the average period of the isotopic variation. From the range 441-952 cm it can be seen that this periodicity dies out with depth. This is as one might expect because of molecular diffusion, compaction and homogenization due to percolating melt-water. The sampling interval is also much more critical at depth, as previously mentioned.

This strong periodicity of 19.7 cm rather than 14.5 cm suggests the isotopes may be more accurate than the stratigraphic indications. Although one would not get exactly the same amount of precipitation each year, a more stable periodicity than offered by the stratigraphic interpretation might be expected. This is not to say that the isotopic technique is totally correct, but rather it offers a more accurate picture of the annual precipitation layers, while the stratigraphy offers more insight into variations within the annual layers because of its continuous rather than discrete sampling. At many depths such as at 255-287 cm in figure 54 stratigraphy would help clarify the isotopic results since the isotope data seems to have been erased, perhaps by percolating melt-waters. Unfortunately, these samples were part of the snow core and stratigraphy is often impossible to decipher in cores.

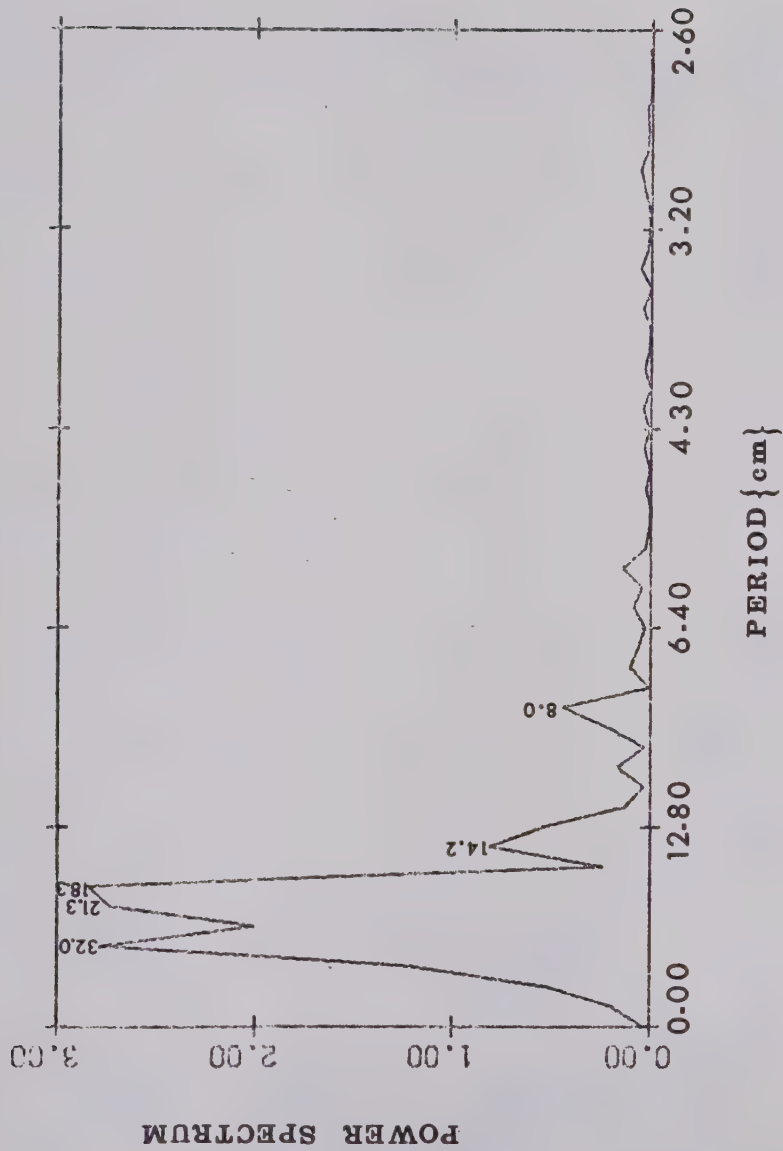


Fig. 56. Power Spectra of the Isotope Profile of the Northern Ellesmere Snow-Pit and Core (0-128 cm.).

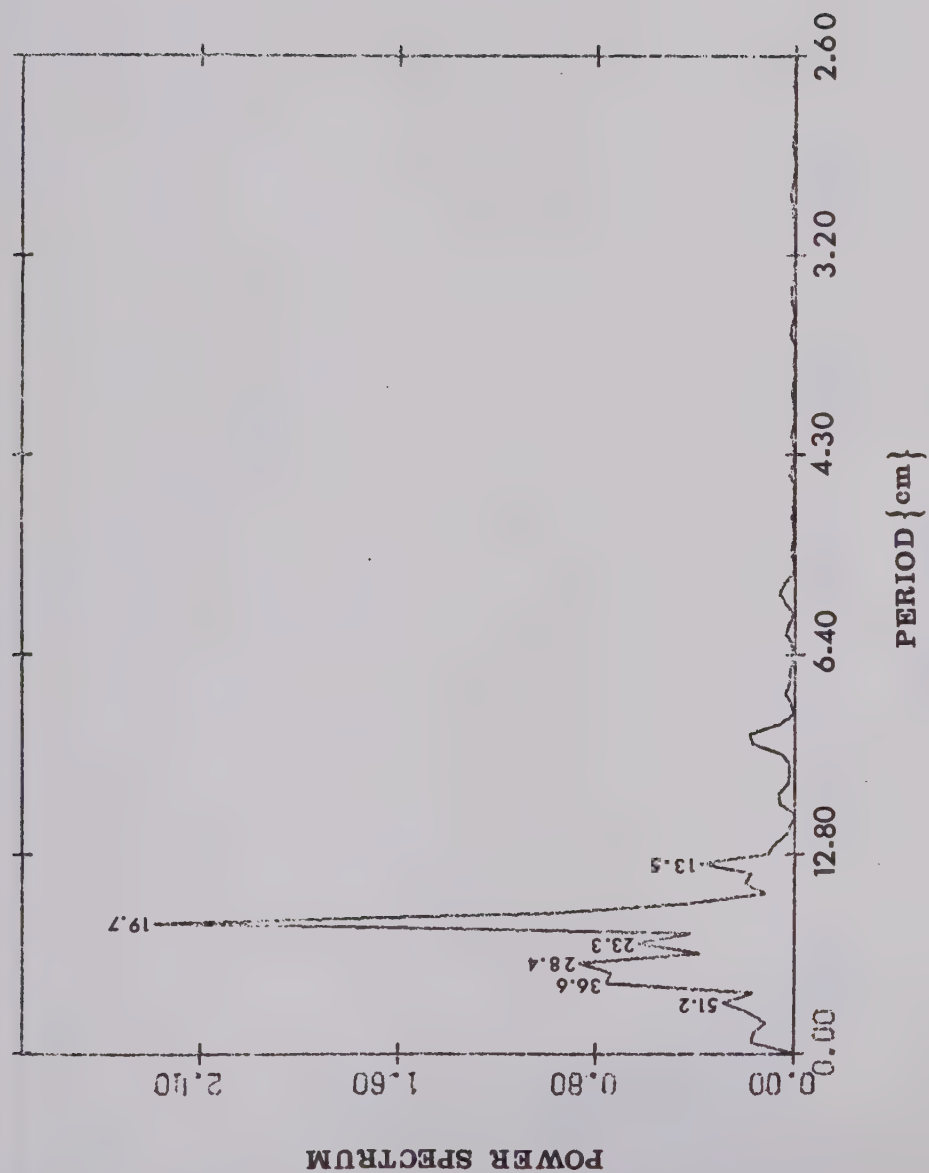


Fig. 57. Power Spectra of the Isotope Profile of the Northern Ellesmere Island Snow-Pit and Core (0-256 cm.).

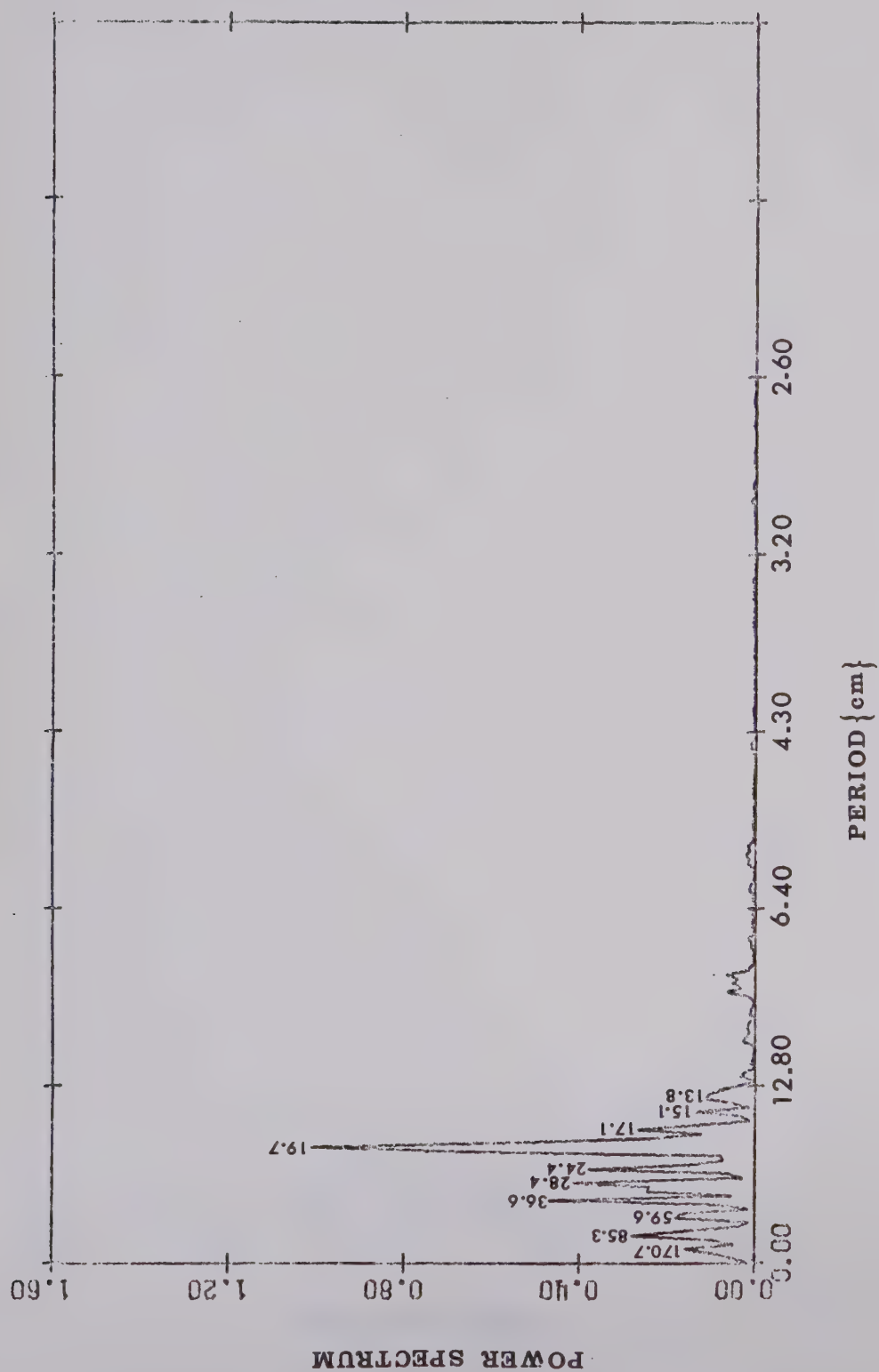


Fig. 58. Power Spectra of the Isotope Profile of the Northern Ellesmere Island Snow-Pit and Core (0-512 cm.).

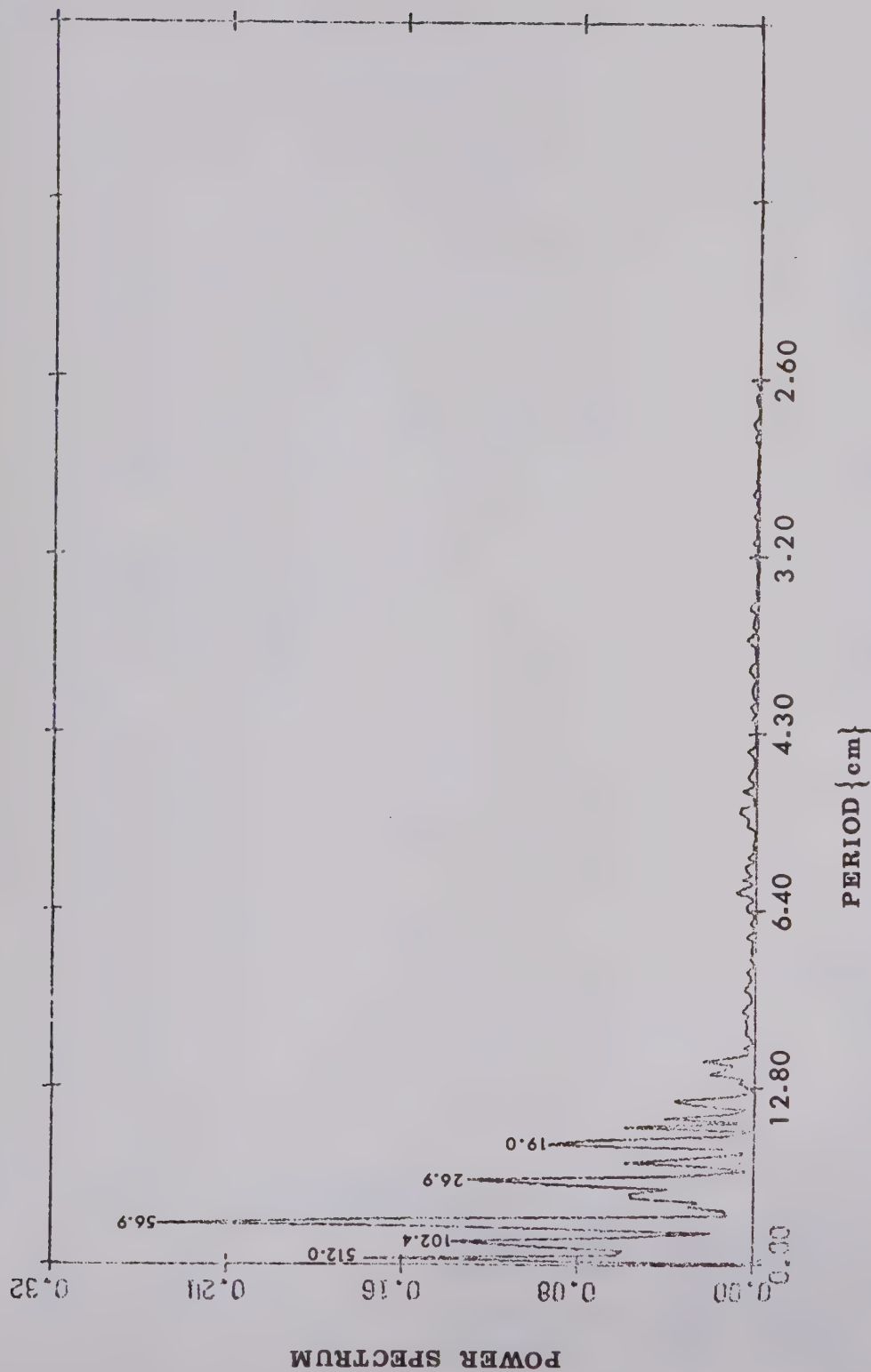


Fig. 59. Power Spectra of the Isotope Profile of the Northern Ellesmere Island Snow-Pit and Core (441-956 cm.).

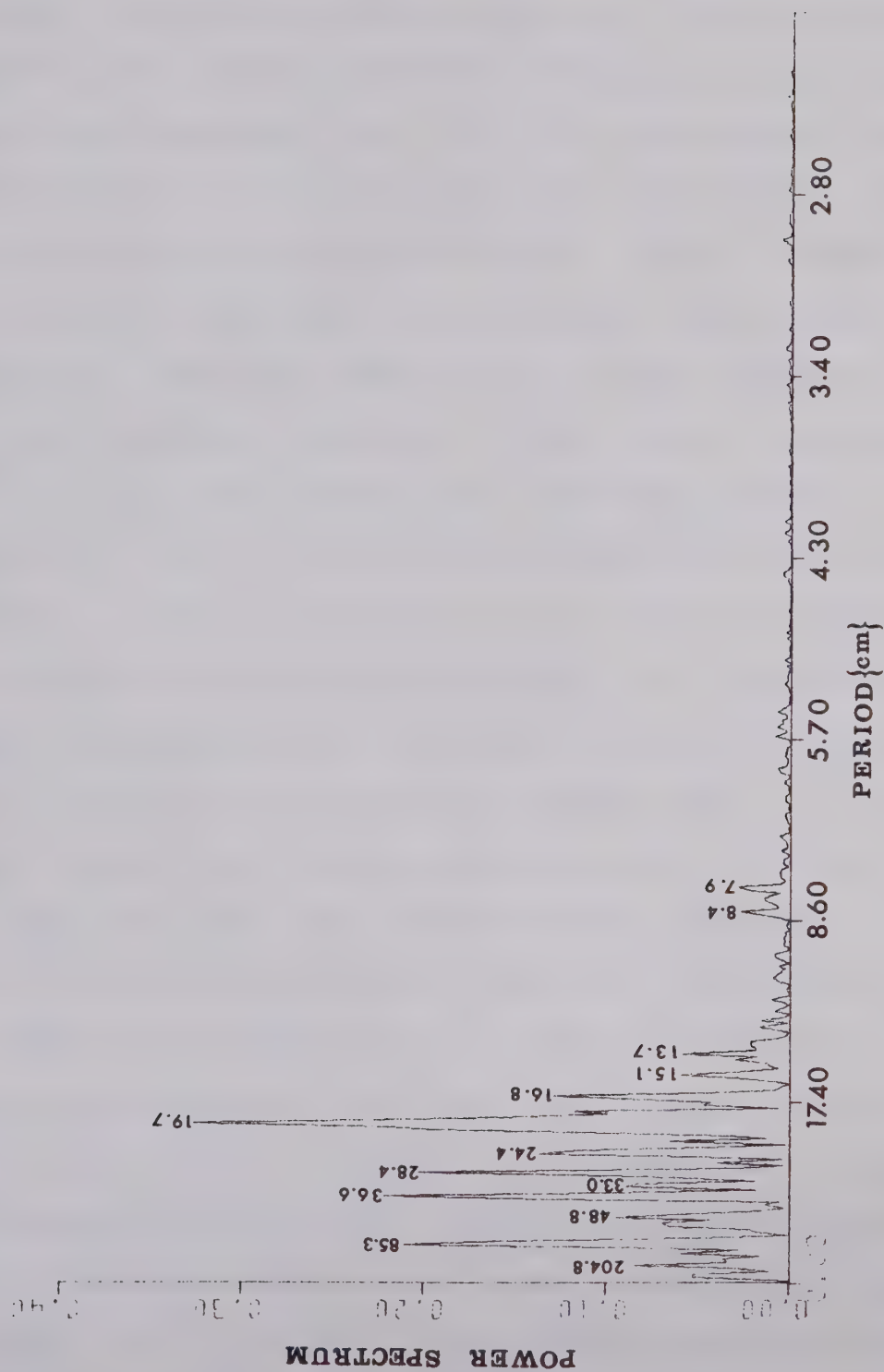


Fig. 60. Power Spectra of the Isotope Profile of the Northern Ellesmere Island Snow-Pit and Core (0-1024 cm.).

c) Climatic Trends

HATTERSLEY-SMITH (1963) compared firn stratigraphy on Gilman Glacier in northern Ellesmere Island to meteorological data from the Upernivik station on the coast of central-west Greenland (lat. $42^{\circ}47'N$) and concluded that the well known climatic warming of the late 1920's and 1930's had affected northern Ellesmere Island. DANSGAARD ET AL (1969b) identified this warm period using oxygen isotopes in a detailed study of an ice core from Camp Century, Greenland. Likewise, in this study, the mean H_2O^{18} value is more positive over the depths between 460-880 cm (fig. 54), the interval identified with this warming. In fact if one looks at the moving mean temperature at Upernivik for this period (fig. 61) the correlation between the isotopic and temperature variation is extremely high. A straight count of summer maxima from the top of the pit labels the isotopic maximum at 462.2 cm (W.E.) as the summer of 1947. The extreme isotopic maximum of $-25.0 \text{ }^{\circ}/\text{oo}$ (S.M.O.W.) at 647.4 cm (W.E.) corresponds to the summer of 1939 which was also one of the warmest recorded at Upernivik (fig. 61). The cooling trend between 1940-45 also shows up isotopically, as does the cooling trend between 1938 and 1931. Again the temperature maximum of 1930 coincides with a local isotopic maximum in figure 54 (depth 811.6 cm, W.E.). The isotopic values then decrease at a slightly faster rate than experienced by the

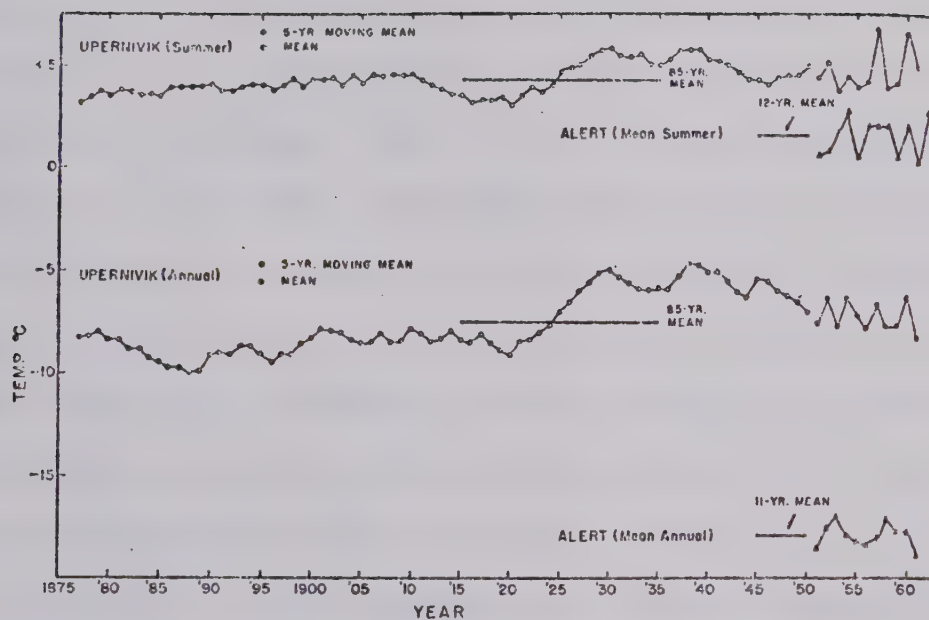


Fig. 61. Temperatures at Upernivik, Greenland, and Alert, N.W.T. (after HATTERSLEY-SMITH, 1963).

decreasing temperatures of Upernivik.

The power spectral analysis of the isotopic data indicates that the isotopic variation and hence the climate varied with periods of approximately 4.3 years, 2 years and 1.5 years (accepting 19.7 cm W.E. as the average precipitation). The 2 and 1.5 year variations were probably caused simply by variation in the annual precipitations from year to year. The 4.3 yr. variation seems real. When a power spectral analysis was done on the mean annual temperatures at Edmonton, the major peak was at 4.6 yrs. This is very close to the variation of a period of 4.3 years found in the isotopic profile of the Ellesmere pit. This indicates that Northern Ellesmere Island seems to experience the same general climatic trends experienced by the rest of the northern half of continental North America. Therefore investigations of deeper pits and cores in the Canadian North might not only give climatic information about the Canadian North, but it also may be possible to gain information of general nature about the past Canadian climate as a whole.

d) Ice Lens Systems

Ice lenses seem to prefer to form in summer or fall precipitation of previous years. This is logical since the loose packing of the large melt crystals, i.e. depth hoar, caused by percolating meltwater offer large pores for the meltwater to run into and refreeze. This

refreezing would release heat which would cause snow in this area to thaw and which might refreeze into small crystals since it is now under pressure. This would especially be true of snow above the ice lens. This effect can be seen in this pit.

Unfortunately $\delta\text{H}_2\text{O}^{18}$ measurements were not made on the ice lenses to determine whether they were isotopically homogeneous. It is striking however that the isotopic composition of the nearby snow continues to display maxima and minima in $\delta\text{H}_2\text{O}^{18}$ values. This implies that the formation of these networks was very localized and water associated with this ice did not interact extensively with the surrounding snow. The stratigraphic description of the snow is in accordance with this conclusion. These observations concur with remarks of BENSON (1959, p. 17) in which he points out that the growth of ice layers is assisted by the fact that meltwater from the surface can percolate down through narrow channels at the melting point although the temperature of the surrounding firn may be many degrees below 0°C .

e) Temperatures

Temperature readings were taken in the first 7 metres of the snow pit. The surface temperature was -9°C . It then dropped steadily, till at a depth of 210 cm., it began to stabilize between -25 and -27°C . In the two pits

dug by HATTERSLEY-SMITH (1963, 1960) the temperatures stabilized at approximately -24.6°C . Applying equation 13 to the average isotope value one gets -21.9°C (average δ value = -28.7 ‰). Applying the temperature lapse rate to the mean temperature of Alert or Eureka also gives a temperature that is more negative than the one calculated from the isotopic average. The most probable reason for this discrepancy is the sparse snowfall. This allows, because of the sampling interval of 6 cm, periods of high snowfall to be heavily weighted; while period of very small snowfall, i.e. the winter, has only a small effect on the average isotope value. Therefore, the isotopic values should have been weighted according to the amount of precipitation that usually occurs during their seasonal period. However, the sampling interval was too large to make such weighting practice. If equation 13 does hold true for this area the average $\delta\text{H}_2\text{O}^{18}$ would be expected to be around -30.6 ‰ (for -24.6°C) after weighting. Only more detailed sampling could show this effect.

f) Relationship with Other Studies

This study is thought to be the first detailed oxygen isotope and stratigraphy study done in the Canadian High Arctic. Oxygen isotopes of an ice core from Meighen Island are being analysed by Dr. H.R. Krouse (University of Calgary) at present. Further studies of a deep core from Devon Island will be carried out in the future. The

rest of the studies of isotopic applications in cold regions have been carried out in Greenland (DANSGAARD ET AL, 1969b; LANGWAY JR., 1967) and Antarctica (EPSTEIN ET AL, 1970; LORIUS ET AL, 1968; GONFIANTINI, 1965; PICCIOTTO ET AL, 1960).

EPSTEIN ET AL (1965) found that the oxygen and deuterium profiles of snow pits near the South Pole gave reliable accumulation and annual layer determinations when compared to direct measurements of snow accumulations over a six year period (average accumulation was 70 mm of H_2O). LORIUS ET AL (1968) found that stable isotopic results (deuterium) were unreliable when the annual accumulation was about 100 mm of H_2O or less when compared with artificial β activity measurement. The conflict between these two conclusions suggests that the reliability of profiles of stable isotopes in areas of small accumulation must depend heavily on parameters such as wind and monthly precipitation rates. It is quite conceivable that high winds or a seasonal drought could totally obscure an isotopic maxima or minima in areas of high winds, low temperatures and small precipitations.

In Northern Ellesmere Island, however, the meteorological situations are different from that of the Antarctic and Greenland Ice Caps. The winds, at least in the summer (LOTZ and SAGAR, 1962), tend to be of low velocity. Also melting in the summer would decrease the

effect of wind scour and wind mixing, at least, as far as the summer is concerned. However, downward percolation of meltwaters adds a parameter not generally encountered in the forementioned areas.

No correlation of annual isotopic variation can be seen between the results from the Greenland Ice Cap and Antarctica and those of Northern Ellesmere Island. It would seem, while they may experience the same large scale climatic variations, annual isotopic variations are indicative of local climatology. The long term climatic trends can be seen in mean isotopic values of tens of years of precipitation (DANSGAARD ET AL, 1969b; EPSTEIN ET AL, 1970).

CHAPTER VI

CONCLUSIONS

Previous $\text{H}_2\text{O}^{18}/\text{H}_2\text{O}^{16}$ studies in St. Elias Mountain Ranges (MACPHERSON and KROUSE, 1967; EPSTEIN and SHARP, 1959a) and in the Rocky and Sierra Nevada Mountains (SHARP ET AL, 1960; FRIEDMAN and SMITH, 1970) obviously show that conclusions derived from the more detailed isotope research programs in Greenland and Antarctica do not describe all of the conditions met in North America's (in our case Canada's) small but numerous ice fields and glaciers. The larger ice caps of Greenland and Antarctica experience weather conditions unlike those of Canada. For example, the only dry snow facies found in studies in Canada are on mountain tops, e.g. Mt. Logan, while a large portion of the research in Greenland and Antarctica is carried out in dry snow facies.

This study has shown that while stable isotopes enable one to understand more clearly some of the local mechanisms in the accumulation, ablation, and motion in the snow and ice of mountainous regions of Canada, they also enable one to relate these mechanisms, past and present, to the North America weather pattern as a whole.

The stable isotope investigations in the various snowfields, or ice caps, rendered a number of successful achievements. The ability of the isotopic abundances to

evaluate the orographic effect in the Logan Plateau as well as excluding snow blown up from lower altitudes as the major source of precipitation is very gratifying. The local meteorological detail exhibited in the Divide snow-pit gives a good picture of the fluctuations of the climatological divide in that area, and hence a deep appreciation of the complex variations in precipitation in that region. The preserved variations in the Ellesmere pit, despite percolating meltwaters, enables one to study the recent and long term meteorological history of Northern Ellesmere Island. However, the discrepancies between the stratigraphy and isotopic variations suggest that great care must be taken when interpreting such a study.

The correlation between the temperature and the δ -values of the precipitation (equation 13) is striking. It would seem that DANSGAARD's (1964) equation for the mean annual temperature of Greenland, also applies to quite a few regions in Canada, when topographic corrections are applied.

The results of the stable isotope investigations of glacier flow are very successful when compared to other such studies (MACPHERSON and KROUSE, 1967; SHARP ET AL, 1960; EPSTEIN and SHARP, 1959a). The ability to separate arms of glaciers that come from different accumulation areas appears possible. However, due to

paleoclimatic variations and other parameters, longitudinal profiles and cores in the lower glaciers are of uncertain value and must be interpreted with care. The isotopic variations, then, can only be used as indicators of general flow, and do not seem to be able to give results suitable for theoretical model fitting. However, the correlation between surface shape and O^{18} variation in an area of high ablation, the Peyto Glacier, warrants further investigation.

Pollution and population problems in recent times have revived interest in ice fields in North America, as they are important future sources of water. This study shows conclusively, that stable isotopes can be a powerful technique when investigating the accumulation and wastage patterns of these resources.

APPENDIX A

CONTOUR PLOTTING OF RAW DATA, TREND SURFACES AND RESIDUALS

A.1 Introduction

The original version of this programme is described in the booklet "Computer Programs for Automatic Contouring" by D.B. McIntyre, D.D. Pollard, and R. Smith (State Geological Survey, University of Kansas, Lawrence, Kansas). Theoretical material may be found in Chapter 13, "An Introduction to Statistical Models in Geology" (KRUMBEIN and GRAYBILL, 1965). Modification for M.T.S. used at the University of Alberta was done with the help of Peter Buttuls of the Computing Centre, University of Alberta.

The whole programme consists of a main programme which calls a number of other subroutines, depending upon what contours are required. It uses 70 K bytes of storage and five scratch files for intermediate storage. If Calcomp plots are required, an extra file for the digital commands is required.

A.2 Raw Data Contouring

This part of the programme performs the calculations and observations necessary to draw reasonably smooth contours through a set of irregularly distributed data taken at different points in a plane, U-V. The following steps are taken to produce this contour map of the raw data.

i) Construction of a grid (subroutine DBMCI 2)

In constructing a grid from the irregularly distributed data, a least squares criterion is used to determine values at regularly spaced intervals, i.e. at grid intersections, and then a polynomial surface is fitted to the points closest to each grid intersection. To avoid too much restriction in the degrees of freedom, a quadratic surface is fitted. Since six coefficients are to be determined, we must use at least six points, and because these may be distributed poorly, we insist on a minimum of eight. A circle is constructed such that the probable number of points contained within it is ten, and if fewer than eight points are found, the radius is incremented and a second count made. The number and magnitude of the increments can be changed, but experience has shown that if more than one increment is allowed the result is likely to be unsatisfactory. Points are weighted inversely as the square of their distance from the grid intersection, and the surface is fitted. On this basis, a value is assigned to the grid point. This value may be unsatisfactory because of the distribution of the data points. Instead of a time consuming test of the distribution, we use the arbitrary criterion that no predicted value may lie outside the range of the values used to compute it by more than 20 percent of that range.

If for any reason the program is not able to assign a satisfactory value to a grid point, it is flagged 999.9 and is ignored during plotting.

ii) Interpolation (subroutine DRAFT)

Once the values at grid intersections have been established, it is necessary to interpolate between these points since a required contour line will not always pass through the calculated grid points. Each grid square is subdivided into 4 triangles by 2 diagonals. This yields six lines along which the interpolation is carried out. All the grid squares are searched for each contour value required and the points of intersection with any of the six lines are written on a scratch file. The plotting of the contours is then carried out by subroutine SIFT.

A.3 Trend Surfaces

Trend surface analysis consists of fitting a polynomial surface to the observed data, Y_j ($1 \leq j \leq N$, where N is number of observations). However, since there are usually more observations than equations, only a least squares fit can be obtained and an error or residual term e_j will remain for each observation;

$$Y_j(U_j, V_j) = Y_j^P + e_j \quad (A-1)$$

i.e. observed value = predicted value + error term.

The predicted value is a polynomial of degree n (up to 8);

$$\begin{aligned} \text{where, } Y_j^P = & B_0 + B_1 U_j + B_2 V_j + B_3 U_j^2 + B_4 U_j V_j \\ & + B_5 V_j^2 + \dots + B_k U_j^n V_j^n \end{aligned} \quad (A-2)$$

The purpose of the least squares fit is thus to find the set of coefficients B_0, B_1, \dots, B_n which will then allow a predicted value to be calculated for any given point (U, V) in the area of interest. The assumptions that are made so that value Y_j of an observation will be equal to the predicted values Y_j^P are;

- 1) e_j is a random variable with an expected value of zero.
- 2) e_j has a variance which is not a function of the coefficients, B_n , or powers of U or V .
- c) Coefficients B_n .

The calculations of the coefficients, B_n , are done by using a least squares fit. Since there are N observed values of Y_j we thus have N equations of the form equation (A-2). The least squares method consists of minimizing the sum of squares of the errors, $L = \sum_{j=1}^W e_j^2$. To obtain a minimum for L , we take the partial derivative of L with respect to each of the B 's. If we then define X as

$$x_{j1} = u_j$$

$$x_{j2} = v_j$$

$$x_{j3} = u_j^2$$

$$x_{j4} = u_j v_j$$

$$x_{j5} = v_j^2$$

$$\vdots$$

$$x_{jk} = u_j^n v_j^n$$

then the above operations yield the following matrix relationship:

$$\begin{bmatrix} N & \sum_j x_{j1} & \sum_j x_{j2} & \cdots & \sum_j x_{jk} \\ \sum_j x_{j1} & \sum_j x_{j1}^2 & \sum_j x_{j1}x_{j2} & \cdots & \sum_j x_{j1}x_{jk} \\ \vdots & \vdots & \vdots & \vdots & \vdots \\ \sum_j x_{jk} & \sum_j x_{jk}x_{j1} & \sum_j x_{jk}x_{j2} & \cdots & \sum_j x_{jk}^2 \end{bmatrix} \begin{bmatrix} B_0 \\ B_1 \\ \vdots \\ B_k \end{bmatrix} = \begin{bmatrix} \sum_j y_j \\ \sum_j x_{j1}y_j \\ \vdots \\ \sum_j x_{jk}y_j \end{bmatrix}$$

$$\text{or } [S] [B] = [G]$$

Thus the B's are readily obtained from the above relationship.

ii) Plotting the trend surfaces

For a given degree n (up to 8), once the set of coefficients have been obtained, predicted values y^p

may be then calculated for any point (U, V) by equation (A-2). Then, in a similar way to that of the formation of the grid for the raw data, a grid for the trend surface is produced and the contours plotted.

A.4 Residuals

The residuals, e_j , are calculated by equation (A-1) and are therefore calculated for each of the observed data points, Y_j . A contour map is then plotted by the same procedure used for the raw data. The coefficient of correlation is then calculated as follows:

$$\left(1 - \frac{\sum_{j=1}^N e_j^2}{\sum_{j=1}^N Y_j^2 - \left(\sum_{j=1}^n Y_j \right)^2} \right) = \left(1 - \frac{\text{variance of unexplainable data}}{\text{variance of explainable data}} \right)$$

Therefore the closer the correlation coefficient is to one, the better the trend surface analysis.

APPENDIX B

 $\text{H}_2\text{O}^{18}/\text{H}_2\text{O}^{16}$ VARIATIONS ON MT. SEYMOUR, B. C.

$\text{H}_2\text{O}^{18}/\text{H}_2\text{O}^{16}$ analysis was done on Mt. Seymour, near Vancouver, B.C., in conjunction with a meteorological project of a graduate student at U.B.C., Blair Fitzharris. Unfortunately the isotopic data seem to be inconclusive.

This could be due to many parameters not met in the previous cases due to the samples' elevation and deposition temperatures. Exchange, severe ablation and perhaps even an amount effect are the most probable parameters altering the isotopic data.

The results are tabulated below with the synoptic situation for storms No. 23, 24 and 30 also being outlined:

Storm No. 23: 8-9 Jan. 1970 $\text{O}^{18}/\text{O}^{16}$ sample taken Jan 9/70

A trough of low pressure, and associated front, moved rapidly eastward through the Mount Seymour area from the Pacific Ocean. At first warmer air was advected into the area with S.E. to S. winds, but the passage of the frontal system (6.30 a.m. PST, on Jan 9/70) was marked by incursion of cooler air and strong N.W. winds. All precipitation occurred as snow at the top of the mountain (1260 m). Below 1000 m, rain fell at first, but turned to snow after the frontal passage.

$\text{O}^{18}/\text{O}^{16}$	Elevations (m)	$\delta\text{H}_2\text{O}^{18}$ (S.M.O.W.)
	1022	
	1220	-14.5

Storm No. 24: 10-11 Jan.1970 O^{18}/O^{16} sample taken Jan 12/70

Low pressure centres in the Gulf of Alaska and over Prince Rupert generated a cold moist W. to S.W. airstream onto the coast. Continental Arctic air from the Yukon and Alaska was modified and heated from below by a short passage over the Pacific. The resultant instability produced extensive cumulus and cumulonimbus clouds giving snow to relatively low levels on Mount Seymour. This airflow was accompanied by a disturbed westerly flow aloft.

O^{18}/O^{16}	Elevations (m)	δH_2O^{18} (S.M.O.W.)
	427	-9.8
	762	-9.3
	945	-8.9
	1022	-9.5
	Average	-9.4

Storm No.30: 26-27 Jan. 1970 O^{18}/O^{16} sample taken Jan 28/70

A low pressure centre and associated front moved through the Mount Seymour area. Storm No. 30 represents the well developed, cool, disturbed, northwesterly airstream which developed between the low pressure centre and a building area of high pressure offshore.

O^{18}/O^{16}	Elevations (m)	δH_2O^{18} (S.M.O.W.)
	838	-21.4
	945	-15.0
	1022	
	1220	-21.3

Storm No. 28: 29-31 Dec. 1970

Elevation (m)	$\delta\text{H}_2\text{O}^{18}$ (S.M.O.W.)
400	-13.2

Storm No. 29: 7-10 Jan. 1971

Elevations (m)	$\delta\text{H}_2\text{O}^{18}$ (S.M.O.W.)
590	-14.2
790	-13.8
970	-14.0
1060	-14.9
1260	-14.4
Average	-14.3

Storm No. 34: 20-21 Jan. 1971

Elevations (m)	$\delta\text{H}_2\text{O}^{18}$ (S.M.O.W.)
490	-11.0
590	-10.9
710	-11.6
790	-12.0
870	-10.7
970	-9.5
1060	-10.5
1260	-10.7
rime at 1260	-9.0
Average	-10.7

	Elevations (m)	$\delta\text{H}_2\text{O}^{18}$ (S.M.O.W.)
Averages at elevation	400	-11.5
	500	-11.0
	600	-12.6
	700	-11.6
	800	-14.1
	900	-11.5
	1000	-9.5
	1100	-12.7
	1200	-17.9
	1300	-12.6

The mechanism believed to be responsible for the lack of an altitude trend is the change of altitude of the freezing levels. This variation in the rain/snow boundary, as the storm proceeds could destroy any altitude or time dependence of the isotopic composition.

In order to make a study of this kind successful it would seem necessary to sample with time as well as altitude. Comparisons between rainfall and snowfall of the same storms could perhaps enable one to find out how much exchange takes place. This could also be checked by comparing the deuterium to the oxygen isotope variations. Monitoring in the summer as well as winter may help clarify some problems, such as amount effects. Such a study would call for a large number of samples and year round meteorological information.

BIBLIOGRAPHY

- ALFORD D. (1967) Density Variations in Alpine Snow, *J. Glac.* 4, No. 46, 495-503.
- and KEELER C. (1968) Stratigraphic Studies of the Winter Snow Layer, Mt. Logan, St. Elias Range, Arctic 21, No. 4, 245-254.
- BAKR A. (1971) Isotopic Studies of Evaporation of Water by Cetyl Alcohol Films, M.Sc. Thesis, University of Alberta, Alberta, Canada.
- BENSON C.S. (1959) Physical Investigations on the Snow and Firn of North-west Greenland 1952, 1953 and 1954, Snow Ice and Permafrost Research Establishment, U.S. Army Research Report 26, 62 pp.
- (1962) Stratigraphic Studies in the Snow and Firn of the Greenland Ice Sheet, U.S. Snow, Ice and Permafrost Research Establishment Research Report 70.
- BREWER T. (1969) Summary of 'Fox' Glacier Mass Balance Study, 1968 (not published).
- CLARKE G.K.C. (1969) Geophysical Measurements on the Kaskawulsh and Hubbard Glaciers, I.R.R.P. Scientific Results, 1, 89-107, pub. by Am. Geog. Soc. and A.I.N.A.
- CLASSEN D. and CLARKE G.K.C. (1971) Basal Hot Spot on a Surge Type Glacier, *Nature* 229, 481-483.
- CRAIG H. (1957) Isotopic Standards for Carbon and Oxygen and Correction Factors for Mass-spectrometric Analysis of Carbon Dioxide, *Geochim. et Coschim. Acta* 12, 133-149.

- (1961a) Standard for Reporting Concentrations of Deuterium and Oxygen-18 in Natural Waters, *Science* 133, 1833-1834.
- (1961b) Isotopic Variation in Meteoric Waters, *Science* 133, 1702-1703.
- (1966) Discussion of Paper by S. Epstein, R.P. Sharp and A.J. Gow, 'Six-year Record of Oxygen and Hydrogen Isotope Variations in South Pole Firn', *J.G.R.* 71, No. 4, 1287-1288.
- DANSGAARD W. (1953) The Abundance of O^{18} in Atmospheric Water and Water Vapour, *Tellus* V, 461-469.
- (1961) The Isotopic Composition of Natural Waters, *Medd. om Grønland* 165, No. 2, 1-120.
- (1964) Stable Isotopes in Precipitation, *Tellus* XVI, No. 4, 436-468.
- and TAUBER H. (1969a) Glacier Oxygen-18 Content and Pleistocene Ocean Temperatures, *Science* 166, 499-502.
- , JOHNSON S.J., MØLLER J. and LANGWAY J.R.C.C. (1969b) One Thousand Centuries of Climatic Record from Camp Century on the Greenland Ice Sheet, *Science* 166, 377-381.
- DERIKX L. and LOIJENS H. (1970) Hydrology of Glacierized Basins—Summary of Research by Glaciology Subdivision, GLACIERS, Proceedings of Workshop Seminar, 1970, Cdn. Ntl. Committee for the I.H.D., Ottawa, Ontario.

- DEUTSCH S., AMBACH W. and EISNER H. (1966) Oxygen Isotope Study of Snow and Firn on an Alpine Glacier, Earth and Planetary Science Letters 1, 197-201.
- DOLE M. (1935) The Relative Atomic Weight of Oxygen in Water and in Air, J. Am. Chem. Soc. 57, 2731.
- (1936) The Relative Atomic Weight of Oxygen in Water and in Air, J. Chem. Phys. 4, 268-275.
- EMILIAN I. (1969) Interglacial High Sea Levels and the Control of Greenland Ice by the Procession of the Equinoxes, Science 166, 1503-1504.
- (1971) The Last Interglacial: Paleotemperatures and Chronology, Science 171, 571-573.
- EPSTEIN S. and MAYEDA T. (1953) Variation of O¹⁸ Content of Water from Natural Sources, Geochim. et Coschim. Acta 4, 213-224.
- and SHARP R.P. (1959a) Oxygen Isotope Variation in the Malaspina and Saskatchewan Glaciers, J. Geol. 67, 88-102.
- and SHARP R.P. (1959b) Oxygen Isotope Studies, IGY Bull. Trans. A.G.U. 40, 81-84.
- and SHARP R.P. (1962) Comments on Annual Rates of Accumulation in West Antarctica, Publ. 58 of the I.A.S.H. Commission of Snow and Ice (Symposium of Obergurgl), 273-285.
- , SHARP R.P. and GOW A.J. (1965) Six-year Record of Oxygen and Hydrogen Isotope Variations in South Pole Firn, J.G.R. 70, No. 8, 1809-1814.

- and SHARP R.P. (1967) Oxygen- and Hydrogen-Isotope Variations in a Firn Core, Eight Stations, Western Antarctica, J.G.R. 72, No. 22, 5595-5598.
- , SHARP R.P. and GOW A.J. (1970) Antarctic Ice Sheet: Stable Isotopes Analyses of Byrd Station Cores and Interhemispheric Climate Implications, Science 168, 1570-1572.
- FRIEDMAN I. and SMITH G.I. (1970) Deuterium Content of Snow Cores from Sierra Nevada Area, Science 169, 467-470.
- GILFILLAN E.S. JR. (1934) The Isotopic Composition of Sea Water, J. Am. Chem. Soc. 56, 406-408.
- GLIOZZI J. (1966) Size-Distribution Analysis of Microparticles in Two Antarctic Firn Cores, J.G.R. 71, No. 8, 1993-1998.
- GONFIANTINI R., TOGLIATTI V, TONGIORGI E., DE BREUCK W. and PICCIOTTO E. (1963) Snow Stratigraphy and Oxygen Isotope Variations in the Glaciological Pit of King Baudouin Station, Queen Maud Land, Antarctica, J.G.R. 68, 3791-3798.
- (1965) Some Results on Oxygen Isotope Stratigraphy in the Deep Drilling at King Baudouin Station, Antarctica, J.G.R. 70, No. 8, 1815-1819.
- GOODISON B. (1970) The Relation between Ablation and Global Radiation over Peyto Glacier, Alberta, GLACIERS, Proceedings of Workshop Seminars, 1970 Cdn. Ntl. Committee for the I.H.D., Ottawa, Ontario.

- GREW E. and MELLOR M. (1969) High Snowfields of the St. Elias Mountains, I.R.R.P. Scientific Results 1, 75-88, published by Am. Geog. Soc. and A.I.N.A.
- HATTERSLEY-SMITH G. (1963) Climatic Inferences from Firn Studies in Northern Ellesmere Island, Geografiska Annaler, XLV, No. 2-3, 139-151.
- (1960) Operation Hazen: Glaciological Studies; Snow Cover, Accumulation and Ablation, D.R.B., Dept. of Nat. Defence, Ottawa, Canada.
- ET AL (1964) Operation Hazen, Operation Tanquary: Preliminary Report, 1963, D.R.B., Dept. of Nat. Defence, Ottawa, Canada.
- HAVENS J.M. and SAARELA D.E. (1964) Exploration Meteorology in the St. Elias Mountains, Yukon, Canada, Weather 19, No. 11, 342-352.
- HERMAN Y., GRAZZINI C.V. and HOOPER C. (1971) Arctic Paleotemperatures in Late Caenozoic Time, Nature 232, 466-469.
- KAMB B. (1967) Ice under Stress and Pressure, Ice in Order and Disorder, Eng. and Sci. 31, No. 2, 27-33.
- (1970) Sliding Motion of Glaciers: Theory and Observation, Reviews of Geophysics and Space Physics 8, No. 4, 673.
- KEELER C.M. (1969) Snow Accumulation on Mt. Logan, Yukon Territory, Canada, Water Resources Research 5, No. 3, 719-723.

- KROUSE H.R. (1970) Glaciers, Canadian National Committee, The International Hydrological Decade, Proceedings of Workshop Seminar, 1970, Cdn. Ntl. Comm. for the I.H.D., Ottawa, Ontario.
- LABELLE J.C. Snow Studies on Mt. Logan, Yukon (in press).
- LACHAPPELLE E.R. (1967) Glaciers in I.U.G.G. Quadrennial Report, Am. Geo. Un. Trans. 48, No. 2, 729-736.
- LANGWAY C.C. JR. (1967) Stratigraphic Analysis of a Deep Ice Core from Greenland, C.R.R.E.L. Research Report 77, Hanover, New Hampshire, U.S.A.
- LLIBOUTRY L.A. (1965) Traité de Glaciologie, Vol. 1 and 2, Masson, Paris.
- (1965) How Glaciers Move? New Scientist 28, No. 473, 734-736.
- (1967) Discussion of Paper by J. Weertman, J.G.R. 72, No. 2, 525-526.
- (1969) Contribution à la théorie des ondes glaciaires, Cdn. J. of Earth Sciences 6, 943-945.
- LLOYD R.M. (1966) Oxygen Isotope Enrichment of Sea Water by Evaporation, Geochim. et Coschim. Acta 30, No. 8, 801-814.
- LORIUS C., LAMBERT G., HAGEMANN R., MERLIVAT L., RAVOIRE J., with the participation of ARDOUIN B., BAUER A., MARTIN J. and RICOU G. (1968) Dating of Firn Layers in Antarctica; Application to the Determination of the Rate of Snow Accumulation, I.S.A.G.E. Symposium, Hanover, U.S.A., 3-7 September 1968.

- LOTZ J.R. (1959) Northern Ellesmere Island, Cape Aldrich to Cape Colgate, Northwest Territories, Canada, A.I.N.A., Scientific Report 1.
- (1961a) Analysis of Meteorological and Micrometeorological Observations, Northern Ellesmere Island - 1959, A.I.N.A., Scientific Report 12.
- (1961b) Operation Hazen: Meteorological Observations on Gilman Glacier, 1960, D.R.B., Dept. of National Defence, Ottawa, Canada.
- (1961c) Meteorological Observations in Northern Ellesmere Island, 1959, A.I.N.A., Scientific Report 11.
- and SAGAR R.B. (1962) Northern Ellesmere Island, An Arctic Desert, Geografiska Annaler, XLIV, No. 3-4, 366-393.
- MCCULLOUGH H. and KROUSE H.R. (1965) Application of Digital Recording to Simultaneous Collection in Mass Spectrometry, Rev. Sci. Instr. 36, No. 8, 1132-1134.
- MCKINNEY C.R., MCCREA J.M., EPSTEIN S., ALLEN H.A. and UREY H.C. (1950) Improvements in Mass Spectrometer for Measurement of Small Differences in Isotopes Abundance Ratios, Rev. Sci. Instr. 21, 724-730.
- MACPHERSON D. (1965) Variations in the Abundance of O^{18} in Ice and Snow from the Kaskawulsh Glaciers, M.Sc. Thesis, University of Alberta, Alberta.
- and KROUSE H.R. (1967) O^{18}/O^{16} Ratios in Snow and Ice of the Hubbard and Kaskawulsh Glaciers; Isotope Techniques in the Hydrological Cycle; A.G.U. Monograph No. 11 pp. 180-194.

- MARCUS M. (1965) Summer Temperature Relationships along a Transect in the St. Elias Mountains, Alaska, and Yukon Territory, *Man and the Earth, Series in Earth Sciences No. 3*, University of Colorado Studies, University of Colorado Press, Boulder.
- MELLOR M. (1961) The Antarctic Ice Sheet, U.S. C.R.R.E.L., Cold Regions Science and Engineering, Pt. II, Sect. B.
- MERLIVAT L., BOTTER R. and NIEF G. (1963) Fractionnement Isotopique au cours de la distillation de l'eau, *J. Chem. Phys.* 60, 56-61.
- MIER F. and POST A. (1969) What are Glacier Surges? *Cdn. Journal of Earth Sciences* 6, 807.
- MÜLLER F. (1962) Zonation in the Accumulation Area of the Glacier of Axel Heiberg Island, N.W.T., Canada, *J. Glac.* 4, 302-318.
- (1969) Introduction: Seminar on the Causes and Mechanics of Glacier Surges, *Cdn. J. of Earth Sci.* 6, No. 4, p. iii.
- NIELSEN L.E. (1969) The Ice-dam, Powder Flow of Theory of Glacier Surges, *Cdn. J. of Earth Sciences* 6, 955.
- NIER A.O. (1947) A Mass Spectrometer for Isotope and Gas Analysis, *Rev. Sci. Instr.* 18, 398-411.
- NYE J.F. (1951) The Flow of Glaciers and Ice Sheets as a Problem in PLasticity, *Proc. Roy. Soc. A*207, 554-572.
- (1952) Mechanics of Glacier Flow, *J. of Glac.* 2, 82-93.

- (1967) Plasticity Solution for a Glacial Snout,
J. of Glac. 6, No. 47, 695-715.
- O'NEIL J.R. and EPSTEIN S. (1966) A Method for Oxygen Analysis
of Milligram Quantities of Water and Some of its
Application, J.G.R. 71, No. 20, 4955-4961.
- ØSTREM G. (1966) Mass Balance Studies on Glaciers in Western
Canada, 1965, Geographical Bull. 8, No. 1, 81-107.
- PATERSON W.S.B. (1969) The Physics of Glaciers, Pergamon Press,
Toronto.
- PICCIOTTO E.E., DEMAERE X. and FRIEDMAN I. (1960) Isotopic Com-
position and Temperature of Formation of Antarctic
Snows, Nature 187, 857-859.
- PICCIOTTO E.E. (1967) Geochemical Investigations of Snow and
Firn Samples from Eastern Antarctica, Antarctic Jour.
of U.S., Nov.-Dec., 1967, p. 236.
- POST A. (1967) Walsh Glacier Surge, J. of Glac. 6, No. 47,
763-765.
- RANKAMA K. (1963) Progress in Isotope Geology, Intersciences
Pub., 1963, New York.
- REID H.F. (1896) The Mechanics of Glaciers, Jour. of Geol. 4,
912.
- ROBIN G. de Q. (1967) Surface Topography of Ice Sheets, Nature
215, No. 5105, 1029-1032.
- (1969) Initiation of Glacier Surges, Cdn. J. of
Earth Sciences 6, 919.

- and BARNES P. (1969) Propagation of Glacier Surges, Cdn. J. of Earth Sciences 6, 969.
- REISENFELD E.H. and CHANG L.T. (1963) Dampfdruck, Siedepunkt und Verdampfungswärme von HDO and H_2O^{18} , Z. Physik Chem. B 33, 127-132.
- SHARP R.P., EPSTEIN S. and VIDZIEMAS (1960) Oxygen-isotope Ratios in the Blue Glacier, Olympic Mountains, Washington, U.S.A., J.G.R. 65, 4043-4059.
- STANLEY A.D. (1970) Combined Studies at Selected Glacier Basins in Canada, GLACIERS, Proceedings of Workshop Seminar, 1970, Cdn. Natl. Committee for the I.H.D., Ottawa, Ontario.
- TAYLOR-BARGE B. (1969) The Summer Climate of the St. Elias Mountains Region, I.R.R.P., Scientific Results 1, 33-50, Pub. by Am. Geog. Soc. and A.I.N.A.
- WAGNER W.P. (1969) Snow Facies and Stratigraphy on the Kaskawulsh Glacier, I.R.R.P., Scientific Results 1, 55-63, pub. by Am. Geog. Soc. and A.I.N.A.
- WALKER E.R. (1961) A Synoptic Climatology for Parts of the Western Cordillera, Publ. in Meteorol. No. 35, McGill University, Montreal.
- WEERTMAN J. (1967) Sliding of Non-temperate Glaciers, U.S. Army, Material Command, C.R.R.E.L., Research Report 216.
- (1967) An Examination of the Llibontry Theory of Glacial Sliding, J. of Glac. 6, No. 46, 489-494.

- (1969) Water Lubrication Mechanism of Glacial Surges, Cdn. J. of Earth Sciences 6, 929.
- WILSON A.T. (1964) Origin of Ice Ages: An Ice Shelf Theory for Pleistocene Glaciation, Nature 201, No. 4915, 147-149.
- WOOD W.A. and RAGLE R.H. (1968) Icefield Ranges Research Project, Arctic 21, 50-51.
- UREY H.E. and GREIFF L.J. (1935) Isotopic Exchange Equilibria, J. Am. Chem. Soc. 57, 321.
- and MILLS G. (1940) The Kinetics of Isotopic Exchange between CO_2 , Bicarbonate Ion, Carbonate Ion and Water, J. Am. Chem. Soc. 62, 1019.
- (1947) The Thermodynamic Properties of Isotopic Substances, J. Chem. Soc., 562-581.
- YOUNG G. (1970) Mass Balance Measurements Related to Surface Geometry on Peyto Glacier, Alberta, GLACIERS, Proceedings of Workshop Seminar, 1970, Cdn. Ntl. Committee for the I.H.D., Ottawa, Ontario.
- ZHAVORONKOV, UVAROV and SEURYUGOVA (1955) Primenie Mechenykh, Atomov Anac. Khim. Akad. Nauk. U.S.S.R., 223-233 [cited in DANSGAARD (1964)].

B30023